



Calhoun: The NPS Institutional Archive
DSpace Repository

Theses and Dissertations

1. Thesis and Dissertation Collection, all items

1980-09

A study of state rate feedback implicit model following control for VSTOL aircraft.

Epley, Lawrence E.

Monterey, California. Naval Postgraduate School

<http://hdl.handle.net/10945/19077>

This publication is a work of the U.S. Government as defined in Title 17, United States Code, Section 101. Copyright protection is not available for this work in the United States.

Downloaded from NPS Archive: Calhoun



<http://www.nps.edu/library>

Calhoun is the Naval Postgraduate School's public access digital repository for research materials and institutional publications created by the NPS community. Calhoun is named for Professor of Mathematics Guy K. Calhoun, NPS's first appointed -- and published -- scholarly author.

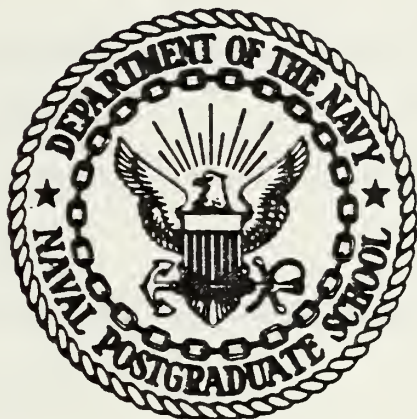
Dudley Knox Library / Naval Postgraduate School
411 Dyer Road / 1 University Circle
Monterey, California USA 93943

A STUDY OF STATE RATE FEEDBACK IMPLICIT
MODEL FOLLOWING CONTROL FOR
VSTOL AIRCRAFT

Lawrence Ernest Epley

NAVAL POSTGRADUATE SCHOOL

Monterey, California



THESIS

A STUDY OF STATE RATE FEEDBACK IMPLICIT
MODEL FOLLOWING CONTROL FOR
VSTOL AIRCRAFT

by

Lawrence Ernest Epley

September 1980

Thesis Advisor:

D. J. Collins

Approved for public release; distribution unlimited

T197425

REPORT DOCUMENTATION PAGE

READ INSTRUCTIONS
BEFORE COMPLETING FORM

1. REPORT NUMBER		2. GOVT ACCESSION NO.	3. RECIPIENT'S CATALOG NUMBER
4. TITLE (and Subtitle) A STUDY OF STATE RATE FEEDBACK IMPLICIT MODEL FOLLOWING CONTROL FOR VSTOL AIRCRAFT			5. TYPE OF REPORT & PERIOD COVERED Engineer's Thesis September 1980
			6. PERFORMING ORG. REPORT NUMBER
7. AUTHOR(s) Lawrence Ernest Epley			8. CONTRACT OR GRANT NUMBER(s)
9. PERFORMING ORGANIZATION NAME AND ADDRESS Naval Postgraduate School Monterey, California 93940			10. PROGRAM ELEMENT, PROJECT, TASK AREA & WORK UNIT NUMBERS
11. CONTROLLING OFFICE NAME AND ADDRESS Naval Postgraduate School Monterey, California 93940			12. REPORT DATE September 1980
			13. NUMBER OF PAGES 157
14. MONITORING AGENCY NAME & ADDRESS (if different from Controlling Office) Naval Postgraduate School Monterey, California 93940			15. SECURITY CLASS. (of this report) Unclassified
			15a. DECLASSIFICATION/DOWNGRADING SCHEDULE
16. DISTRIBUTION STATEMENT (of this Report) Approved for public release; distribution unlimited			
17. DISTRIBUTION STATEMENT (of the abstract entered in Block 20, if different from Report)			
18. SUPPLEMENTARY NOTES			
19. KEY WORDS (Continue on reverse side if necessary and identify by block number) VSTOL Aircraft Control, Aircraft Attitude Stabilization, Model Following, State Rate Feedback Implicit Model Following,			
20. ABSTRACT (Continue on reverse side if necessary and identify by block number) The State Rate Feedback Implicit Model Follower control concept is examined in detail from a classical and modern control theory viewpoint. State Rate Feedback Implicit Model Following (SRFIMF) is a concept whereby control of the dynamic response of a system is achieved by the measurement and feedback of a state rate, normally acceleration. In addition to a basic description of the concept, emphasis is placed on the effect of noise in the measurement of the			

Block 20 continued:

required feedback quantities. Control of the pitch attitude of the AV-8A Harrier VTOL aircraft is used as an example of the application of the control concept. The model of the Harrier used in this study includes the effect of both sensor measurement errors and gust load inputs.

Approved for public release; distribution unlimited

A Study of
State Rate Feedback Implicit Model Following Control
for VSTOL Aircraft

by

Lawrence E. Epley
Lieutenant, United States Navy
B.S., Purdue University, 1973

Submitted in partial fulfillment of the
requirements for the degree of

AERONAUTICAL ENGINEER

from the

NAVAL POSTGRADUATE SCHOOL
September 1980

ABSTRACT

The State Rate Feedback Implicit Model Follower control concept is examined in detail from a classical and modern control theory viewpoint. State Rate Feedback Implicit Model Following (SRFIMF) is a concept whereby control of the dynamic response of a system is achieved by the measurement and feedback of a state rate, normally acceleration. In addition to a basic description of the concept, emphasis is placed on the effect of noise in the measurement of the required feedback quantities. Control of the pitch attitude of the AV-8A Harrier VTOL aircraft is used as an example of the application of the control concept. The model of the Harrier used in this study includes the effect of both sensor measurement errors and gust load inputs.

TABLE OF CONTENTS

I.	INTRODUCTION -----	15
II.	DESCRIPTION OF THE SRFIMF CONTROLLER -----	19
	A. THE BASIC SCHEME -----	19
	B. THE GENERAL FORM OF THE SRFIMF CONTROLLER ---	29
	C. PRACTICAL EXAMPLES OF THE SRFIMF CONTROLLER -	32
III.	TIME AND FREQUENCY DOMAIN ANALYSIS OF THE SRFIMF -----	38
	A. REPRESENTATIVE AIRCRAFT PLANT DYNAMICS -----	38
	B. FREQUENCY RESPONSE AND BODE ANALYSIS -----	44
	C. ROOT LOCUS ANALYSIS -----	47
	D. SRFIMF SIMULATIONS -----	60
IV.	SENSOR NOISE ANALYSIS -----	73
	A. SRFIMF STOCHASTIC MODEL -----	73
	B. COVARIANCE ANALYSIS -----	85
	C. ALTERNATE MEASUREMENT SCHEMES -----	94
V.	APPLICATION OF THE SRFIMF CONCEPT TO THE HARRIER AIRCRAFT -----	107
	A. PITCH ATTITUDE CONTROL -----	107
	B. PITCH ATTITUDE GUST RESPONSE -----	122
VI.	CONCLUSIONS -----	130
	APPENDIX A - COMPUTER LISTINGS -----	132
	APPENDIX B - DATA -----	150
	LIST OF REFERENCES -----	155
	INITIAL DISTRIBUTION LIST -----	157

LIST OF TABLES

III-1	ASSUMED MODEL CONSTANTS -----	38
III-2	TYPICAL AIRCRAFT POLE LOCATIONS -----	41
III-3	AIRCRAFT MODES USED IN SIMULATIONS -----	43
III-4	PLANT PARAMETERS FOR ROOT LOCUS ANALYSIS ---	55
IV-1	SENSOR ERROR MODEL PARAMETERS -----	75
IV-2	STEADY STATE ERRORS AS A RESULT OF MEASUREMENT ERRORS -----	88
IV-3	STEADY STATE TRACKING ERRORS PRODUCED BY STRAPDOWN AND INERTIAL NAVIGATION SENSORS --	89
IV-4	STEADY STATE ERROR IN x_1 , x_2 AND x_3 FOR MEASUREMENTS MADE BY STRAPDOWN SENSORS -----	106
V-1	STEADY STATE VALUES OF σ_1 , σ_2 AND σ_5 AS A RESULT OF POSITION, VELOCITY AND ACCELERATION MEASUREMENT ERROR -----	118
V-2	STANDARD DEVIATION OF STEADY STATE TRACKING ERRORS IN x_1 , x_2 AND x_5 AS A RESULT OF SENSOR NOISE IN THE HARRIER AIRCRAFT -----	122
B-1	TABULATED DATA FOR FIGURES 4-4 THROUGH 4-6 -	150
B-2	TABULATED DATA FOR FIGURE 4-7 -----	151
B-3	TABULATED DATA FOR FIGURES 4-9 THROUGH 4-11 -----	152
B-4	TABULATED DATA FOR FIGURES 5-4 THROUGH 5-6 -	153
B-5	TABULATED DATA FOR FIGURE 5-7 -----	154

LIST OF FIGURES

2-1	IMPLICIT MODEL FOLLOWING SCHEME -----	21
2-2	SRFIMF POSITION CONTROLLER DEVELOPED BY INTUTIVE ARGUMENTS -----	24
2-3	THE GENERAL FORM OF THE SRFIMF CONTROLLER -----	30
2-4	PHYSICALLY REALIZABLE SRFIMF POSITION CONTROLLER -----	33
2-5	PHYSICALLY REALIZABLE SRFIMF RATE CONTROLLER --	33
2-6	SRFIMF CONTROLLER EMPLOYED ON THE RTA FOR SPEED CONTROL -----	37
2-7	SRFIMF CONTROLLER EMPLOYED ON RTA FOR PITCH ATTITUDE CONTROL -----	37
3-1	TYPICAL AIRCRAFT POLE LOCATIONS -----	42
3-2	FREQUENCY RESPONSE OF SRFIMF POSITION CONTROLLER, $KRL = 1$ -----	48
3-3	FREQUENCY RESPONSE OF SRFIMF POSITION CONTROLLER, $KRL = 10$ -----	49
3-4	FREQUENCY RESPONSE OF THE SRFIMF POSITION CONTROLLER, $KRL = 25$ -----	50
3-5	FREQUENCY RESPONSE OF SRFIMF POSITION CONTROLLER, $KRL = 50$ -----	51
3-6	FREQUENCY RESPONSE OF SRFIMF POSITION CONTROLLER, $KRL = 100$ -----	52
3-7	ROOT LOCUS PLOT OF OSCILLATORY POLE OF A SRFIMF POSITION CONTROLLER. THE OPEN LOOP PLANT HAS A NATURAL FREQUENCY OF 1.47 RAD/SEC AND A DAMPING RATIO OF -.441 -----	56
3-8	ROOT LOCUS OF THE OSCILLATORY POLE OF A SRFIMF POSITION CONTROLLER. THE OPEN LOOP PLANT HAS TWO POLES AT THE ORIGIN -----	57

3-9	ROOT LOCUS OF THE OSCILLATORY POLE OF A SRFIMF CONTROLLER. THE OPEN LOOP PLANT HAS A NATURAL FREQUENCY OF .95 RAD/SEC AND DAMPING RATIO OF 0.475 -----	58
3-10	ROOT LOCUS OF THE OSCILLATORY POLE OF A SRFIMF POSITION CONTROLLER. THE OPEN LOOP PLANT HAS REAL POLES AT -1.0 AND -.6 -----	59
3-11	PERFECT MODEL RESPONSE -----	62
3-12	SIMULATION OF SRFIMF POSITION CONTROL FOR AIRCRAFT MODE 1, TABLE III-3. THE OPEN LOOP PLANT HAS A NATURAL FREQUENCY OF 2.94 RAD/SEC AND DAMPING OF .2 -----	63
3-13	SIMULATION OF SRFIMF POSITION CONTROL FOR AIRCRAFT MODE 2, TABLE III-3. THE OPEN LOOP PLANT HAS A NATURAL FREQUENCY OF 2.5 RAD/SEC AND DAMPING RATIO OF 0.06 -----	64
3-14	SIMULATION OF SRFIMF POSITION CONTROL FOR AIRCRAFT MODE 3, TABLE III-3. THE OPEN LOOP PLANT HAS A NATURAL FREQUENCY OF 0.954 RAD/SEC AND A DAMPING RATIO OF 0.314 -----	65
3-15	SIMULATION OF SRFIMF POSITION CONTROL FOR AIRCRAFT MODE 4, TABLE III-3. THE OPEN LOOP PLANT HAS A NATURAL FREQUENCY OF 0.283 RAD/SEC AND DAMPING RATIO OF 0.353 -----	66
3-16	SIMULATION OF SRFIMF POSITION CONTROL FOR AIRCRAFT MODE 5, TABLE III-3. THE OPEN LOOP PLANT HAS REAL POLES AT -0.2 AND 0 -----	67
3-17	SIMULATION OF SRFIMF POSITION CONTROL FOR AIRCRAFT MODE 6, TABLE III-3. THE OPEN LOOP PLANT HAS A NATURAL FREQUENCY OF 1.47 RAD/SEC AND DAMPING RATIO OF -.204 -----	68
3-18	SIMULATION OF SRFIMF POSITION CONTROL FOR AIRCRAFT MODE 7, TABLE III-3. THE OPEN LOOP PLANT HAS REAL POLES AT 0.30 AND 0 -----	69
3-19	SIMULATION OF SRFIMF POSITION CCNTROL FOR AIRCRAFT MODE 8, TABLE III-3. THE OPEN LOOP PLANT HAS A NATURAL FREQUENCY OF 0.17 RAD/SEC AND DAMPING RATIO OF 0.590 -----	70

3-20	SIMULATION OF SRFIMF POSITION CONTROL OF AIRCRAFT MODE 9, TABLE III-3. THE OPEN LOOP PLANT HAS TWO POLES AT THE ORIGIN -----	71
3-21	SIMULATION OF SRFIMF POSITION CONTROL OF AIRCRAFT MODE 10, TABLE III-3. THE OPEN LOOP PLANT HAS REAL POLES AT -1.0 AND -0.6 -----	72
4-1	EXPONENTIALLY CORRELATED NOISE SHAPING FILTER -----	74
4-2	HIGH FREQUENCY ERROR MODEL, POSITION CONTROLLER -----	76
4-3	TRACKING ERRORS IN x_1 AS A RESULT OF MEASURE- MENT ERROR IN POSITION, VELOCITY AND ACCELERATION -----	91
4-4	TRACKING ERRORS IN x_2 AS A RESULT OF MEASURE- MENT ERROR IN POSITION, VELOCITY AND ACCELERATION -----	92
4-5	TRACKING ERRORS IN x_3 AS A RESULT OF MEASURE- MENT ERROR IN POSITION, VELOCITY AND ACCELERATION -----	93
4-6	FIRST ALTERNATE MEASUREMENT SCHEME. MEASURED ACCELERATION AND IMPLIED POSITION AND VELOCITY -----	94
4-7	ERROR IN x_1 , x_2 , AND x_3 AS A RESULT OF MEASUREMENT ERRORS IN ACCELERATION -----	97
4-8	SECOND ALTERNATE MEASUREMENT SCHEME, MEASURED POSITION AND VELOCITY. ESTIMATED ACCELERATION -----	98
4-9	TRACKING ERRORS OF x_1 AS A RESULT OF MEASURE- MENT ERRORS IN POSITION AND VELOCITY -----	103
4-10	TRACKING ERRORS OF x_2 AS A RESULT OF MEASURE- MENT ERRORS IN POSITION AND VELOCITY -----	104
4-11	TRACKING ERRORS OF x_3 AS A RESULT OF MEASURE- MENT ERRORS IN POSITION AND VELOCITY -----	105
5-1	ROOT LOCUS OF THE OSCILLATORY POLES OF THE LONGITUDINAL AXIS OF THE HARRIER USING SRFIMF POSITION CONTROL -----	109

5-2	HARRIER LONGITUDINAL SIGNAL FLOW GRAPH TRANSFER FUNCTION SIMULATION -----	111
5-3	SIMULATION OF THE UNIT STEP RESPONSE OF THE PITCH ATTITUDE OF THE AV-8A HARRIER WITH SRFIMF CONTROL -----	112
5-4	SCHEMATIC REPRESENTATION OF THE AV-8A HARRIER PITCH AXIS WITH THE SRFIMF CONTROLLER. INCLUDING SENSOR NOISE -----	114
5-5	TRACKING ERROR IN x_1 AS A RESULT OF MEASURE- MENT ERROR IN POSITION, VELOCITY AND ACCELERATION FOR THE HARRIER LONGITUDINAL AXIS POSITION CONTROL -----	119
5-6	TRACKING ERROR IN x_2 AS A RESULT OF MEASURE- MENT ERROR IN POSITION, VELOCITY AND ACCELERATION FOR THE HARRIER LONGITUDINAL AXIS POSITION CONTROL -----	120
5-7	TRACKING ERROR IN x_5 AS A RESULT OF MEASURE- MENT ERROR IN POSITION, VELOCITY AND ACCELERATION FOR THE HARRIER LONGITUDINAL AXIS POSITION CONTROL -----	121
5-8	GUST SHAPING FILTER -----	124
5-9	SCHEMATIC REPRESENTATION OF THE AV-8A PITCH CONTROL USING A SRFIMF CONTROLLER WITH WIND GUST INPUT -----	126
5-10	STANDARD DEVIATION OF VEHICLE PITCH ACCELERA- TION AND PLANT INPUT, x_5 , AS A RESULT OF A GUST -----	129

LIST OF SYMBOLS

A	matrix of coefficients of the closed loop controller
A*	modal transformation of the matrix of coefficients of the closed loop controller
A(s)	SRFIMF controller compensator transfer function
B	matrix of control input coefficients
B*	modal transformation of the matrix of input coefficients
b	damping term in aircraft rigid-body second order modes
c	stiffness term in aircraft rigid-body second order modes
C*	modal transformation of the SRFIMF output matrix
C	SRFIMF output matrix
CPG	constant plant gain or control power gradient depending upon use
F	implicit model following feedback matrix
f	value of the highly damped root of a SRFIMF system
G	matrix of coefficients of the noise inputs to the SRFIMF system
G(s)	Laplace transform of airplane rigid-body modes
H(s)	transfer function representing the dynamic behavior of control force or moment application
h	height in feet of aircraft center of gravity
K	forward loop gain of SRFIMF controller
KRL	SRFIMF controller gain parameter
K_x	position feedback gain
$K_{\dot{x}}$	rate feedback gain

L matrix of coefficients of the model
 L_w characteristic length of atmospheric turbulence
 NASA National Aeronautics and Space Administration
 P matrix of SRFIMF system covariances
 Q matrix of SRFIMF exponentially correlated white noise strengths
 RTA Research and Technology Aircraft
 s Laplace transform variable
 SRFIMF State Rate Feedback Implicit Model Following
 T transformation matrix between state variable coordinates and modal coordinates
 T_r correlation time of exponentially correlated sensor noises
 T_g correlation time of exponentially correlated wind gust noise
 U Vector of SRFIMF system inputs
 V_{wind} nominal surface wind
 $W(s)$ SRFIMF control law
 $W_t(t)$ white noise
 $X(s)$ controlled variable
 X vector of SRFIMF state variables
 X^* vector of SRFIMF modes
 X_c commanded input
 X_a^* acceleration error mode
 X_p^* position error mode
 X_v^* velocity error mode
 Y SRFIMF output vector

z	vector of model states
δ	general transfer function control input
δ_g	gust input
δ_e	control stick input
ζ	second order response damping ratio
θ	pitch attitude angle
μ	white noise strength
ξ	exponentially correlated noise
σ	standard deviation
σ_a	standard deviation of acceleration error
σ_g	standard deviation of gust input
σ_p	standard deviation of position error
σ_v	standard deviation of velocity error
τ	control actuator time constant
ω_n	natural frequency of second order response

ACKNOWLEDGMENT

With sincere gratitude, the help and encouragement of numerous individuals is acknowledged. Most important, is the patient assistance of my teacher and advisor, Prof. Daniel Joseph Collins. The advise of Dr. J. Franklin and Mr. V. Merrick of the Guidance and Central Branch of the NASA Ames Aeronautical Research Center; Dr. Tsuyoshi Goka of Analytical Mechanics Associates, Inc., and the faculty of the Aeronautics Department of the U.S. Naval Postgraduate School has been invaluable in the production of this study. The work was made considerably easier with the help of Mrs. Adrian Schueneman who scrutinized and typed the early drafts.

Special thanks goes to my wife, Mary Anne, and my family for their support during the long and trying months required to produce this work.

I. INTRODUCTION

A State Rate Feedback Implicit Model Following (SRFIMF) flight controller has been proposed as a possible approach to improving the handling qualities of Vertical and Short Field Take Off and Landing (VSTOL) aircraft by Merrick at the NASA Ames Aeronautical Research Laboratory [1, 2]. The SRFIMF concept has potential applications in various types of control problems encountered in aircraft design, among which are attitude, guidance, and engine control. The concept has not been used in actual flight tests, however several detailed simulations [2, 3] have been conducted at NASA Ames in which SRFIMF control was applied. The most notable features of the control scheme are that:

1. The Input-output relationship of a system using SRFIMF control is insensitive to changes in airframe and propulsion dynamic characteristics.
2. The dynamic relationship of the output to the input is approximately that of a second order system whose frequency and damping is chosen by the designer.
3. The system is self trimming and the commanded output variable is independent of external disturbances.
4. The system has good gust alleviation.

This study presents a detailed analysis of the SRFIMF control concept as applied to the attitude control of VSTOL aircraft.

The following discussion is given to clarify the meaning of State Rate Feedback Implicit Model Following as used in this study. Model following refers to the ability of a control scheme to impart specified dynamic characteristics, given by a model, to the closed loop system. The model being considered here is a second order response in which the parameters of natural frequency and damping ratio are chosen by the designer. Typically a second order response is mathematically defined in terms of the states position and velocity. The state rate of the second order model is the acceleration. The State Rate Feedback Implicit Model Following controller, studied here, achieves model following by measurement and feedback of the system's state rate, acceleration. The result is that a priori knowledge of the plant is not required to produce model following.

To illustrate the use of state rate feedback, consider a plant of second order. With the states of the system X_1 and X_2 , defined as position and velocity, the representation of the plant in matrix notation is

$$\begin{matrix} \dot{X}_1 \\ \dot{X}_2 \end{matrix} = \begin{bmatrix} 0 & 1 \\ -c & -b \end{bmatrix} \begin{Bmatrix} X_1 \\ X_2 \end{Bmatrix} + \begin{Bmatrix} 0 \\ 1 \end{Bmatrix} U(t) \quad 1-1$$

The acceleration, \dot{X}_2 , equation is thus

$$\dot{X}_2 = -cX_1 - bX_2 + U(t) \quad 1-2$$

The values of b and c define the dynamic behavior of the plant. Design of a control system would in general require that b and c be known. The feedback scheme or control law of the SRFIMF controller is formulated so that the plant dependent quantities of b and c are only involved in the total quantity of $(-cX_1 - bX_2)$. With this arrangement the quantity, $(-cX_1 - bX_2)$, can be obtained by measurement of the state rate, acceleration, minus the input, U . Model following by measurement of the state rate, as in this illustration, is the basic concept of the SRFIMF controller.

The intent of this study is to provide a detailed analysis of the SRFIMF controller from a modern and classical control viewpoint. Particular emphasis will be placed on a basic description of the control scheme and the effects of measurement errors on the output of the closed loop system. The first two sections deal with a classical analysis of the controller as applied to the attitude position control of a general VSTOL aircraft. The third section considers the effect of measurement errors on the system from a modern control viewpoint. From that analysis, the steady state covariance of the state variables, as a result of measurement uncertainties, will be found. Finally, the previously developed analysis technique will be applied to an example where SRFIMF is used for pitch control of the Harrier aircraft. The effect of sensor errors will be examined and the response of the Harrier to gust inputs will be determined.

The following assumptions are made in this study:

1. The system is linear. Non-linear effects such as control saturation and actuator hysteresis are not considered.
2. The dynamic response of the plant will be represented at a single point by linearized, rigid-body, transfer functions.
3. Measurement uncertainties are represented as exponentially correlated noise and the effect of bias error is not considered. The basic description and development of the SRFIMF controller will be considered in section II.

II. DESCRIPTION OF THE SRFIMF CONTROLLER

A. THE BASIC SCHEME

It is desirable for a flight controller to impart specific dynamic characteristics to the closed loop response of an aircraft system. Often the desired response is given in terms of a natural frequency and damping ratio. Piloted simulations at NASA Ames [2] have indicated that a desirable response from the pilot's stick to the aircraft attitude is a second order response whose natural frequency, ω_n , is approximately 2 rad/sec and damping ratio, ζ , of 0.75. One possible approach to the design of an attitude controller is to apply model following techniques. Mathematically the model for attitude control dynamics can be represented by a transfer function in the frequency domain. If, as an example we let $\theta(s)$ represent the aircraft pitch angle and $\delta(s)$ the elevator control input, then the transfer function of a model for pitch attitude control can be written as

$$\frac{\theta(s)}{\delta(s)} = \frac{1}{s^2 + 2\zeta\omega_n s + \omega_n^2} \quad 2-1$$

In this example, if the desired response has a natural frequency of 2 rad/sec and damping ratio of 0.75, and equation 2-1 becomes

$$\frac{\theta(s)}{\delta(s)} = \frac{1}{s^2 + 3s + 4} \quad 2-2$$

This transfer function will be used to illustrate model following techniques in the development of the SRFIMF concept. The desired model response, given by 2-1, can also be expressed in state variable notation with states Z_1 of position and Z_2 velocity. The matrix of coefficients of the model is given the symbol L and equation 2-1 can be written as

$$\begin{aligned}\dot{Z} &= [L]Z + [B]U \\ &= \begin{bmatrix} 0 & 1 \\ -\omega_n^2 & -2\zeta\omega_n \end{bmatrix} Z + \begin{Bmatrix} 0 \\ 1 \end{Bmatrix} U\end{aligned}\quad 2-3$$

Given somewhat arbitrary open loop plant dynamics, the object of model following is to produce a closed loop system whose dynamic characteristics are given by equation 2-1 or equation 2-3.

For a general system

$$\begin{aligned}\dot{X} &= AX + BU \\ Y &= CX\end{aligned}\quad 2-4$$

the object of implicit model following is to force the output of the system to follow the model equation

$$\dot{Z} = LZ + BU\quad 2-5$$

That is to say, the output, Y , should approximate Z ($Y \approx Z$) so that

$$\dot{Y} \approx LY + BU\quad 2-6$$

By proper choice of the feedback gain F , as shown in figure 2-1, the output is forced to follow equation 2-6. The

implied model shown in the upper portion of the figure, is not actually generated but implied by the behavior of \underline{Y} .

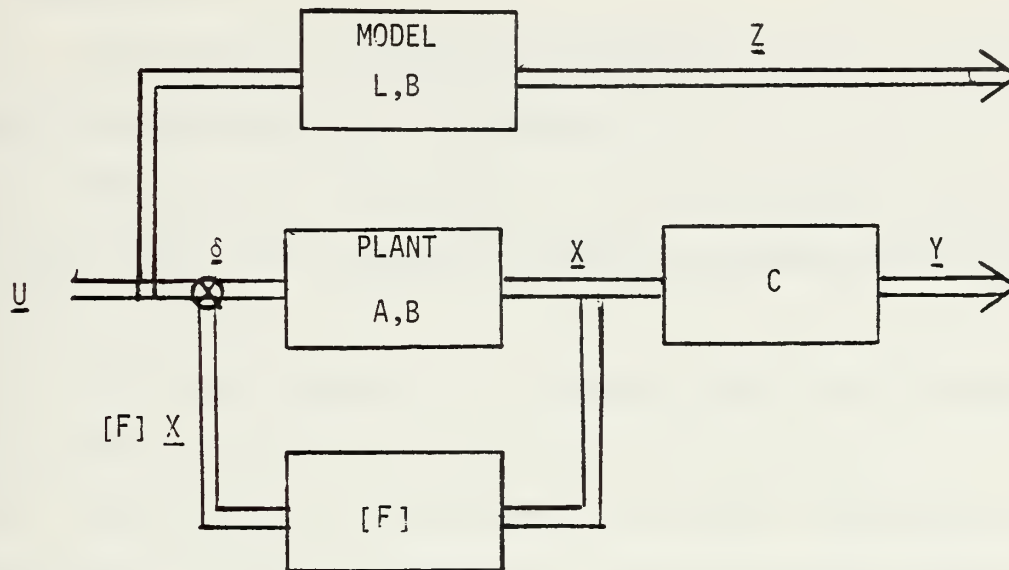


Figure 2-1 Implicit Model Following scheme

The formulation of the feedback law required in model following has been determined by Taylor [4] using optimal control techniques. In addition, Erzberger [5] has defined algebraic methods for determining if perfect model following can be achieved. This algorithm will be examined later in this section. In aircraft applications certain physical facts about the system allow a form of implicit model following to be obtained by simple intuitive reasoning.

Consider the problem of stabilizing the pitch attitude of a VSTOL aircraft. The following assumptions can be made and will lead to a simplified SRFIMF controller:

1. The desired model response is of second order with frequency, ω_n , of 2 rad/sec and damping ratio, ζ , of 0.75 from equation 2-1.

2. Measurements of angular position, angular rate and angular acceleration are available.

3. The control U is either a thrust or control deflection whose net result is to produce angular acceleration of the vehicle.

4. The open loop plant is arbitrary and the transfer function for θ , $\theta(s)/U(s) = G(s)$, may be unknown.

5. The control law which produces model following will be developed so that it represents the difference between the vehicle's angular acceleration, as measured, and the angular acceleration which would be implied by the model given in 1, above.

From assumption 1 we obtain the desired closed loop response as that of the model and express it as

$$\frac{\theta(s)}{U(s)} = \frac{1}{s^2 + K_{\dot{x}}s + K_x} \quad 2-7$$

where $\theta(s)$ is the pitch attitude and the constants $K_{\dot{x}}$ and K_x are defined for convenience and will be used throughout this study as

$$K_{\dot{x}} = 2\zeta\omega_n = 3 \quad 2-8$$

$$K_x = \omega_n^2 = 4 \quad 2-9$$

By requiring the model, equation 2-7, to hold we observe that the implied angular acceleration is

$$s^2\theta(s) = -K_x\theta(s) - K_{\dot{x}}s\theta(s) + U(s) \quad 2-10$$

$\theta(s)$ and $s\theta(s)$ are angular position and angular rates which, by assumption 2, are available from measurements. The quantity $U(s)$ is the input to the open loop plant. Given $\theta(s)$, $s\theta(s)$ and $U(s)$, the quantity $s^2\theta(s)$ can be calculated from equation 2-10.

We will define $W(s)$ as the control law for the system. $W(s)$ will be taken as the difference between the implied model acceleration $s^2\theta(s)$ and the actual measured acceleration

$$W(s) = s^2\theta(s) - (\text{measured acceleration}) \quad 2-11$$

Using equation 2-10 and substituting for $s^2\theta(s)$ one has

$$W(s) = -K_x\theta(s) - K_{\dot{x}}s\theta(s) + U(s) - (\text{measured acceleration}) \quad 2-12$$

Further the quantities $\theta(s)$ and $s\theta(s)$ will be determined by sensors so that

$$W(s) = -K_x \cdot (\text{measured position}) - K_{\dot{x}} \cdot (\text{measured rate}) + U(s) - (\text{measured angular acceleration}) \quad 2-13$$

The quantity $U(s)$ could be considered pilot or other control input to the plant. Since we also defined $W(s)$ as the control there is some ambiguity in the notation. The symbol $U(s)$ will be used consistently for the control feedback quantity as indicated in figure 2-2.

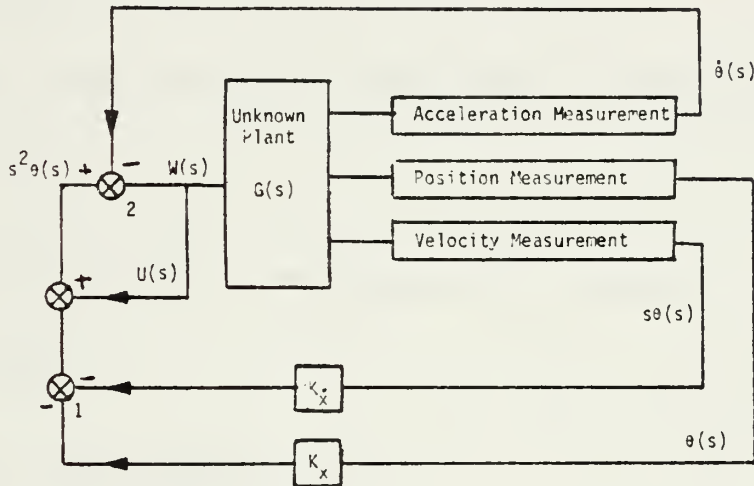


Figure 2-2 SRFIMF position controller developed by intuitive arguments.

Figure 2-2 shows schematically the control law and unknown plant $G(s)$. It can also be seen that the plant input, $U(s)$ is a feedback quantity and the implied acceleration, $s^2\theta(s)$ is compared to the measured acceleration at point 2 of the figure. The term state rate feedback is applied to this type of control because of acceleration feedback. It is this measurement which brings to the controller information about the plant making a priori knowledge of the transfer function for $\theta(s)$ unnecessary. This aspect of the SRFIMF controller is most clearly seen by application of the Erzberger criterion mentioned earlier.

The Erzberger criterion for exact implicit model following is obtained by analysis of the system in state space representation where the system is given by

$$\dot{X} = AX + BU \quad 2-14$$

$$Y = CX \quad 2-15$$

For implicit model following the output is approximated by

$$\dot{Y} = LY \quad 2-16$$

Taking the derivative of equation 2-15, one has

$$\dot{Y} = C\dot{X} \quad 2-17$$

Substituting from equation 2-14

$$\dot{Y} = C(AX + BU) \quad 2-18$$

or

$$\dot{Y} = CAX + CBU$$

but from equations 2-15 and 2-16 one has

$$\dot{Y} = LY = LCX \quad 2-19$$

so that one has, on equating 2-18 and 2-19,

$$CAX + CBU = LCX \quad 2-20$$

or

$$CBU = (LC - CA) \cdot X$$

Solving for the control, U, from 2-20 we have that

$$U = \left[(CB)^+ \cdot (LC - CA) \right] X \quad 2-21$$

where $(CB)^+$ is the pseudo, or generalized, inverse of (CB) .

Eliminating U from 2-20 and 2-21, the condition for perfect model following becomes

$$[(CB)(CB)^+ - I][(LC) - (CA)] \cdot X = 0 \quad 2-22$$

The use of the pseudo inverse is based on the property of the pseudo inverse that $(CB)(CB)^+$ is an orthogonal projection operator on the range of (CB) . It then follows that if 2-22 holds for all X, the range of CB must contain the range of $(LC-CA)$. This implies that 2-16 is valid which has already been assumed to be the case.

We will now apply equation 2-22 to the pitch attitude controller given earlier. In this case $\theta(s)/U(s)$ is assumed to be the transfer function of an arbitrary second order system.

$$\frac{\theta(s)}{U(s)} = \frac{1}{s^2 + bs + c}$$

The desired closed loop performance is given by the model as in equation 2-7. For this example we initially take the feedback quantities to be angular position and angular rate. Defining the quantities in state variable representation we have the plant where

$$X_1 = \theta(t)$$

$$X_2 = \dot{\theta}(t)$$

$$\begin{aligned}\dot{X} &= [A] X + BU \\ &= \begin{bmatrix} 0 & 1 \\ -c & -b \end{bmatrix} \begin{Bmatrix} X_1 \\ X_2 \end{Bmatrix} - \begin{Bmatrix} 0 \\ 1 \end{Bmatrix} U\end{aligned}\tag{2-23}$$

and

$$Y = CX$$

or

$$Y = \begin{bmatrix} 1 & 0 \\ 0 & 1 \end{bmatrix} \begin{Bmatrix} X_1 \\ X_2 \end{Bmatrix}\tag{2-24}$$

Calculation of the pseudo inverse depends upon the relative rank of C and B in this case, following Noble [6], the pseudo inverse of (CB) is given as

$$(CB)^+ = [(CB)^+ \cdot (CB)]^{-1} \cdot (CB)^T$$

From 2-23 and 2-24

$$(CB) = \begin{Bmatrix} 0 \\ 1 \end{Bmatrix}$$

therefore

$$(CB)^+ = [0 \ 1]$$

To determine if perfect model following is possible, we substitute into 2-22 using 2-23, 2-24, 2-8, 2-9 and the above for (CB) and $(CB)^+$

$$[(CB) (CB)^+ - I] = \begin{bmatrix} -1 & 0 \\ 0 & 0 \end{bmatrix} \quad 2-25$$

$$[(LC) - (CA)] = \begin{bmatrix} 0 & 0 \\ -(K_x + c) & -(K_{\dot{x}} + b) \end{bmatrix} \quad 2-26$$

The result is that

$$[(CB) (CB)^+ - I] [(LC) - (CA)] \equiv 0 \quad 2-27$$

Equation 2-27 shows that perfect model following is possible for all X using position and rate feedback only. The control can be determined by equation 2-21 with the result

$$U_c = [(-K_x + c) (-K_{\dot{x}} + b)] \begin{Bmatrix} X_1 \\ X_2 \end{Bmatrix} \quad 2-28$$

$$= -K_x X_1 - K_{\dot{x}} X_2 + cX_1 + bX_2 \quad 2-29$$

The control law given in equation 2-29 requires that the constants c and b be known in order to produce the desired model following. In the previous discussion we stated that the addition of acceleration feedback provided the needed information about the plant. To show this, note that the latter two terms of equation 2-29, $cX_1 + bX_2$, can be interpreted in terms of the acceleration of the system, X_2 , since

$$\dot{X}_2 = -cX_1 - bX_2 + U(s) \quad 2-30$$

one has

$$\dot{X}_2 - U(s) = -cX_1 - bX_2 \quad 2-31$$

or rewriting equation 2-29 one has

$$U_c = -K_x X_1 - K_{\dot{x}} \dot{X}_2 + U(s) - \dot{X}_2 \quad 2-32$$

We can compare this to equation 2-13 rewritten in the same notation

$$W(s) = -K_x X_1 - K_{\dot{x}} \dot{X}_2 + U(s) - (\text{measured} \quad 2-33 \\ \text{angular acceleration})$$

Note, X_1 and X_2 are the measured angular position and measured angular rate. This comparison shows that the measured acceleration supplies the terms needed for perfect model following without a need for a knowledge of the plant dynamics.

The significance of this result is that state rate feedback can be used to provide information about the plant in applications where the plant has unknown and changing dynamic characteristics. This conclusion was reached based upon the assumption that the plant was of second order. We shall now consider a more general form of the SRFIMF controller and we will show that model following can be achieved by measurement of state rate for a higher order plant.

B. THE GENERAL FORM OF THE SRFIMF CONTROLLER

The preceding discussion presented an intuitive description of the principal operation of the SRFIMF controller and the use of state rate feedback. It is the intent of this section to develop a general form of state rate feedback and

to show again that model following can be achieved without a priori knowledge of the plant by using measurement of the state rate. We begin by examining the basic SRFIMF controller as developed by Merrick at NASA Ames. The block diagram of this controller is shown in figure 2-3.

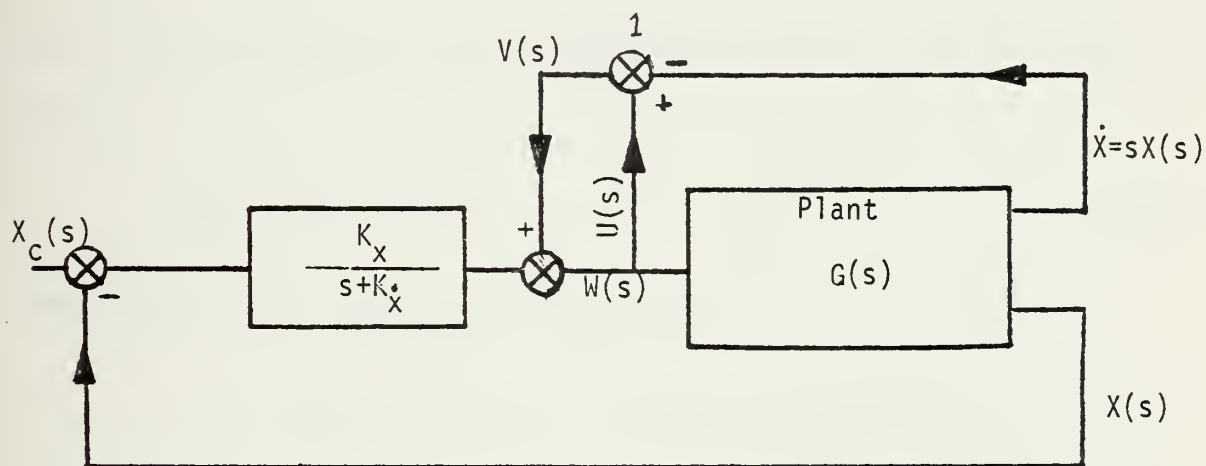


Figure 2-3 The general form of the SRFIMF controller.

Assume that figure 2-3 represents a velocity controller, then the feedback quantities $X(s)$ and $sX(s)$ are velocity and acceleration respectively. It can be seen that at position 1 we are summing $(- \text{acceleration} + U(s))$. It will be shown that the transfer function between the input $X_c(s)$ and the output $X(s)$ does not depend upon the plant transfer function $G(s)$ and that the closed loop response is that of a second order system whose damping and natural frequency are determined by the choice of feedback constants K_x and K_x^* .

From figure 2-3 $W(s)$ is given by

$$W(s) = U(s) - sX(s) + [X_C(s) - X(s)] \cdot \left[\frac{K_X}{s + K_X} \right] \quad 2-34$$

and for $V(s)$ we write

$$V(s) = U(s) - sX(s) \quad 2-35$$

from the definition of the transfer function $G(s)$ we have that

$$X(s) = W(s) G(s) \quad 2-36$$

Combining 2-34 and 2-36 we have that

$$X(s) = \left\{ U(s) - sX(s) + \frac{(X_C(s) - X(s)) K_X}{s + K_X} \right\} G(s) \quad 2-37$$

Since $U(s) = W(s)$ as seen from figure 2-3, we have

$$X(s) = U(s) \cdot G(s) \quad 2-38$$

and equation 2-37 can be rewritten as

$$X(s) = X(s) - sX(s)G(s) + \frac{(X_C(s) - X(s)) K_X}{s + K_X} G(s) \quad 2-39$$

and

$$sX(s)G(s) = \frac{(X_C(s) - X(s)) K_X}{s + K_X} \cdot G(s) \quad 2-40$$

$G(s)$ on both sides of equation 2-40 cancels and the result becomes

$$\frac{X(s)}{X_C(s)} = \frac{K_X}{s^2 + K_X s + K_X} \quad 2-41$$

Equation 2-41 shows that the closed loop response of the SRFIMF is identically that of a second order system whose natural frequency and damping ratio is completely determined by the constant feedback gains which are given by

$$\omega_n = K_x \quad \zeta = \frac{K_{\dot{x}}}{2\sqrt{K_x}}$$

The results of this analysis indicate that the SRFIMF controller is an excellent candidate for VSTOL aircraft applications. The form of the controller shown in figure 2-2 could be used to control a position such as attitude while the general form shown in figure 2-3 might be used to control rates or velocity. It will now be necessary to examine the requirements necessary to implement a SRFIMF controller in an aircraft. In particular, the exact relationship between $U(s)$ and $W(s)$ must be considered. The next section will examine practical examples of SRFIMF controllers in a realistic aircraft environment.

C. PRACTICAL EXAMPLES OF THE SRFIMF CONTROLLER

Two types of controllers are illustrated in this section, a position controller, figure 2-4, and a velocity controller, figure 2-5. A first order actuator is included in the plant of each controller. Also included is a compensator in the control feedback loop involving $U(s)$. The system is not realizable without the compensator. These controllers will be used in the analysis of this report.

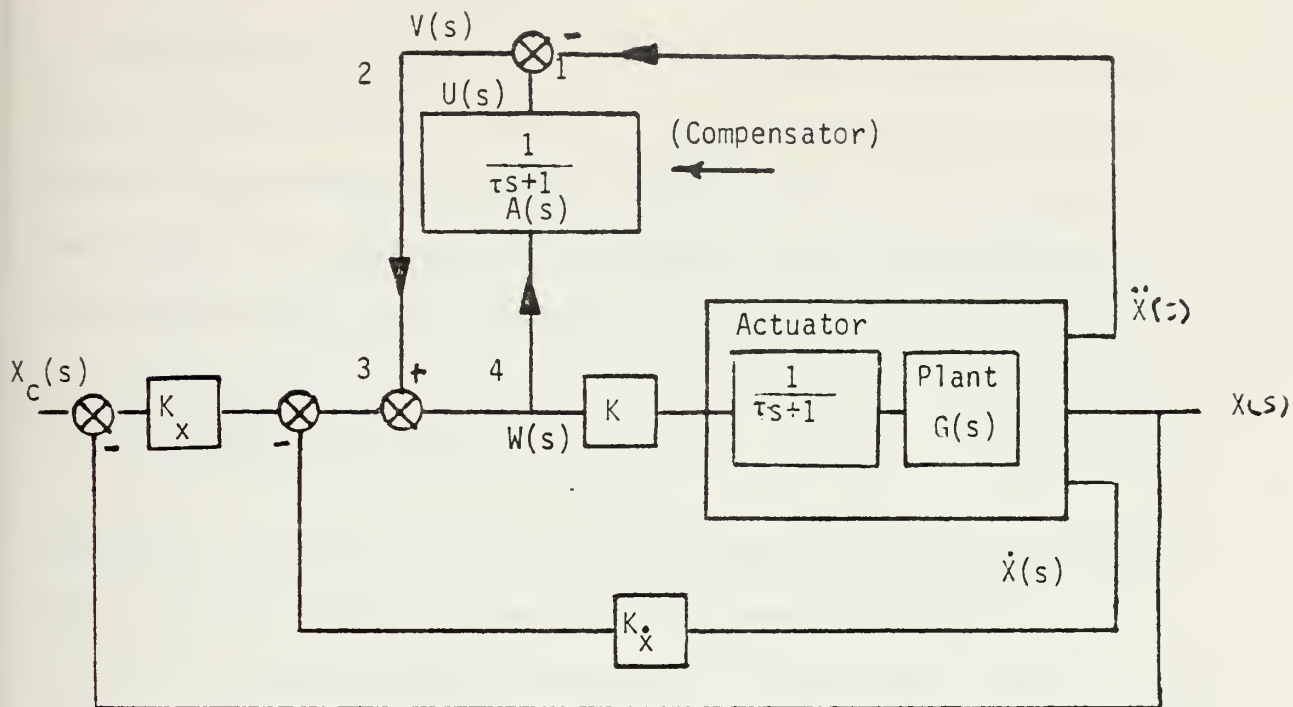


Figure 2-4 Physically realizable SRFIMF position controller.

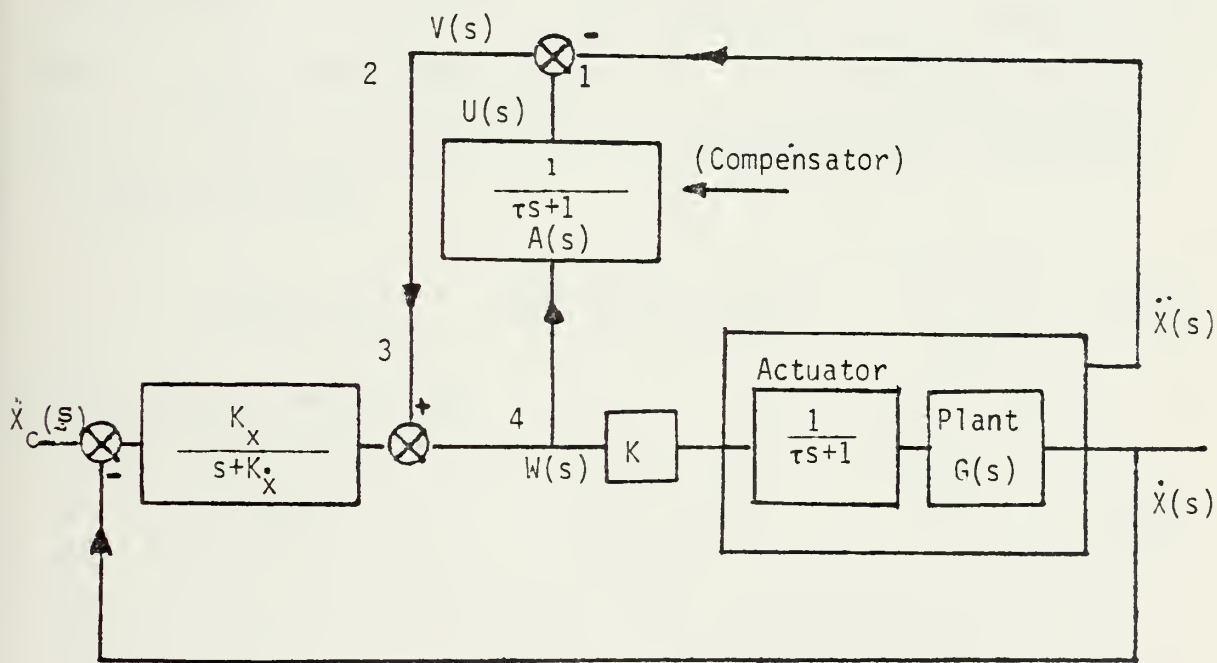


Figure 2-5 Physically realizable SRFIMF rate controller.

The plant is assumed to be driven by a control actuator and because of that a phase lag can be expected to exist between the commanded control signal, $W(t)$ and the input of the plant. The effect of the actuator will be modeled by using the first order transfer function

$$\frac{H(s)}{W(s)} = \frac{1}{(\tau s + 1)} \quad 2-42$$

where $H(s)$ is the output of the actuator, $W(s)$ is the input and τ is the actuator time constant assumed to be 0.1 sec for all of the examples considered in this work. Recall from a previous section that SRFIMF feedback contained a term $U(t)$ which represented the control input to the plant and that $W(t)$ was assumed to equal $U(t)$. Because of the fact that $U(t)$ was equal to $W(t)$ the output signal of the controller could be used to cancel the $U(t)$ term in the acceleration feedback. It was shown that

$$\text{acceleration} = -cX_1 - bX_2 + U(t) \quad 2-43$$

and it was assumed that

$$U(t) = W(t) \quad 2-44$$

In order for equation 2-44 to be valid, the system would need to have instantaneous response to any input. Because of the action of the control actuator this is not possible and a compensator is placed in the feedback loop between $W(s)$ and the summing junction at 1, as shown in figures 2-4 and 2-5. The compensator transfer function is $A(s)$. $A(s)$ is chosen so that the output of the compensator is dynamically identical to the input of the plant, after the control actuator. When the control is represented by a first order lag, as in this case, $A(s)$ is the same as the transfer function of the actuator. In cases of higher order actuator dynamics the result is more complicated. An algorithm for determining the necessary transfer function, $A(s)$, which must be used in the feedback is given by Merrick [2]. We will assume a first order actuator and a compensator of the form $1/(\tau s + 1)$ as shown in figures 2-4 and 2-5, for the remainder of this work.

Actual controllers used at NASA Ames are illustrated in figures 2-6 and 2-7. Figure 2-6 is a speed controller. The quantities VD and VDD represent the measured speed and acceleration. VC is the commanded speed and $W(s)$ is the output of the controller. Figure 2-7 is a SRFIMF position controller used to control the pitch attitude, θ , of the RTA vehicle. The limiters seen in the figures are not included in the model studied here. The purpose of the limiter is to prevent the control feedback loop from acting as an integrater when the plan control is saturated. This condition could occur

when a large difference between the commanded variable, X , and the input variable, X_c , existed and the plant control was saturated. In this condition $W(s)$ would increase without bound and a reversal of the input would be delayed because of the very high value of $W(t)$ at the time the control reversal was applied. The limiter was not considered here because of the assumption of linearity.

III. TIME AND FREQUENCY DOMAIN ANALYSIS OF THE SRFIMF

A. REPRESENTATIVE AIRCRAFT PLANT DYNAMICS

The State Rate Feedback Implicit Model Follower controller presented in section II, figure 2-4 will now be examined using Root Locus, Bode Analysis and Time Simulations. Root Locus analysis will show the asymptotic behavior of the closed loop poles and Bode analysis will show the filter characteristics of the controller. Simulated time response of the controller will be shown in order to demonstrate the ability of the SRFIMF to follow the given model and to show graphically the self trimming feature of the controller. The model and representative plant will next be defined.

The model for the system is taken as a second order system with a transfer function given by

$$\frac{M(s)}{U(s)} = \frac{K_x}{s^2 + K_{\dot{x}}s + K_x} \quad 3-1$$

The gains K_x and $K_{\dot{x}}$ are selected to yield two different models, one a position controller and the other a rate controller as shown in the following table.

	ω_n	ζ	K_x	$K_{\dot{x}}$	Pole Location	
Attitude Control	2 rad/sec	.75	4	3	-1.5	1.32i
Rate Control	1.23 rad/	.7023	1.57	1.76	-.88	.89i

TABLE 3-1 Assumed Model Constants.

The values listed in table 3-1 are based upon piloted simulations at NASA Ames [2] and reflect what has been judged to be representative of good handling qualities.

The plant transfer function is also taken as a second order system

$$G(s) = \frac{CPG}{s^2 + bs + c} \quad 3-2$$

While initially this assumption may seem unrepresentative of a real aircraft, proper choice of b and c can represent the dynamic behavior of the individual modes of any aircraft, provided that first order modes are taken two at a time. To illustrate, consider the general transfer function

$$C(s) = \frac{K \prod_{i=1}^M (s + z_i)}{s \prod_{J=1}^q (s + p_J) \prod_{K=1}^r (s^2 + 2\zeta_K \omega_K s + \omega_K^2)} \quad 3-3$$

If the poles are distinct then equation 3-3 can be expanded into partial fractions as follows

$$C(s) = \frac{a}{s} + \sum_{J=1}^q \frac{a_J}{s + p_J} + \sum_{K=1}^r \frac{b_K (s + \zeta_K \omega_K) + C_K W_n \sqrt{1 - \zeta_K^2}}{s^2 + 2\zeta_K \omega_K s + \omega_K^2} \quad 3-4$$

It can be seen from the above that the response of a higher order system is composed of a summation of first and second order terms. When the first order terms are taken two at a

time, the total system response can be expressed as the sum of only second order terms with constant numerators. The assumption of linearity allows us to analyze the modes independently. It remains to choose values of b and c which represent typical aircraft modes. To do this, it will be necessary to survey several representative aircraft. From this survey a number of modes will be selected as typical of VSTOL applications. It will be assumed that acceptable control of each of the modes will lead to acceptable control of the system. This method of analysis leads to considerable simplification since it allows the plant to be taken as a second order system. While this simplified plant will serve the majority of the analysis, a more complex plant will be examined in section V.

Table 3-2 is a listing of pole locations for selected aircraft. Figure 3-1 is a sketch of these poles in the complex plane and an assumed envelope of VSTOL pole locations. Table 3-3 lists points which will be considered by time simulation. From this list, four representative modes will be examined by root locus.

AIRCRAFT	FLIGHT CONDITION	FREQUENCY/DAMPING		OSCILLATORY POLES		REAL POLES	
		ω_n	ζ	Re.	Im.	$1/T_1$	$1/T_2$
F106	S.L. M=.2	2.42	.62	-1.5	1.9	-.169	-.59
Lateral/Directional	20,000', M=.9	3.01	.159	-.48	3.0	-1.84	+.006
A4 Longitudinal	S.L. M=.2 short period	1.56	.31	-.48	1.5		
	long period	1.52	.087	-.013	.15		
	15,000', M=.9 short period	.623	.344	+.20	.585		
	long period	.12	-.078	+.01	.12		
A4	S.L. M=.2	1.89	.05	-.09	1.89	-.065	-.56
Lateral/Directional	15,000', M=.9	6.61	.096	-.641	6.6	-2.48	-.006
VZ4	0 kts.	.731	-.439	+.32	.66	-.82	-.137
Longitudinal	26.5 kts.	2.16	.4	+.086	.20		
	75.6 kts. short period	3.4	.374	-.127	3.4		
	long period	.316	.346	-.11	.30		
VZ4	0 kts.	.669	-.347	+.30	.63	-.65	-.90
Lateral/Directional	75 kts.	1.59	.421	-.67	1.4		
H19 (helo)	0 kts.	.43	-.250	+.10	.42	-.69	-.87
	115 kts.	.38	-.043	+.016	.40	-.9	-1.05
Harrier	0 kts.	.31	-.48	+.148	.27	-.33	-.02
Longitudinal	60 kts.	.32	-.91	+.30	.13	-.073	-1.0
	Harrier	.52	-.50	+.26	.45	-.015	-.58
Lateral/Directional	60 kts.	1.2	-.28	+.336	1.15	-.068	-1.26
	120 kts.	1.8	-.15	+.27	1.78	-.056	-1.73

Table 3-2 Typical aircraft pole locations where the characteristic equation has the form

$$(s + 1/T_1)(s + 1/T_2)(s^2 + 2\zeta\omega_n s + \omega_n^2) = 0$$

Source: References [4 & 6]

TYPICAL AIRCRAFT POLES

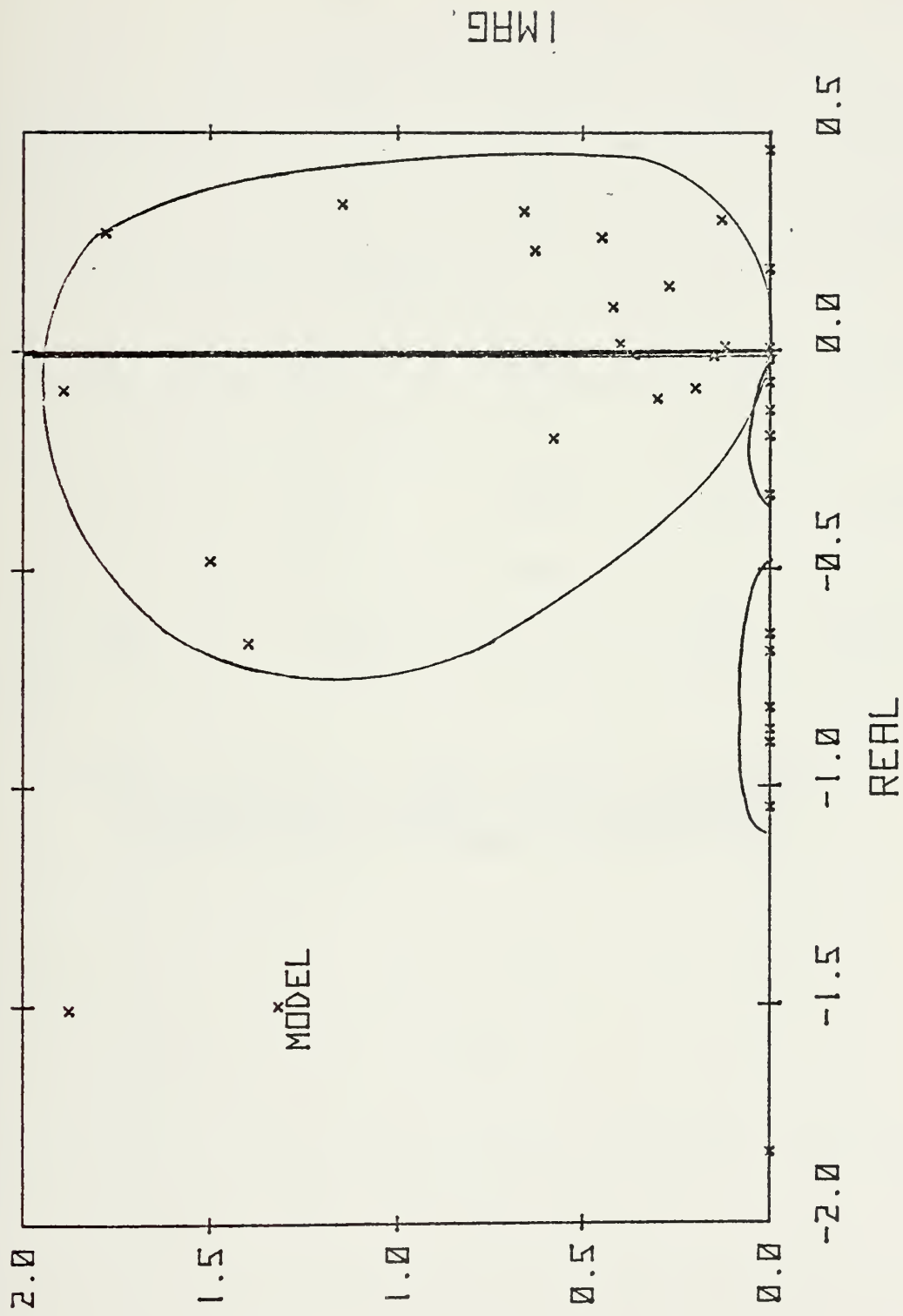


Figure 3-1 Typical aircraft pole locations.

<u>Mode #</u>	<u>Real</u>	<u>Im.</u>	<u>b</u>	<u>c</u>
1	-.6	3.	1.2	8.64
2	-.15	2.15	0.3	6.23
3	-.3	1.0	0.6	0.91
4	-0.1	0.3	0.2	0.08
5	-0.2/0.		0.2	0.0
6	0.3	1.5	-0.6	2.16
7	0.3	0.0	-0.6	0.0
8	0.1	0.14	-0.2	0.03
9	0.0	0.0	0.0	0.0
10	-1.0/ 0.6		1.6	0.6

Table 3-3 Aircraft modes used in simulations.
The modes were choosen to be typical of
VSTOL aircraft as seen in figure 3-1.

B. FREQUENCY RESPONSE AND BODE ANALYSIS

The object of Bode Analysis is to examine the frequency response characteristics of the SRFIMF controller. It will be necessary to develop the transfer function of the position controller shown in figure 2-4. The plant transfer function is given in general as

$$G(s) = \frac{X(s)}{W(s)} = \frac{CPG}{s^2 + bs + C}$$

As in earlier sections the control actuator transfer function, $H(s)$, is assumed to be of the form

$$H(s) = \frac{1}{(\tau s + 1)} \quad 3-5$$

The transfer function of the plant is given by $G(s)$, the output position, defined as $X(s)$ and the commanded input is $X_c(s)$. The compensator shown in figure 2-4, and described in section 2-3 is

$$A(s) = \frac{1}{(\tau s + 1)} \quad 3-6$$

From figure 2-4 we can write at point 1, the equation

$$V(s) = A(s)W(s) - s^2X(s)$$

where $s^2X(s)$ is now the acceleration feedback. We write the control quantity, $W(s)$, from figure 2-4 as

$$W(s) = U(s) - K_x sX(s) - K_x [-X(s) - X_c(s)] \quad 3-7$$

and also note

$$X(s) = K \cdot G(s) \cdot H(s) \cdot W(s) \quad 3-8$$

Combining and rearranging the above expressions we have that

$$X_c(s) K_x = \left(\frac{(1 - A(s))}{K} \cdot \frac{1}{G(s)H(s)} + s^2 + K_x s + K_x \right) \cdot X(s)$$

and further rearrangement leads to the transfer function for the input-output relation

$$\frac{X(s)}{X_c(s)} = \frac{K_x}{\left(\left[\frac{1-A(s)}{K} \right] \cdot \frac{1}{G(s)H(s)} \right) + s^2 + K_x s + K_x} \quad 3-9$$

It will be convenient to separate the constant plant gain, CPG, from the plant transfer function. The remaining transfer function, defined as $G'(s)$, has a unity constant gain. Stated another way

$$G(s) = \text{CPG} \cdot G'(s) \quad 3-10$$

The parameter KRL is thus defined as

$$\text{KRL} = K \cdot \text{CPG} / \tau$$

Substituting for $A(s)$, $H(s)$, and KRL and, rearranging 3-9 we are left with

$$\frac{X(s)}{X_c(s)} = \frac{\text{KRL} \cdot K_x}{s \left(\frac{1}{G'(s)} \right) + \text{KRL} (s^2 + K_x s + K_x)} \quad 3-12$$

Equation 3-12 shows the effect of the SRFIMF gain parameter, KRL. As KRL increases, the model term $(s^2 + K_x s + K_x)$,

becomes more dominant in the closed loop transfer function. Using equation 3-12, we can examine the frequency response of the controller.

Assuming the plant transfer function to be a second order system given by $G(s)$, equation 3-2, equation 3-12 can be rewritten as

$$\frac{X(s)}{X_c(s)} = \frac{KRL \cdot K_x}{s^3 + (KRL + b)s^2 + (KRL K_x + c)s + K_x \cdot KRL} \quad 3-13$$

The dominant effect of KRL in equation 3-13 is again seen in the coefficients of the s and s^2 terms. From table 3-2 we see that a likely range in the values of b and c are $-0.6 \leq b \leq 1.6$ and $0.0 \leq c \leq 8.64$. If KRL is of the order of 25 and b and c are in the range of 2 and 8 respectively, then KRL will dominate the terms of equation 3-13 which contain b and c . Equation 3-13 can be simplified by neglecting b and c with resulting transfer function for the closed loop system written as

$$\frac{X(s)}{X_c(s)} = \frac{KRL \cdot K_x}{s^3 + KRL(s^2 + KRL K_x s + K_x)} \quad 3-14$$

From this later representation it is clear that the plant dynamics which were determined by the coefficients b and c no longer play a role in the frequency response analysis.

Equation 3-14 expressed in Bode form becomes

$$\frac{X(s)}{X_c(s)} = \frac{KRL \cdot K_x}{(i\omega)^3 + KRL(i\omega)^2 + KRL K_x(i\omega) + KRL K_x} \quad 3-15$$

Equation 3-15 was plotted for frequencies from .01 to 100 and for KRL values of 1, 10, 25, 50 and 100. Figures 3-2 to 3-6 are the plots of the frequency response of the closed loop system. It can be seen that the frequency response of the system is that of a low pass filter with a break frequency of around 3.0 and a 40 db/Dec roll off. It is also seen that the response is very nearly in phase with the input for frequencies lower than 3.0. The results of the frequency response analysis show that the controller possesses good frequency response characteristics from the input to the output in that it has a flat response for all input frequencies of interest and little, if any phase shift. It has also been shown by Merrick [2] that the controller attenuates plant disturbances in the form of applied accelerations. The question of control disturbances will be examined from a different point of view in section V. We shall now consider the requirements for the gain, KRL, by root locus analysis.

C. ROOT LOCUS ANALYSIS

The intent of the root locus analysis is to determine the magnitude of the SRFIMF controller gain parameter, KRL, necessary for acceptable model following. Plots of the root locus of the oscillatory pole will show that the desired closed loop pole location is approached asymptotically as KRL is increased. Acceptable performance is determined by the specific application for which the SRFIMF controller is used. We begin by examining the equations for the closed loop system developed in the preceeding section.

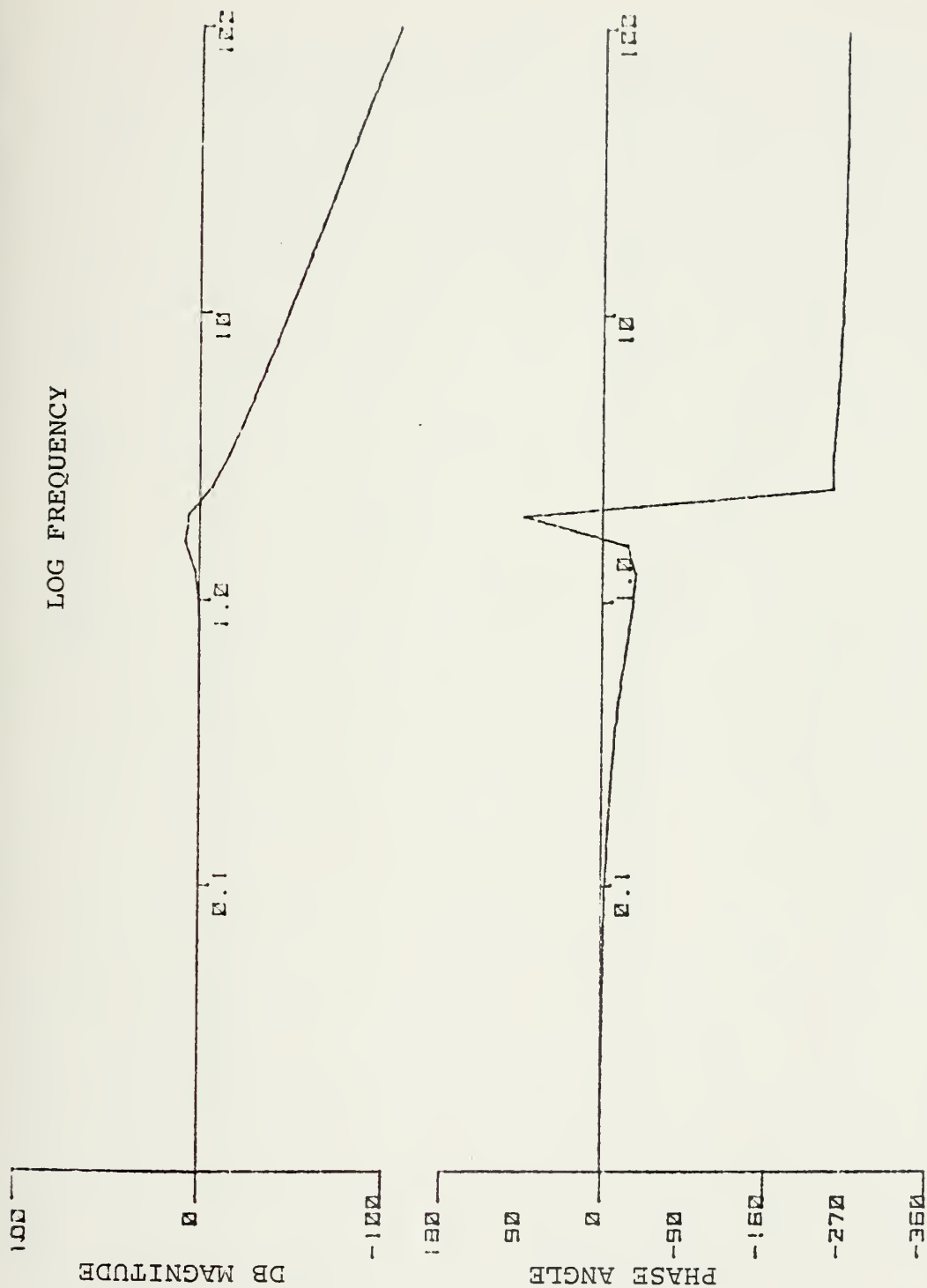


Figure 3-2 Frequency response of SRFIMF position controller, $KRL = 1$.

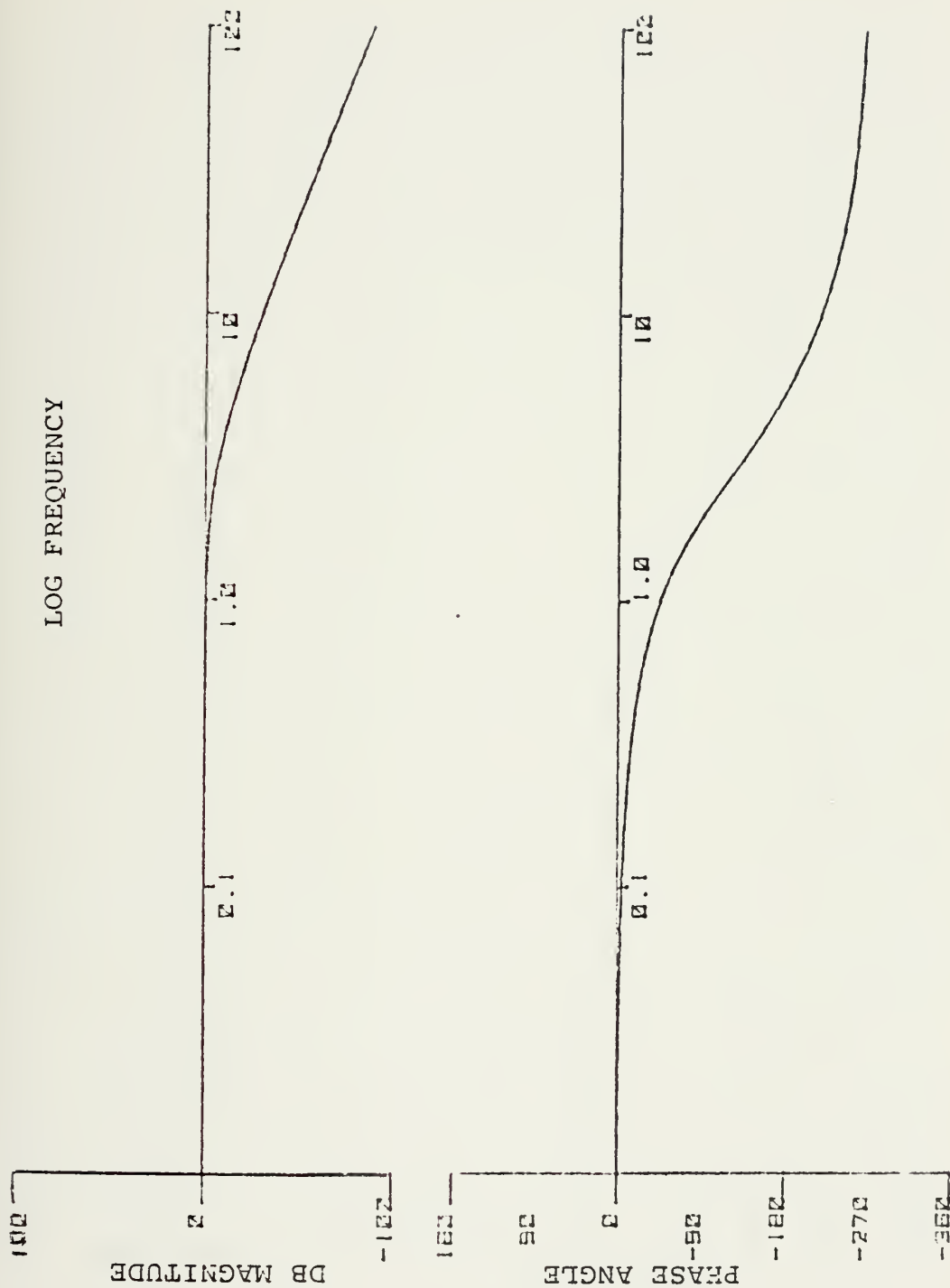


Figure 3-3 Frequency response of SRFIMF position controller, $KRL = 10$.

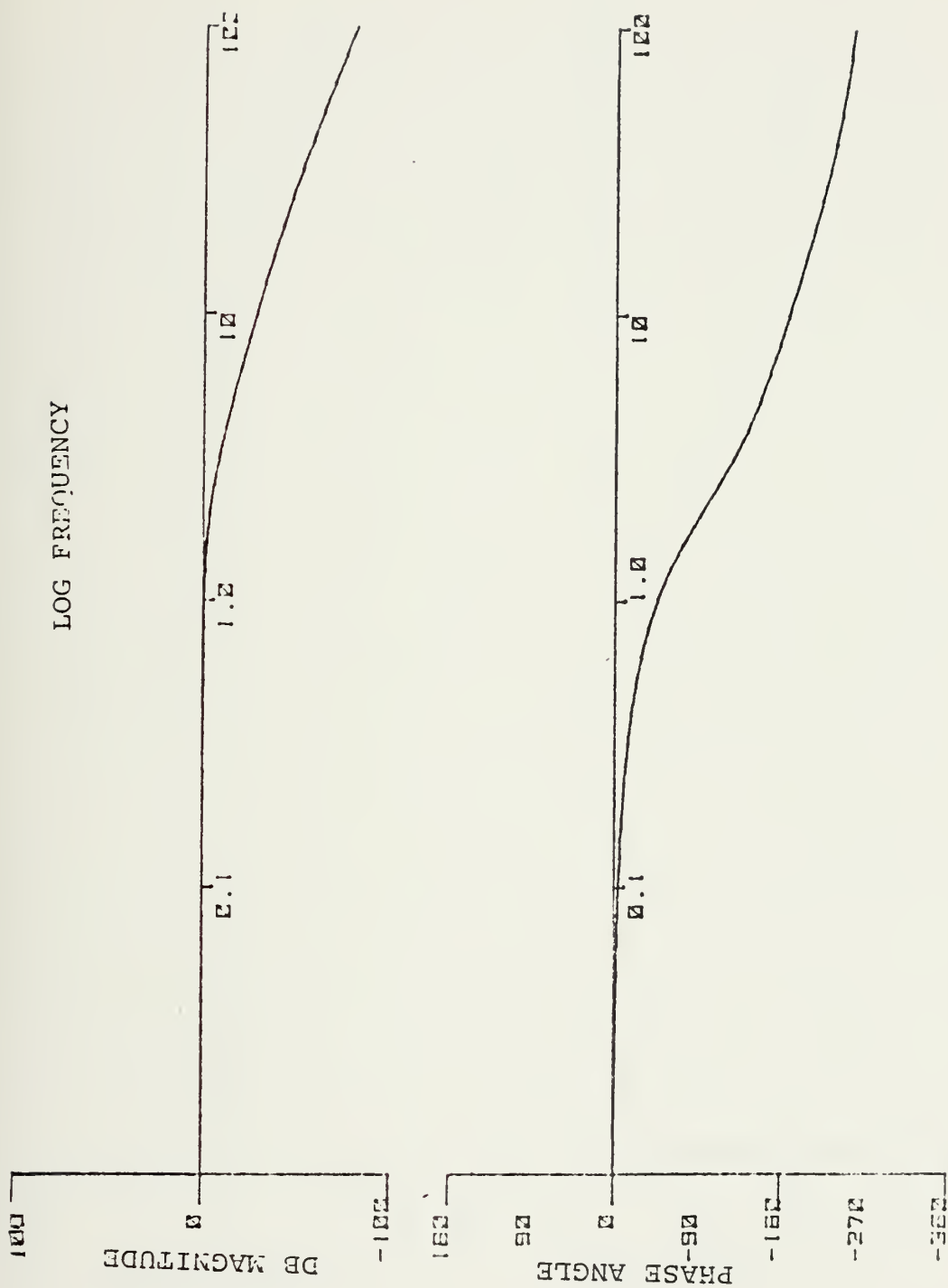


Figure 3-4 Frequency response of the SRFIMF position controller, KRL = 25.

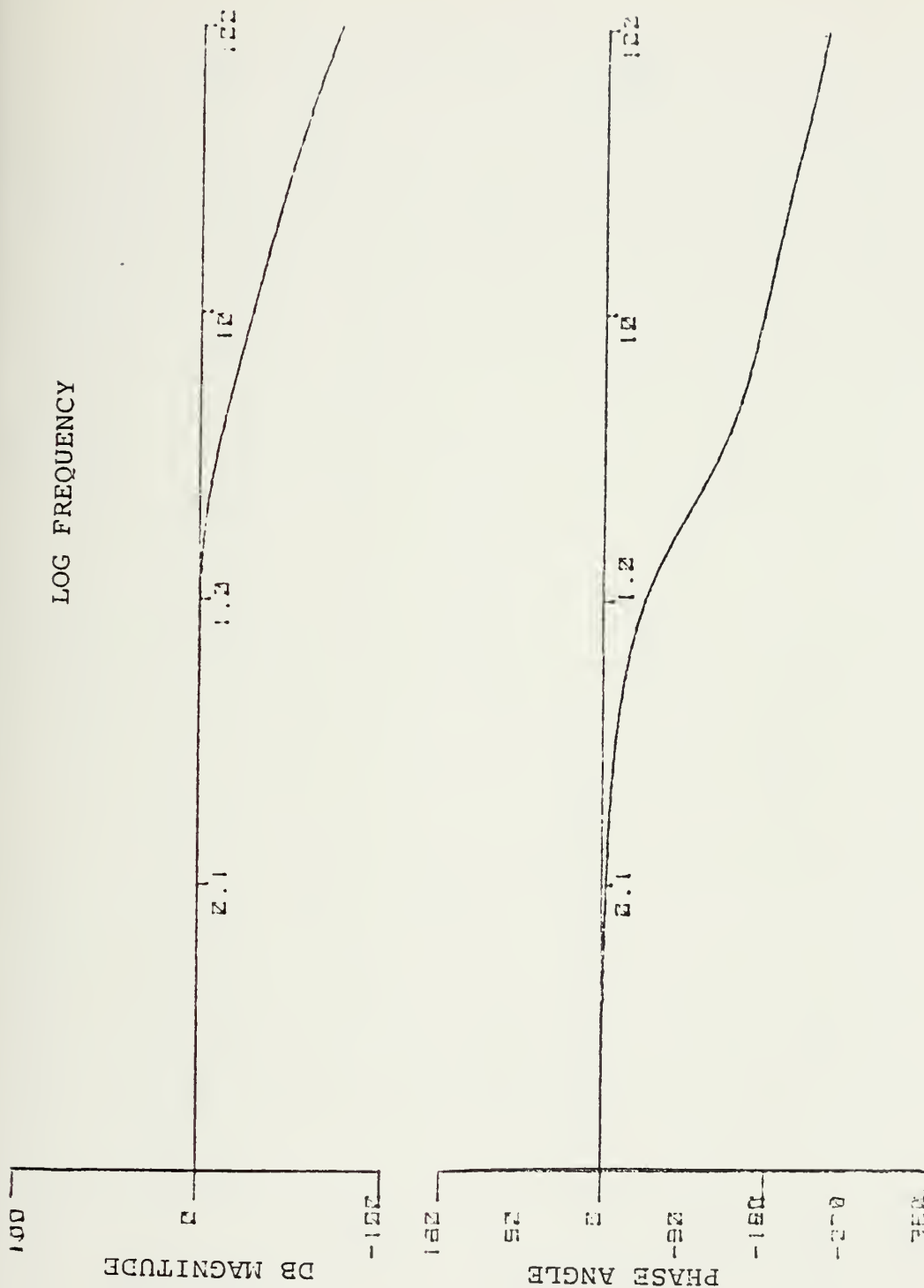


Figure 3-5 Frequency response of SRFIM position controller, KRL = 50.

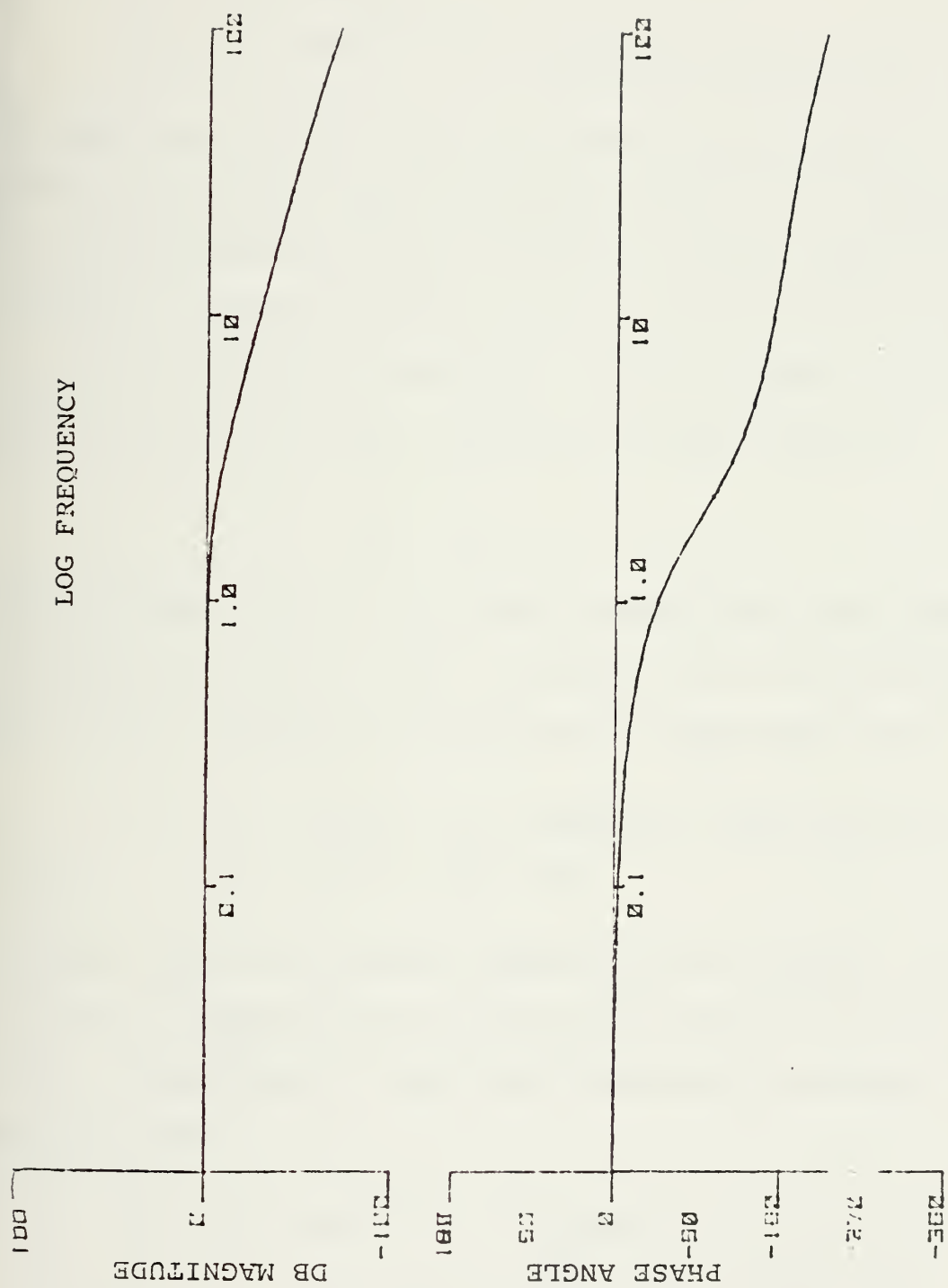


Figure 3-6 Frequency response of SRIMF position controller, KRL = 100.

The characteristic equation for the system can be obtained by setting the denominator of equation 3-13 to zero. The resulting equation is

$$s^3 + (b + KRL)s^2 + (c + K_{\dot{x}} KRL)s + KRL \cdot K_x = 0 \quad 3-16$$

At least one root of 3-16 must be real and the factor corresponding to the real root is defined as $(s + f)$. Assuming that the system described by the transfer function, equation 3-13, represents a model following system, then the second factor of 3-16 must be given by the model. In other words, assuming perfect model following, equation 3-16 must factor as

$$(s + f)(s^2 + K_{\dot{x}}s + K_x) = 0 \quad 3-17$$

As KRL becomes large, the SRFIMF closed loop system response does approach perfect model following, and it can be stated that as KRL increases the condition is approached where

$$\frac{s^3 + (b + KRL)s^2 + (c + K_{\dot{x}}KRL)s + KRL \cdot K_x}{(s + f)(s^2 + K_{\dot{x}}s + K_x)} \longrightarrow \quad 3-18$$

In other words, the dynamic behavior of the system's oscillatory mode is approximately given by the model parameters $K_{\dot{x}}$ and K_x . Expanding the right hand side of 3-18 we have for increasing KRL

$$\begin{aligned} s^3 + (b + KRL)s^2 + (c + K_{\dot{x}}KRL)s + KRL \cdot K_x &\longrightarrow \\ s^3 + (K_{\dot{x}} + f)s^2 + (K_x + K_{\dot{x}}f)s + f \cdot K_x &\quad 3-19 \end{aligned}$$

Comparing coefficients reveals that for increasing KRL

$$b + KRL \rightarrow K_x + f \quad 3-20a$$

$$c + K_x KRL \rightarrow K_x f + K_x \quad 3-20b$$

$$KRL \rightarrow f \quad 3-20c$$

The relationships of 3-20 are not equalities, but they indicate that while KRL is increasing, the difference between KRL and f remains finite.

Therefore, it can be said that one real pole is on the negative real axis and its location is approximated by the value of KRL since f is approaching KRL as KRL becomes large relative to b or c . To examine the behavior of the oscillatory pole as KRL is increased, it will be necessary to rearrange equation 3-9 into root locus form. Setting the denominator of 3-9 equal to zero yields

$$\left[\frac{1 - A(s)}{K} \right] \cdot \left[\frac{1}{H(s) G(s)} \right] + s^2 + K_x s + K_x = 0 \quad 3-21$$

Substituting for $A(s)$, $H(s)$ and $G(s)$ and rearranging, the general relation for the root locus is

$$0 = 1 + \frac{KRL (s^2 + K_x s + K_x)}{s} G'(s) \quad 3-22$$

where $G'(s)$ is an arbitrary plant transfer function divided by its constant gain, CPG, as was shown by equation 3-10.

Equation 3-21 will now be used to determine the root locus for the position controller where $G'(s)$ is given by one of four of the modes assumed to be typical of VSTOL aircraft as listed in table 3-4. The cases considered are

	Mode # from Table 3-2	<u>b</u>	<u>c</u>
Case 1	6	-.6	2.16
Case 2	3	.6	.91
Case 3	9	0	0
Case 4	10	1.6	.6

Table 3-4 Plant Parameters for Root Locus Analysis

The root locus computer program developed by Melsa and Jones [7] was used to evaluate and plot the root locus given by equation 3-21. The gain constant, KRL, was varied from 0 to 100. The resulting root locus trajectory of the oscillatory poles for the four mode cases are shown in figures 3-7 to 3-10. From the figures it can be seen that in all cases the oscillatory pole approaches the desired value given by the model, in this case $-1.5, 1.32i$. Because of scaling, the real pole described earlier is not shown in the figures. It can also be seen that the pole location of the closed loop system is within 5 percent of the desired value for KRL of between 25 and 50. Although a value of KRL equal to 25 is normally sufficient, a KRL value of 50 will be used for the remainder of this work.

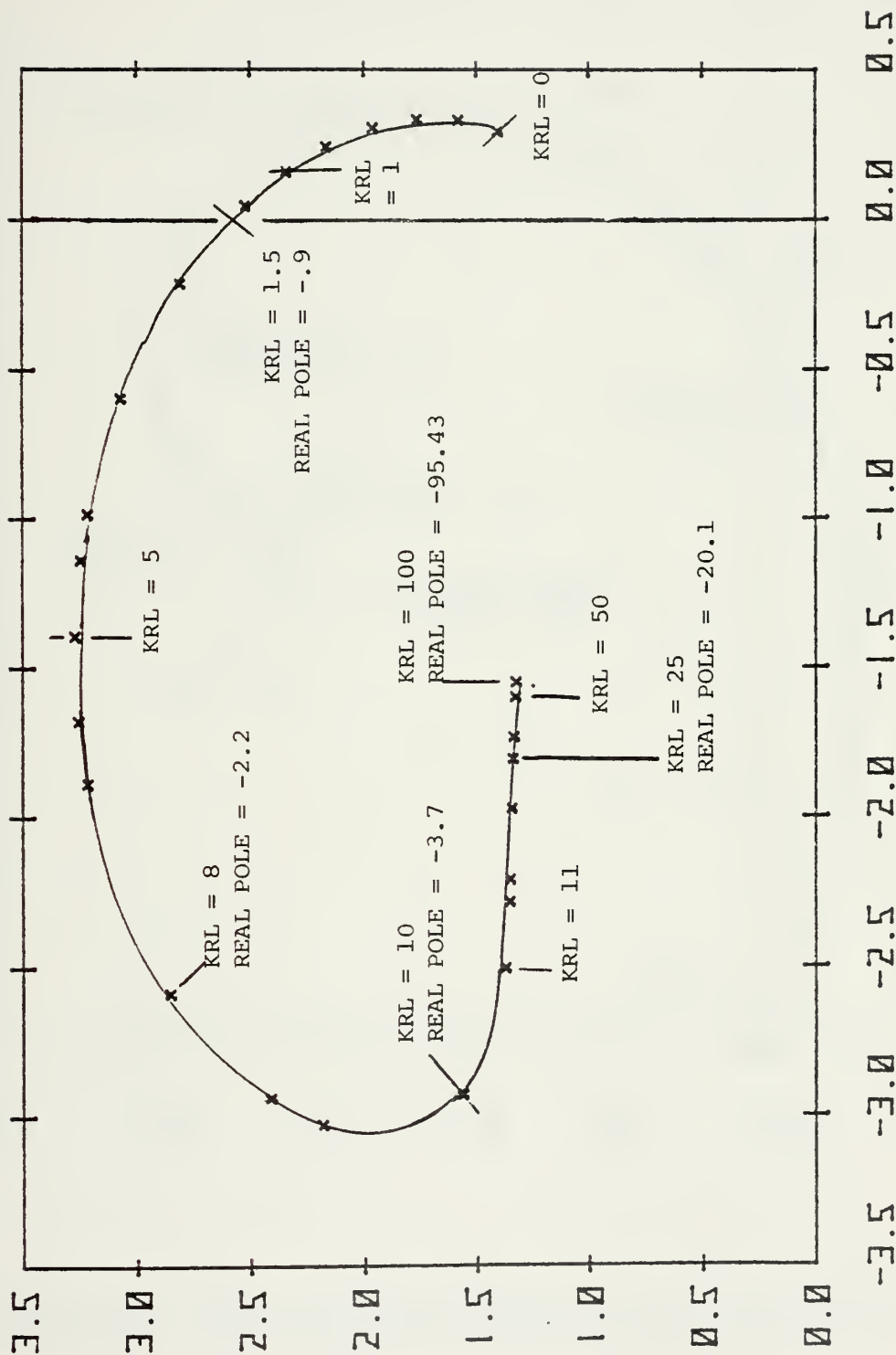


Figure 3-7 Root locus plot of oscillatory pole of a SRFIM position controller. The open loop plant has a natural frequency of 1.47 rad/sec and a damping ratio of -0.441.

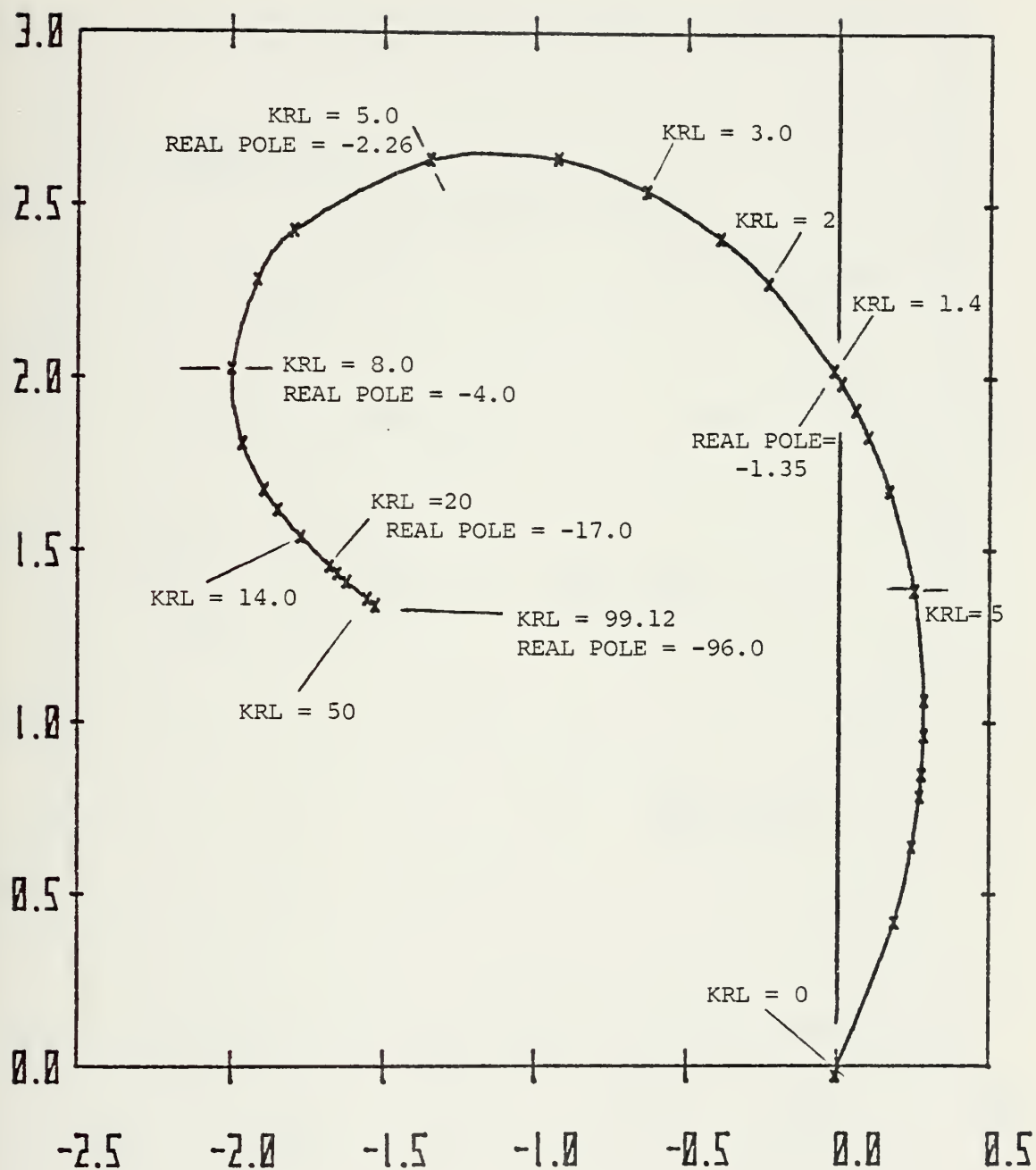


Figure 3-8 Root locus of the oscillatory pole of a SRFIMF position controller. The open loop plant has two poles at the origin.

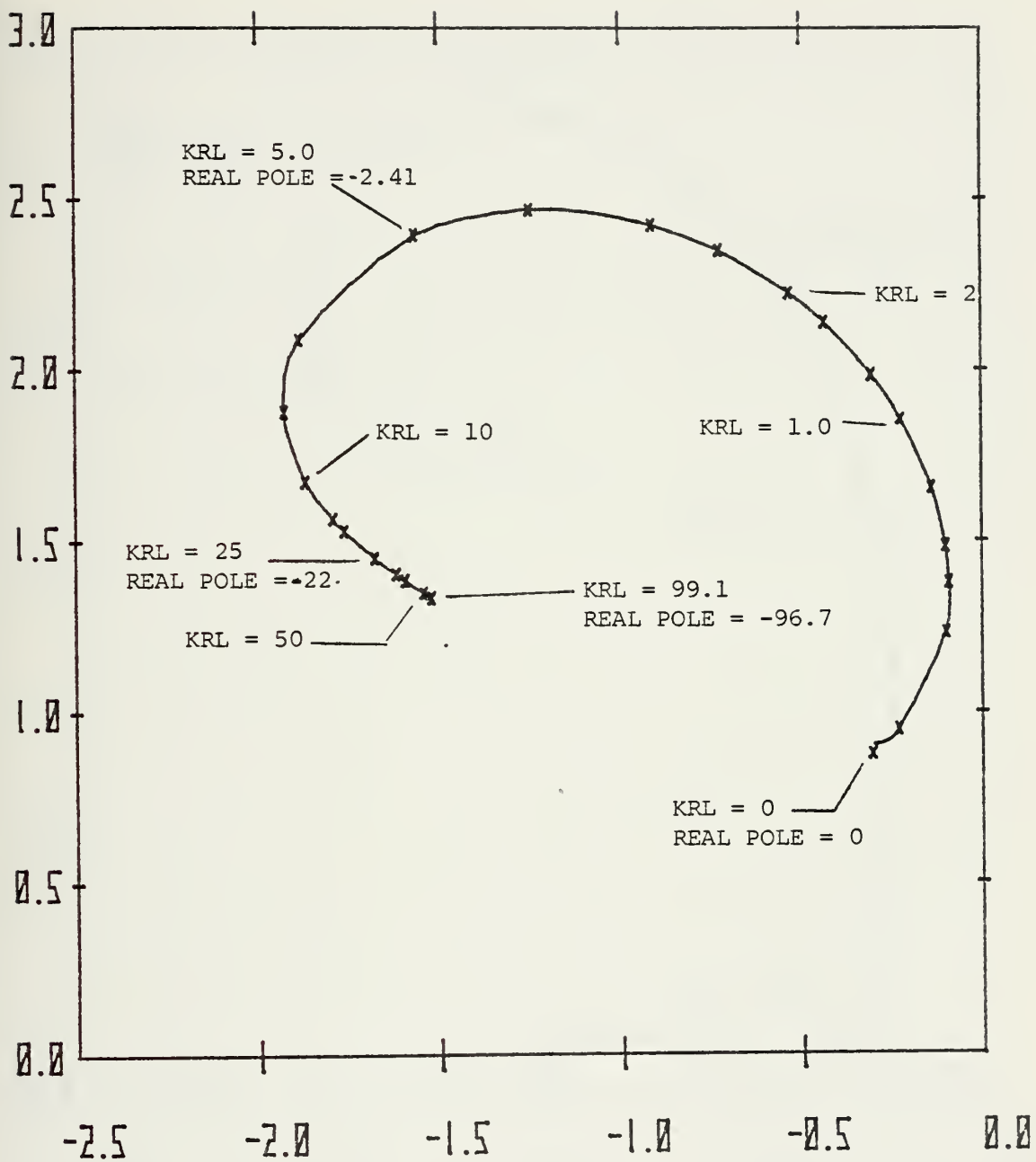


Figure 3-9 Root locus of the oscillatory pole of a SRFIMF controller. The open loop plant has a natural frequency of .95 rad/sec and damping ratio of 0.475.

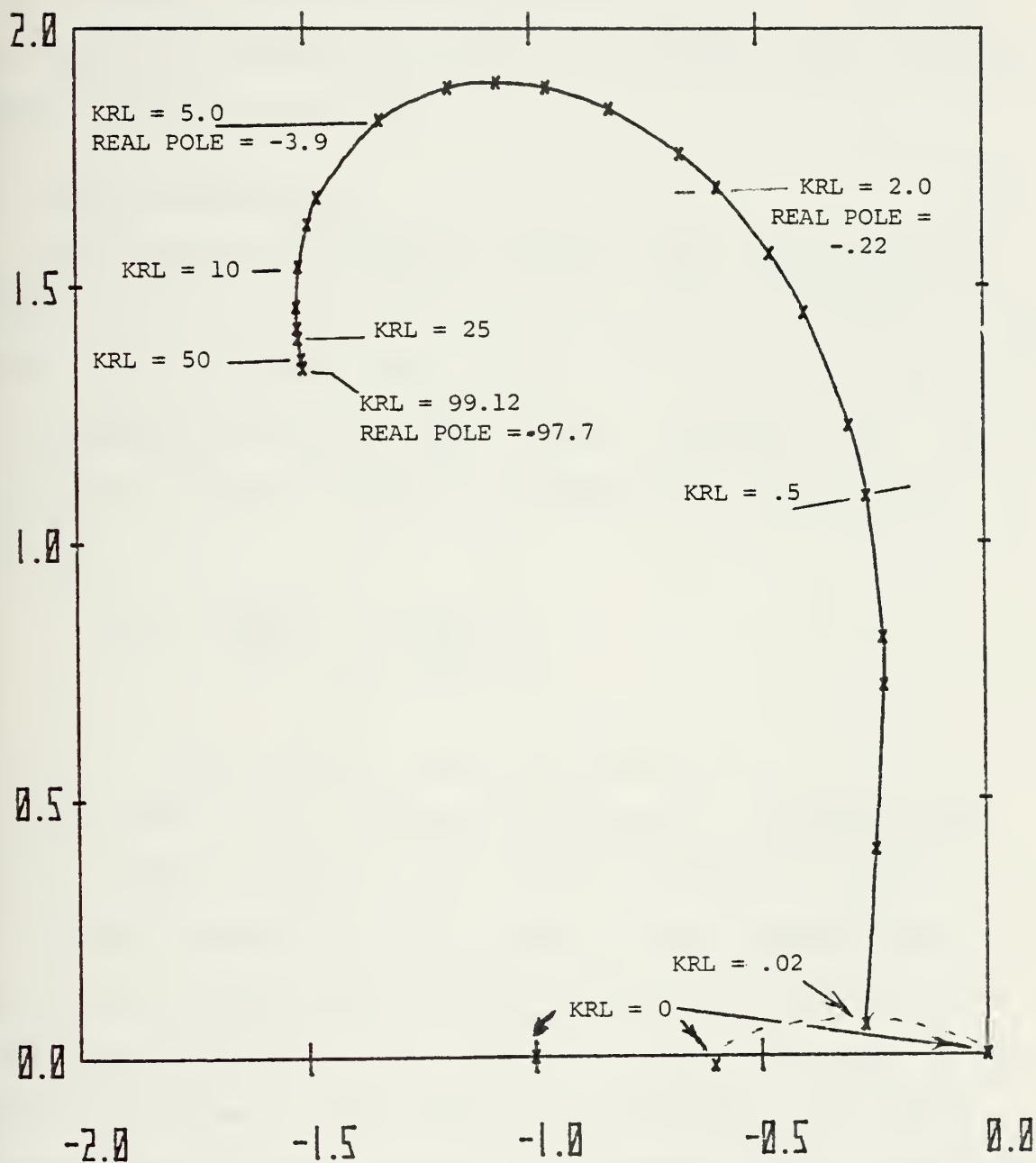


Figure 3-10 Root locus of the oscillatory pole of a SRFIMF position controller. The open loop plant has real poles at -1.0 and -0.6.

The root locus behavior of a more complex plant will be shown in section V where the SRFIMF controller will be applied to a transfer function of the Harrier aircraft. The system will next be simulated for each of the sample VSTOL aircraft modes listed in table 3-2.

D. SRFIMF SIMULATIONS

The simulated response of a plant under the control of SRFIMF position controller was done for all ten of the typical VSTOL aircraft modes listed in table 3-2. The time histories were generated using the CSMP program, reference [6]. The open loop plant for each of the ten systems was assumed to be of the form

$$G(s) = \frac{X(s)}{\delta(s)} = \frac{CPG}{s^2 + bs + c}$$

with $CPG = 1$ and b and c given in table 3-2.

The model was as assumed in section II, a second order with a natural frequency of 2 rad/sec and damping ratio, of 0.75. The constants K_x and $K_{\dot{x}}$ were 3 and 4 respectively as determined by equations 2-8 and 2-9. The simulation of the model response is shown in figure 3-9. The rise time of the modeled response is approximately 1.2 seconds. The model response has a slight overshoot (2.9 percent) with a peak time at 2.4 seconds. Settling to within 1 percent occurs immediately after the peak response. For the simulations, KRL was taken to be 50 and the actuator time constant, τ , was 0.10 seconds. The

input to the system and to the open loop plant was a unit step function, representing X_c , at $t = 0$. A sample listing of the CSMP source code is given in Appendix A.

Figures 3-11 to 3-21 show the time histories of the open and closed loop response of each of the ten simulated systems. It can be seen from the figures that the closed loop response of each system is indistinguishable from the model response. Figures 3-11 to 3-21 graphically show that the response of the closed loop system is approximated by the model response regardless of the plant being controlled. In addition, the self trimming feature of the controller is seen. In all cases the steady state value of the output of the closed loop system is the same as the input, X_c , namely 1.

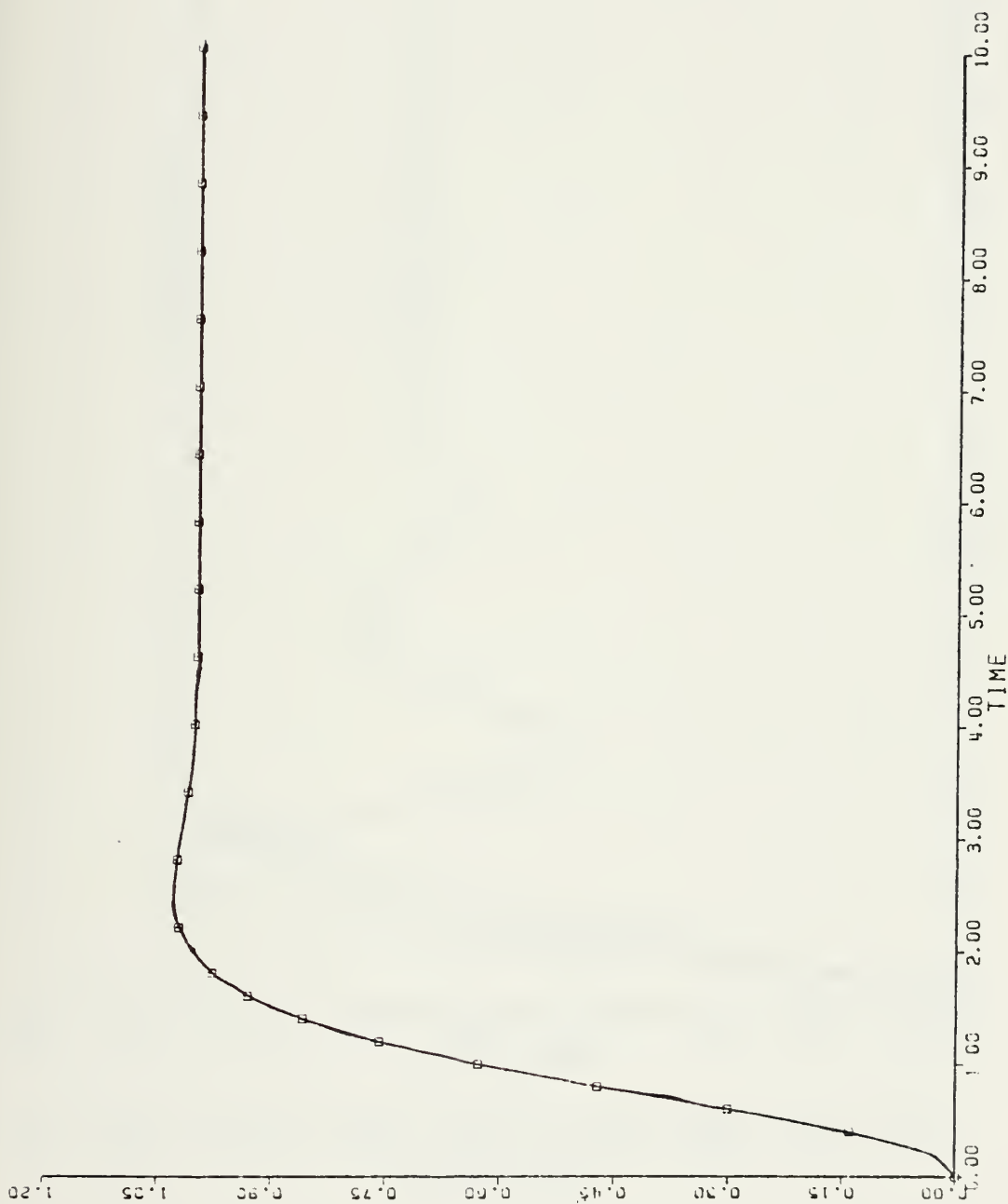


Figure 3-11 Perfect model response. $K_x = 4$, $K_{\dot{x}} = 3$, $\omega_n = 2$, $\zeta = 0.75$.

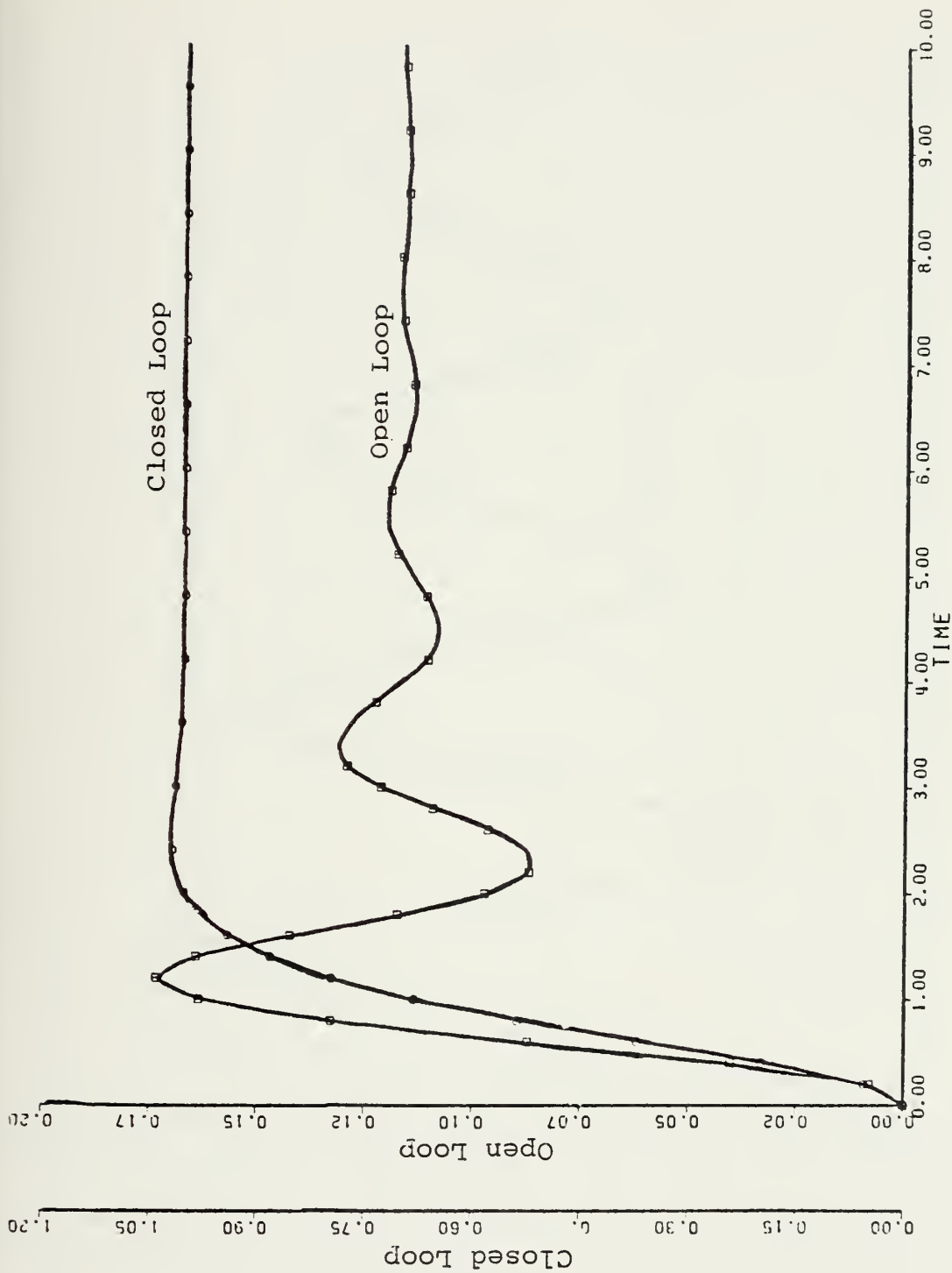


Figure 3-12 Simulation of SRFIMF position control for aircraft mode 1, table 3-3. The open loop plant has a natural frequency of 2.94 rad/sec and damping of .2.

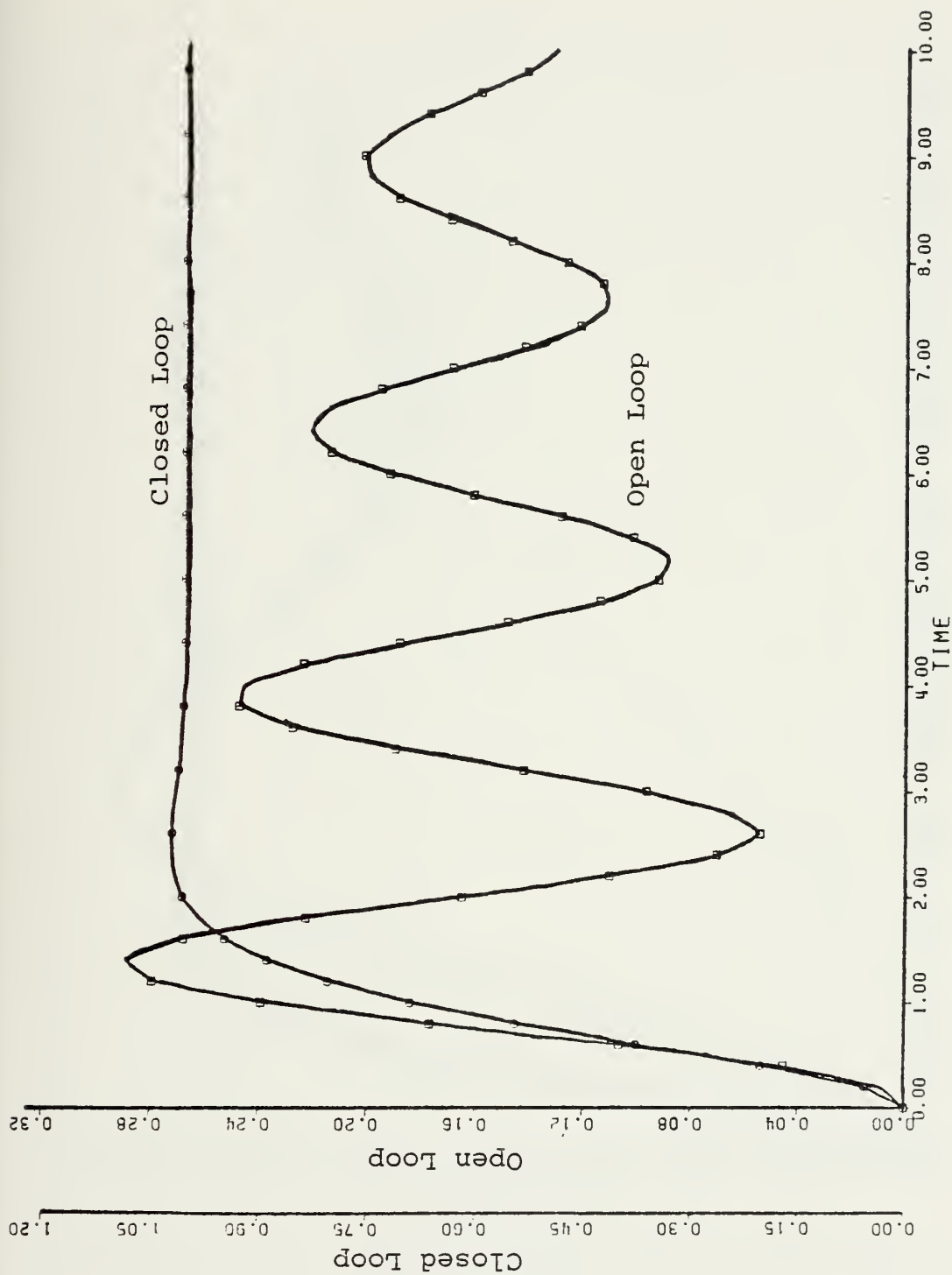


Figure 3-13 Simulation of SRFIMF position control for aircraft mode 2, table 3-3. The open loop plant has a natural frequency of 2.5 rad/sec and damping ratio of 0.06.

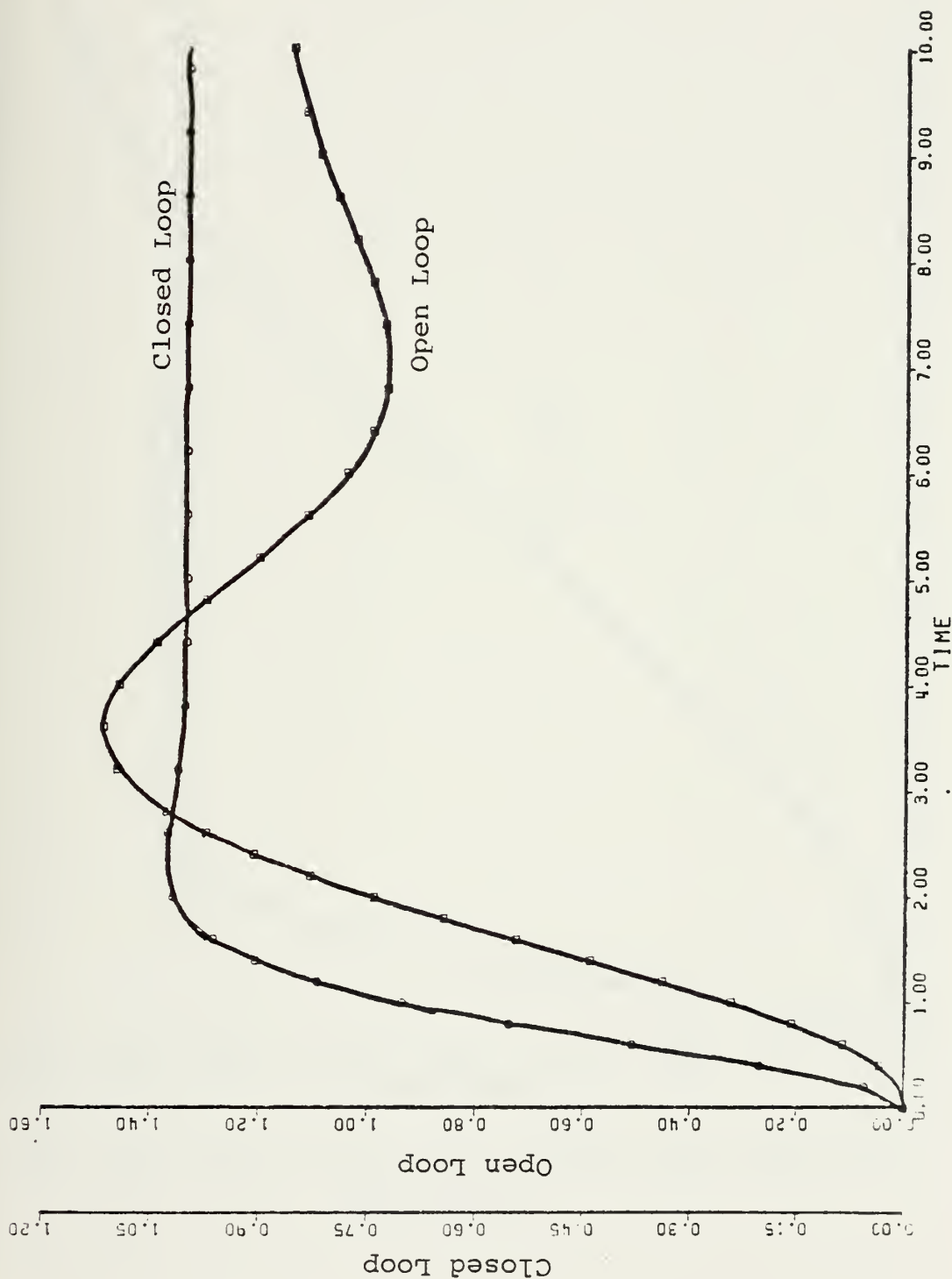


Figure 3-14 Simulation of SRFIMF position control for aircraft mode 3, table 3-3. The open loop plant has a natural frequency of 0.954 rad/sec and a damping ratio of 0.314.

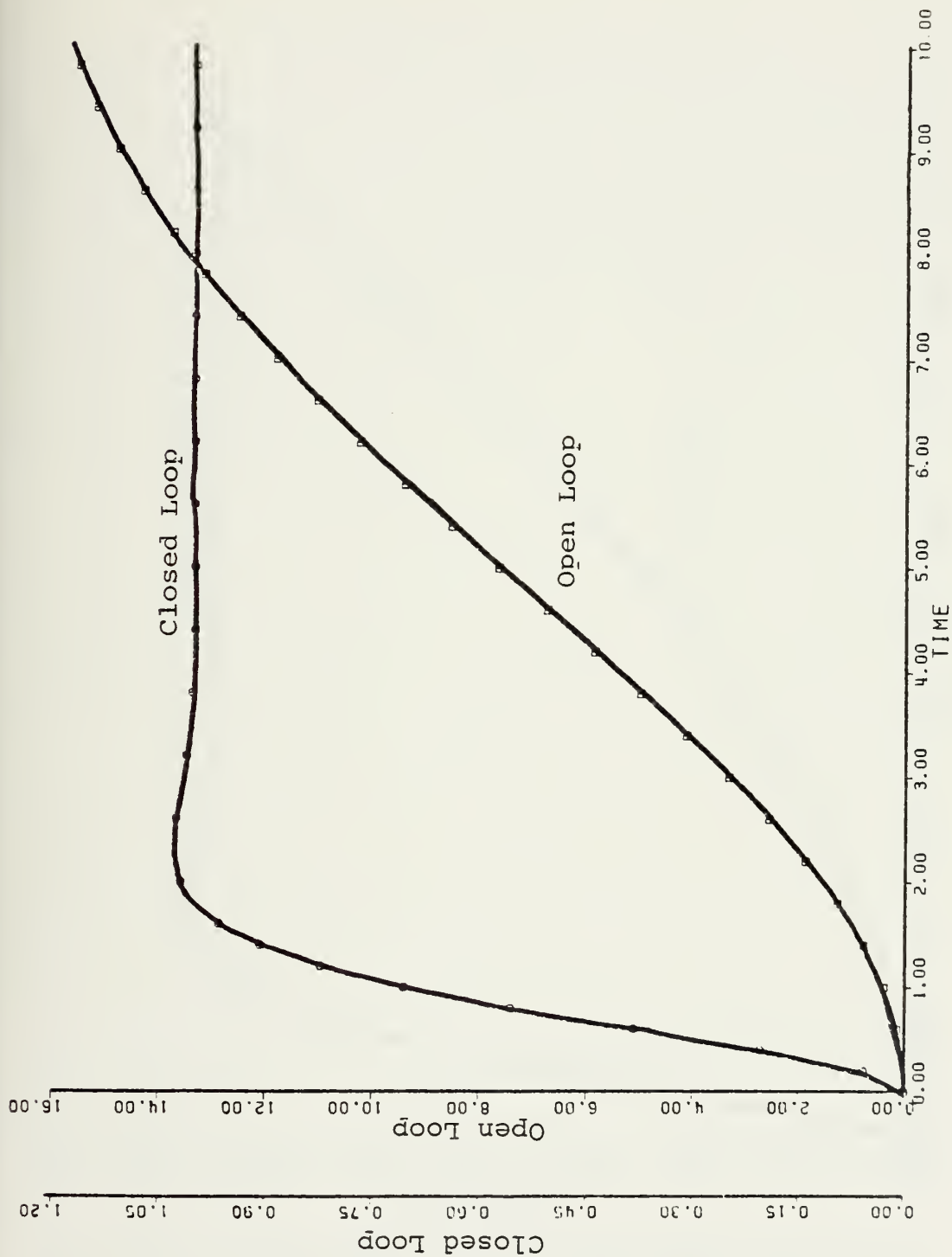


Figure 3-15 Simulation of SRFIMF position control for aircraft mode 4, table 3-3. The open loop plant has a natural frequency of 0.283 rad/sec and damping ratio of 0.353.

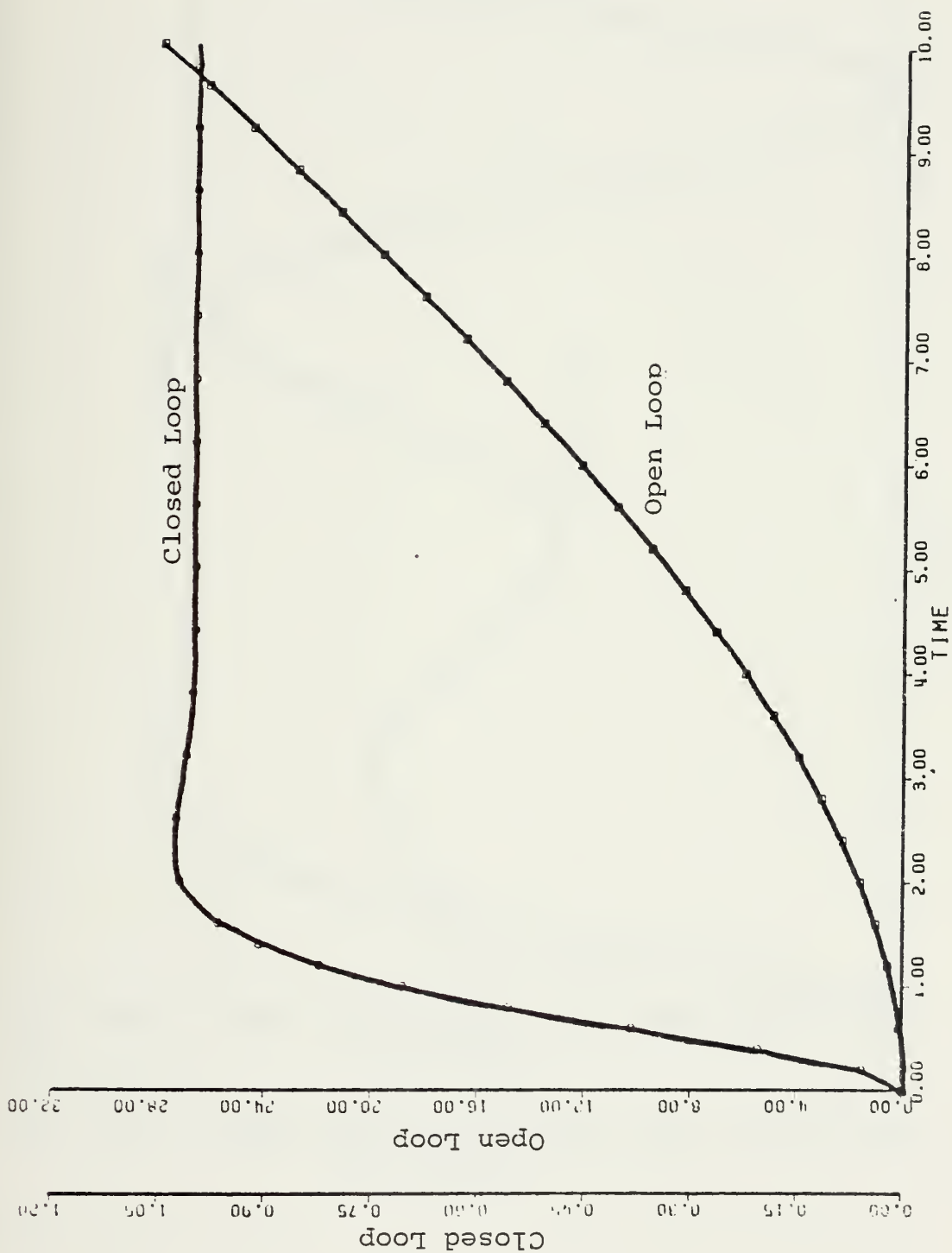


Figure 3-16 Simulation of SRFIMF position control for aircraft mode 5, table 3-3. The open loop plant has real poles at -0.2 and 0.

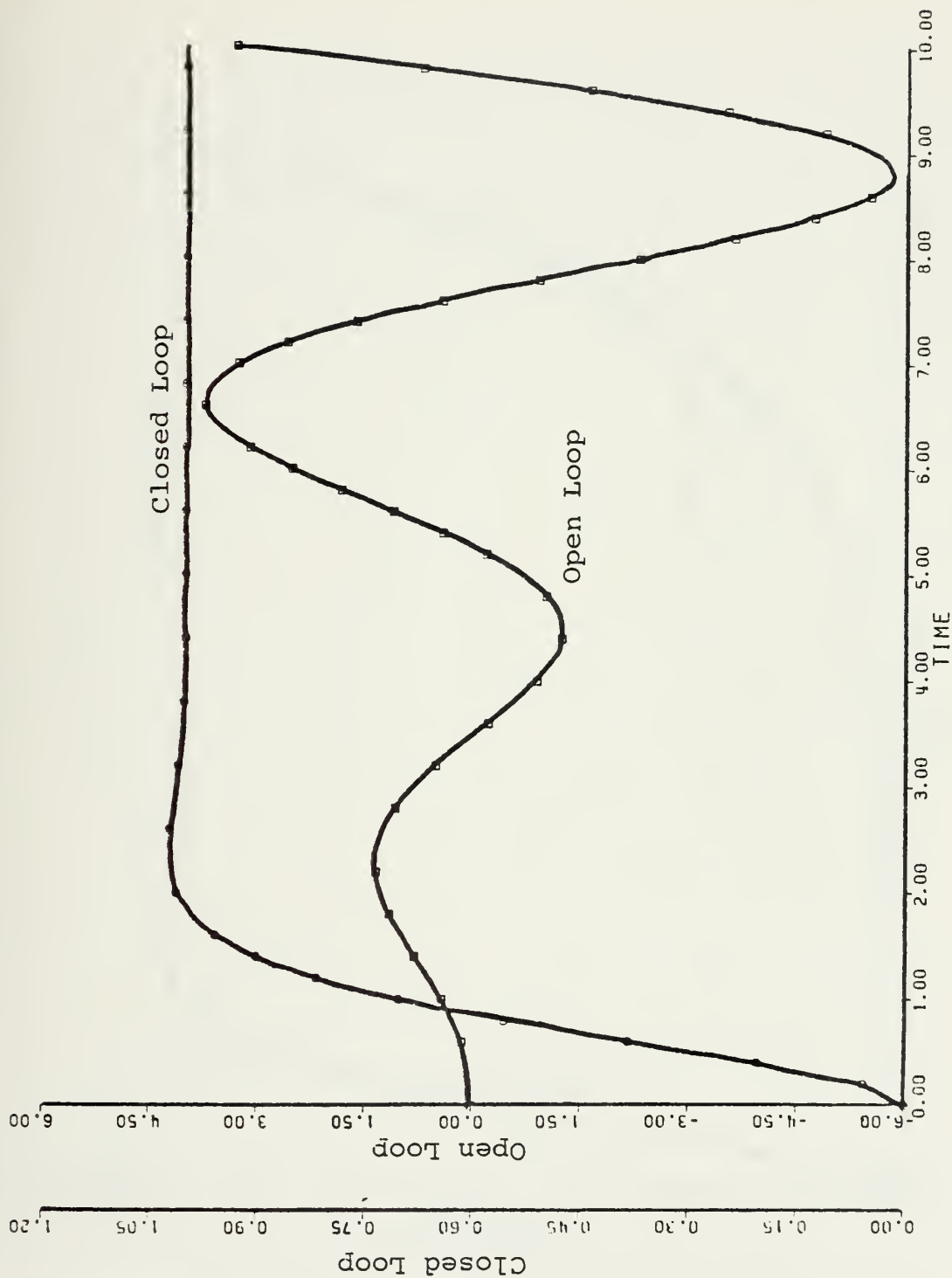


Figure 3-17 Simulation of SRFIMF position control for aircraft mode 6, table 3-3. The open loop plant has a natural frequency of 1.47 rad/sec and damping ratio of -.204.

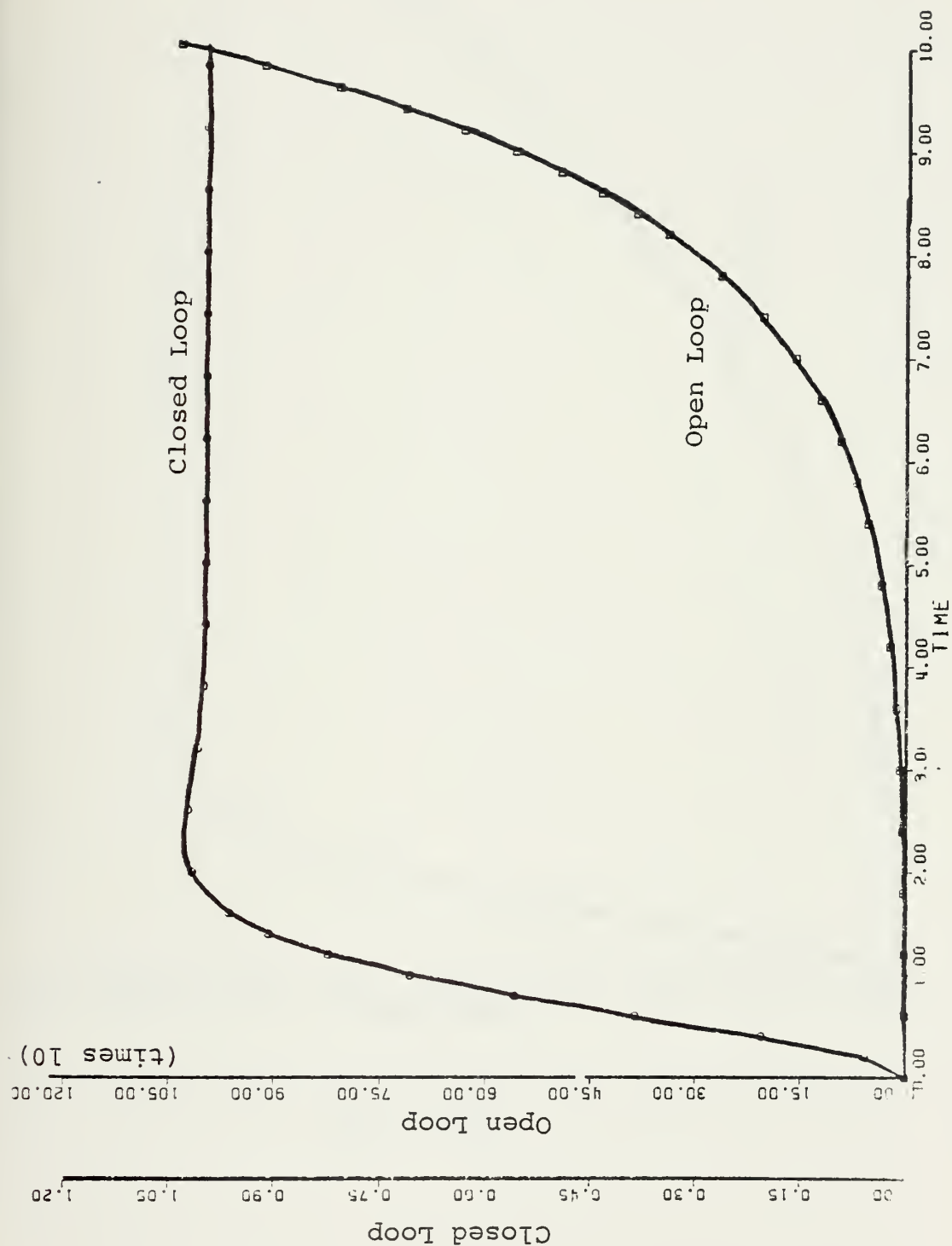


Figure 3-18 Simulation of SRFIMF position control for aircraft mode 7, table 3-3. The open loop plant has real poles at 0.30 and 0.

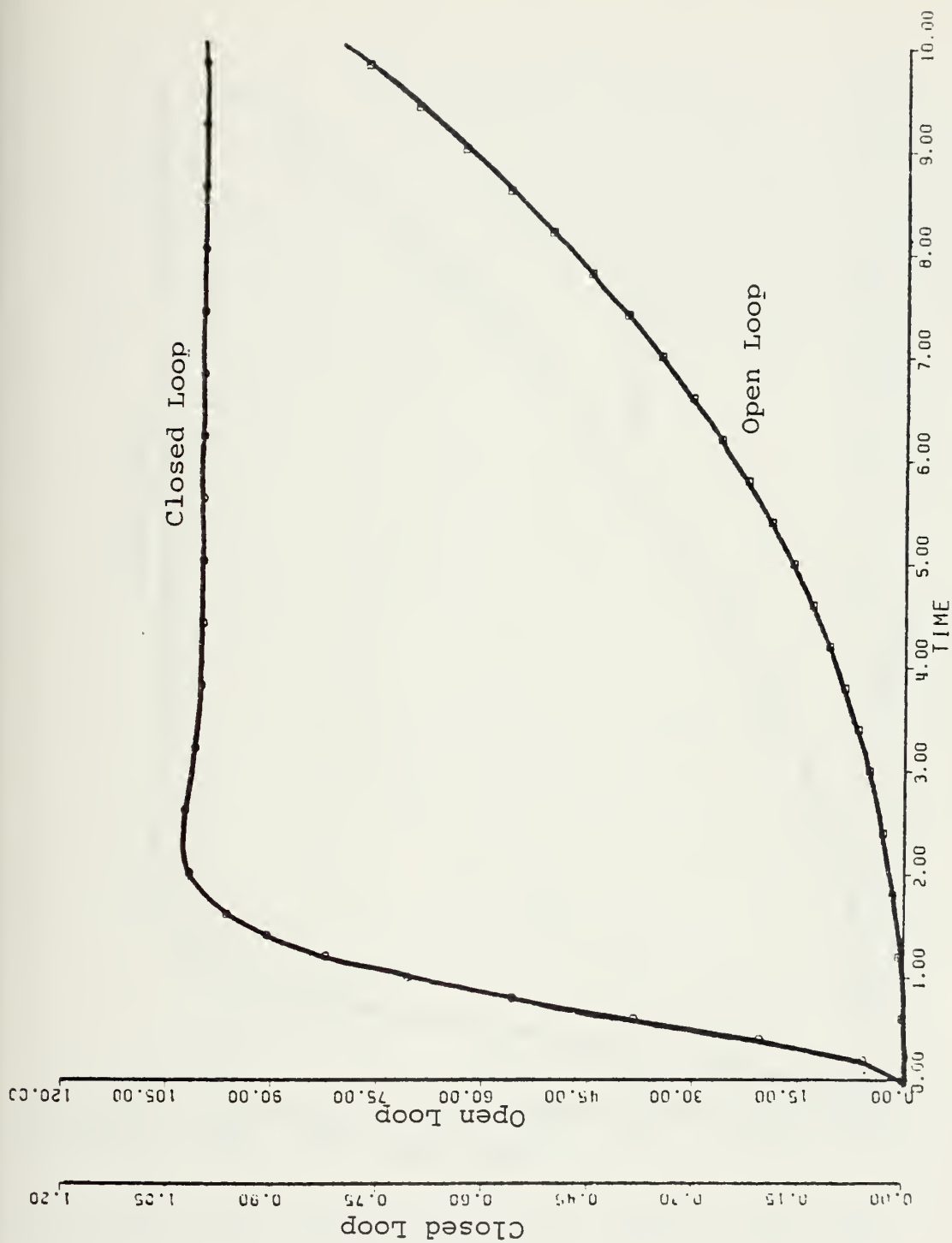


Figure 3-19 Simulation of SRFIMF position control for aircraft mode 8, table 3-3. The open loop plant has a natural frequency of 0.17 rad/sec and damping ratio of 0.590.

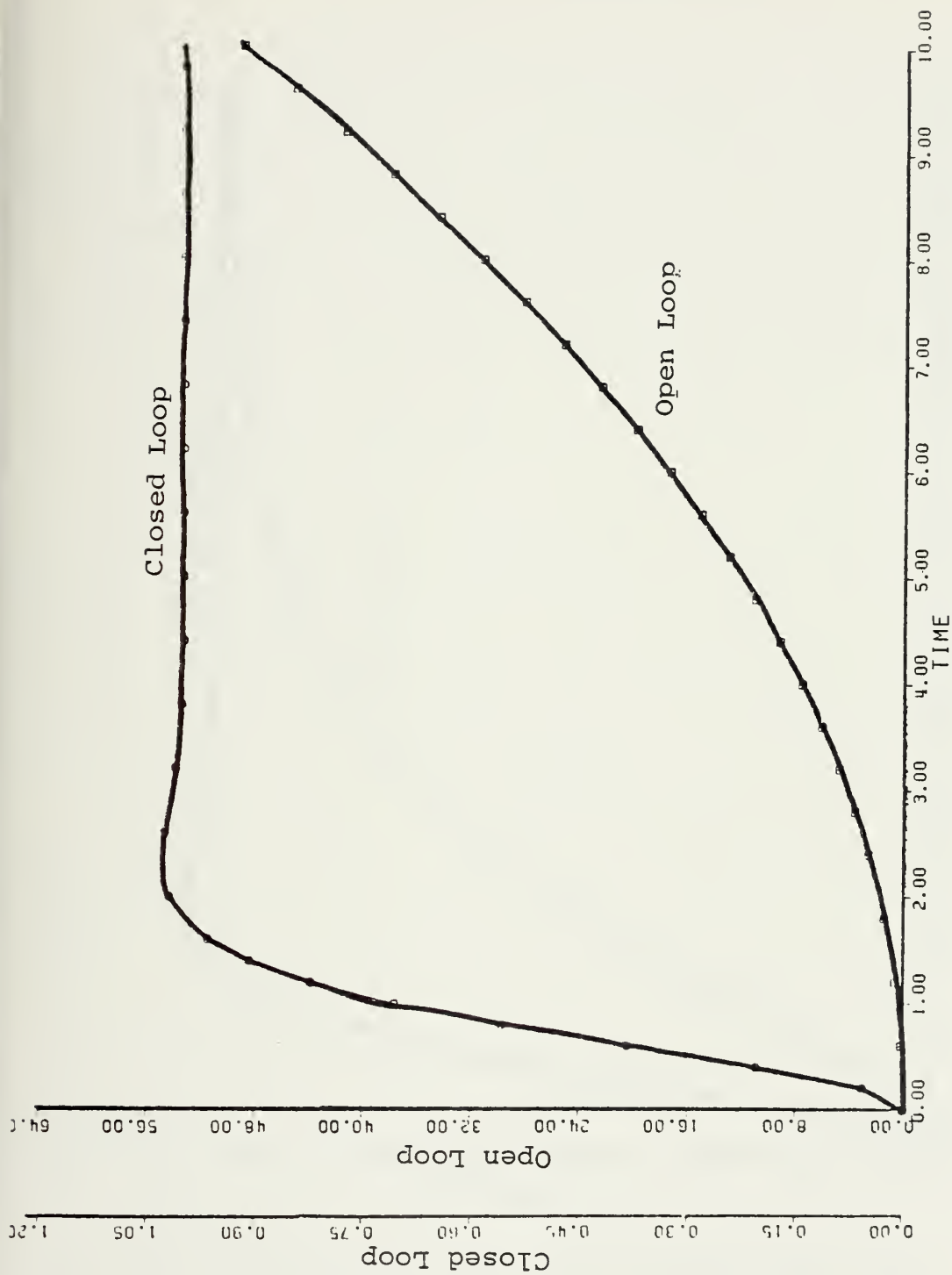


Figure 3-20 Simulation of SRFIM position control of aircraft mode 9, table 3-3. The open loop plant has two poles at the origin.

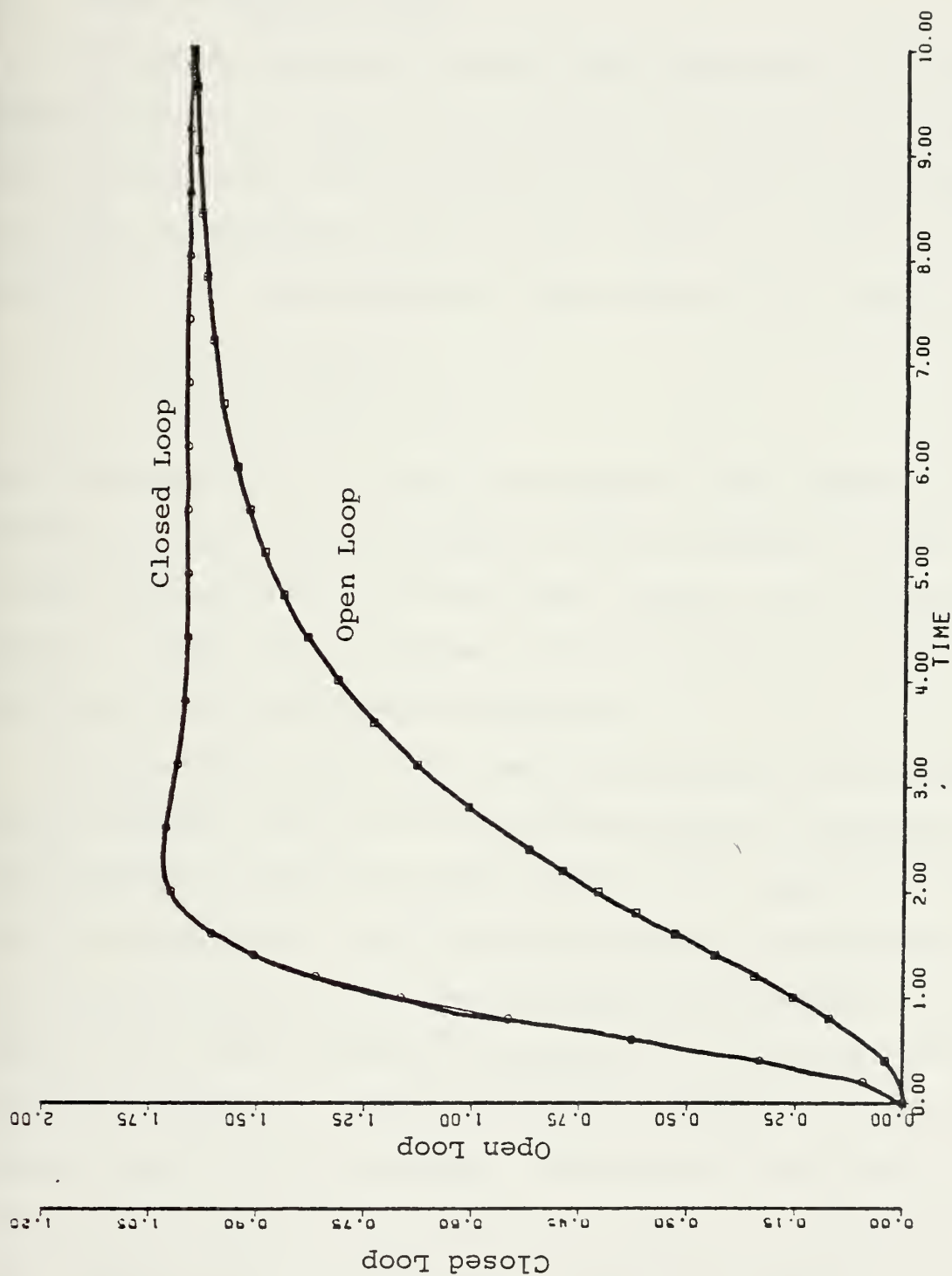


Figure 3-21 Simulation of SRFIMF position control of aircraft mode 10, table 3-3. The open loop plant has real poles at -1.0 and -0.6.

IV. SENSOR NOISE ANALYSIS

A. SRFIMF STOCHASTIC MODEL

The SRFIMF controller relies upon measurements to produce model following. We shall now examine the effect of measurement uncertainty on the operation of the closed loop system. In order to accomplish this we will consider a position controller with a representative second order plant given by

$$G(s) = \frac{CPG}{s^2 + bs + c} \quad 4-1$$

The position controller will be augmented with sensor noise sources and the observability and controllability of the closed loop system with these noise sources will be analyzed. Errors in the state variables will be determined by covariance analysis using the Lyapunov equation.

The measured quantities that are considered to be contaminated by sensor noise are the attitude position, attitude rate and attitude acceleration measurements. Two types of sensors will be considered. One is of high accuracy and typical of good quality inertial navigation system measurements. The second is of lower accuracy and might be considered typical of strapdown sensors. Sensor errors are assumed to be of two types, bias and high frequency. Bias errors are usually small relative to measured quantities and they are of constant value. Bias errors have little effect on the dynamic behavior of the control system and will not be considered in this study.

High frequency errors can be modeled in various ways. It is assumed that the sensor noise sources can be modeled by exponentially correlated noise. Exponentially correlated noise is obtained by passing Gaussian white noise through a first order shaping filter. A first order filter is represented by the differential equation

$$\dot{\xi} = -1/T_r \xi + W_t(t) \quad 4-2$$

where $W_t(t)$ is a scalar white, zero mean, Gaussian noise of constant strength, μ . μ is chosen so that the steady state value produced by the filter is the square of the sensor error standard deviation, σ^2 . Following Maybeck [9], the required value of μ as the input to the filter is given by

$$\mu = 2\sigma^2/T_r \quad 4-3$$

where T_r is the correlation time of the exponentially correlated noise. Figure 4-1 is a schematic representation of a typical shaping filter, in Laplace transform notation. $\xi(s)$ is resulting exponentially correlated noise.

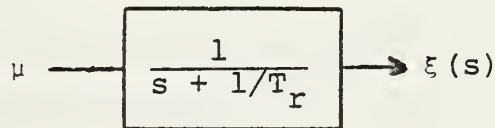


Figure 4-1 Exponentially correlated noise shaping filter

The standard deviation, σ , of the sensor error is a function of the sensors. The values of σ and T_r were obtained from a study by Analytical Mechanics Association (AMA), reference [10], in which an aircraft using a SRFIMF controller was studied. Table 4-1 is a list of the standard deviation estimates which were obtained from the AMA study. Also based upon the AMA study, we assume a value of T_r to be 10 seconds for both sensor models.

	<u>Strapdown</u>	<u>Inertial</u>
Attitude position, σ_p	1°	$0.1^\circ/$
Attitude rate, σ_v	$0.5^\circ/\text{sec}$	$0.5^\circ/\text{sec}$
Attitude acceleration, σ_a	$1^\circ/\text{sec}^2$	$0.1^\circ/\text{s}^2$

($T_r = 10$ seconds in all cases)

Table 4-1 Sensor error model parameters

The position controller shown in figure 2-4 is augmented with the sensor error sources and the resulting system is shown in figure 4-2.

To analyze the closed loop controller, we first obtain the state space representation of the plant given by equation 4-1. Taking position and velocity as the state variable of the plant we write

$$\text{Position} = X_1 \quad 4-4a$$

$$\text{Velocity} = \dot{X}_1 = X_2 \quad 4-4b$$

$$\text{Acceleration} = \dot{X}_2 = -cX_1 - bX_2 + \text{CPGX}_3 \quad 4-4c$$

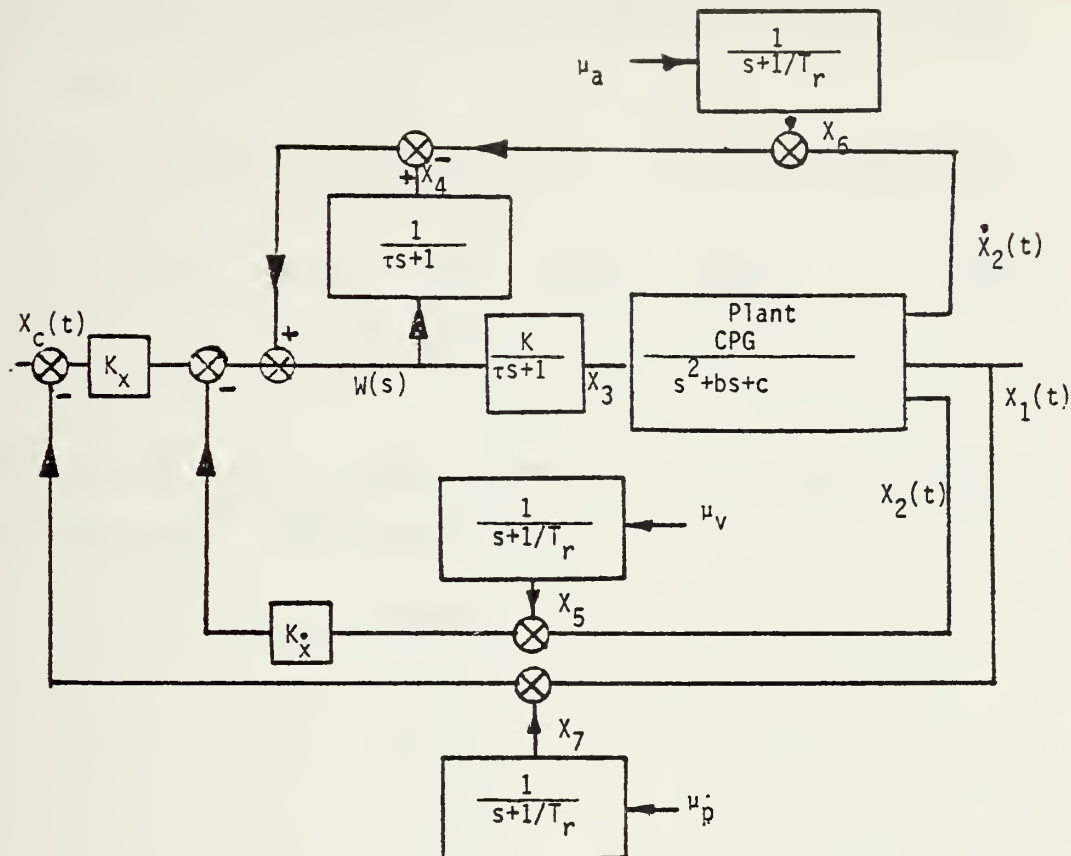


Figure 4-2 High frequency error model,
position controller

The additional state variables required for analysis of the controller as shown in figure 4-2 are

- x_3 = output of the actuator which is also input to the plant
- x_4 = output of the actuator compensator
- x_5 = state variable representing the error in the velocity measurement
- x_6 = state variable representing the error in acceleration measurement
- x_7 = state variable representing the error in position measurement

From the figure we can write the control law $W(s)$, with

$X_c = 0$ as

$$\begin{aligned} W(t) &= -K_x(X_1 + X_7) - K_{\dot{x}}(X_2 + X_5) - (-cX_1 - bX_2 + CPGX_3 + X_6) + X_4 \\ &= (-K_x + c)X_1 + (-K_{\dot{x}} + b)X_2 - CPGX_3 + X_4 - K_{\dot{x}}X_5 - \\ &\quad X_6 - K_xX_7 \end{aligned} \quad 4-5$$

The remaining first order differential equations, obtained from figure 4-1, are given as

$$\dot{X}_3 = -1/\tau X_3 + K/\tau W(t) \quad 4-6a$$

$$\dot{X}_4 = -1/\tau X_4 + 1/\tau W(t) \quad 4-6b$$

$$\dot{X}_5 = -1/T_r X_5 + 2\sigma_v^2/T_r \quad 4-6c$$

$$\dot{X}_6 = -1/T_r X_6 + 2\sigma_a^2/T_r \quad 4-6d$$

$$\dot{X}_7 = -1/T_r X_7 + 2\sigma_p^2/T_r \quad 4-6e$$

Combining equation 4-4, 4-5 and 4-6 and expressing the system in matrix form*, we have the closed loop system whose inputs are the random sensor noise quantities given by

$$X = [A] X + [B][Q] \quad 4-7$$

$$Y = [C] X$$

where σ_p , σ_v , and σ_a are the standard deviation of the position measurement error of the velocity measurement error and of acceleration measurement error respectively and $[Q]$ is the matrix of input white noise powers given by

$$Q_{ii} = \mu_i = 2\sigma_i^2/T_r$$

*Matricies A, B, Q and C are shown on following page.

$$A = \begin{bmatrix} 0 & 1 & 0 & 0 & 0 & 0 & 0 \\ (c - K_X) \frac{K}{\tau} & 0 & -(CPG \cdot K + 1)/\tau & K \frac{1}{\tau} & -\frac{K_X \cdot K}{\tau} & -\frac{K \cdot K_X}{\tau} & 0 \\ (c - K_X)/\tau & (b - K_X) \frac{K}{\tau} & -CPG/\tau & 0 & -\frac{K_X}{\tau} & -\frac{K_X}{\tau} & 0 \\ 0 & 0 & 0 & 0 & -1/Tr & 0 & 0 \\ 0 & 0 & 0 & 0 & 0 & -1/Tr & 0 \\ 0 & 0 & 0 & 0 & 0 & 0 & -1/Tr \end{bmatrix}$$

$$B = \begin{bmatrix} 0 & 0 & 0 & 0 & 0 & 0 & 0 \\ 0 & 0 & 0 & 0 & 0 & 0 & 0 \\ 0 & 0 & 0 & 0 & 0 & 0 & 0 \\ 1 & 0 & 0 & 0 & 0 & 0 & 0 \\ 0 & 1 & 0 & 0 & 0 & 0 & 0 \\ 0 & 0 & 0 & 0 & 0 & 0 & 1 \end{bmatrix}$$

$$Q = \begin{bmatrix} 2\sigma_v/Tr & 0 & 0 \\ 0 & 2\sigma_a/Tr & 0 \\ 0 & 0 & 2\sigma_p/Tr \end{bmatrix}$$

$$C = \begin{bmatrix} -c & 0 & 0 & 0 & 0 & 0 & 1 \\ 0 & -b & 0 & 1 & 0 & 0 & 0 \\ -c & -b & CPG & 0 & 1 & 0 & 0 \end{bmatrix}$$

Having the matrix representation of the closed loop controller being driven by the sensor noise inputs, we can analyze the effect of the sensor error by considering the controllability and observability of the system with respect to the noise inputs and outputs of position, velocity and acceleration.

The linear control system computer programs, developed by Melsa and Jones [7], were first used with the result that the system is both observable and controllable. In order to gain a better understanding of the controllability and observability of the system, a second approach, following a method suggested by Bryson [11], was used. In the later method we decouple the system of equations by diagonalizing the system given by equation 4-7. This produces a system of equations in modal coordinates. The diagonalization procedure requires that we calculate the eigenvalues and eigenvectors of the A matrix. The transformation matrix, T, from the original coordinates to the new coordinates, is obtained by normalizing, in a complex sense, the matrix of eigenvectors. The matrix quantities corresponding to the modal coordinates are denoted with a superscript, *. The system, in modal coordinates is expressed as

$$X^* = A^*X^* + B^*Q \quad 4-8a$$

$$Y = C^*X^* \quad 4-8b$$

and the transformation is as follows

$$X^* = T^{-1}X \quad 4-9a$$

$$A^* = T^{-1}AT \quad 4-9b$$

$$B^* = T^{-1}B \quad 4-9c$$

$$C^* = CT \quad 4-9d$$

We will now apply the above coordinate transformation to examine the observability and controllability of the system when the plant is a specific second order system.

For this example we chose one of the representative VSTOL second order plants given by mode number 6 of table 3-2. The transfer function for this plant is given by

$$G(s) = \frac{1}{s^2 + .6s + 2.16} \quad 4-10$$

We will assume the following additional parameters

$$\tau = .1 \text{ sec}, K_x = 4, K_v = 3, K = 5, T_r = 10 \text{ sec}$$

with these choices the gain parameter KRL is

$$KRL = K \text{ CPG} / \tau = 50$$

Because the system is linear with respect to the noise inputs we can solve the problem in general assuming a unit value for the individual noise standard deviations, or

$$\sigma_p = \sigma_v = \sigma_a = 1$$

where σ_p , σ_v and σ_a is the standard deviation of the position, velocity and acceleration measurement error. The original system and the resulting diagonalized system was determined by a fortran computer code called MODAL, listed in Appendix A.

The results are given

$$X = AX + BQ$$

$$Y = CX$$

$$X^* = A^*X^* + B^*Q$$

$$Y = C^*X^*$$

Matricies A, B, C, A*, B* and C* are shown on the following pages.

$$A = \begin{bmatrix} 0.0 & 1.0 & 0.0 & 0.0 & 0.0 & 0.0 \\ -2.16 & -0.6 & 1.0 & 0.0 & 0.0 & 0.0 \\ -92.0 & -120.0 & -60.0 & 50.0 & -150.0 & -200.0 \\ -18.4 & -24.0 & -10.0 & 0.0 & -30.0 & -40.0 \\ 0.0 & 0.0 & 0.0 & 0.0 & -0.1 & 0.0 \\ 0.0 & 0.0 & 0.0 & 0.0 & 0.0 & 0.0 \\ 0.0 & 0.0 & 0.0 & 0.0 & -0.1 & 0.0 \end{bmatrix}$$

$$B = \begin{bmatrix} 0.0 & 0.0 & 0.0 \\ 0.0 & 0.0 & 0.0 \\ 0.0 & 0.0 & 0.0 \\ 0.0 & 0.0 & 0.0 \\ 1.0 & 0.0 & 0.0 \\ 0.0 & 1.0 & 0.0 \\ 0.0 & 0.0 & 1.0 \end{bmatrix}$$

$$C = \begin{bmatrix} 1.0 & 0.0 & 0.0 & 0.0 & 0.0 & 1.0 \\ 0.0 & 1.0 & 0.0 & 0.0 & 1.0 & 0.0 \\ -2.16 & -0.6 & 1.0 & 0.0 & 0.0 & 0.0 \end{bmatrix}$$

$$A^* = \begin{bmatrix} -1.56 & 1.34 & 0.0 & -0.0 & 0.0 & -0.0 & 0.0 \\ -1.34 & -1.56 & -0.0 & 0.0 & -0.0 & -0.0 & -0.0 \\ -0.0 & -0.0 & -47.48 & 0.0 & 0.0 & 0.0 & 0.0 \\ -0.0 & 0.0 & -0.0 & -10.0 & 0.0 & 0.0 & 0.0 \\ 0.0 & 0.0 & 0.0 & 0.0 & -0.1 & 0.0 & 0.0 \\ 0.0 & 0.0 & 0.0 & 0.0 & 0.0 & -0.1 & 0.0 \\ 0.0 & 0.0 & 0.0 & 0.0 & 0.0 & 0.0 & -0.1 \end{bmatrix}$$

$$B^* = \begin{bmatrix} Q_v & Q_a & Q_p \\ 15.48 & 5.16 & 20.64 \\ 17.91 & 5.97 & 23.88 \\ -3.41 & -1.14 & -4.54 \\ 0.0 & 0.0 & 0.0 \\ 2.17 & 0.0 & 0.0 \\ 0.0 & 1.19 & 0.0 \\ 0.0 & 0.0 & 2.75 \end{bmatrix}$$

$$C^* = \begin{bmatrix} 0.05 & 0.0 & -0.0 & 0.01 & -0.87 & X_v^* & X_p^* \\ 0.08 & 0.07 & 0.02 & -0.08 & 0.5 & X_a^* & -0.03 \\ 0.03 & -0.22 & -0.99 & 0.82 & -0.0 & 0.84 & 0.04 \\ & & & & & & -0.0 \end{bmatrix}$$

It is instructive to observe the A matrix of the system. In the upper right corner, rows and columns 1 and 2 represent the plant. Row 3 is derived from the controller terms, $K \cdot W(t)/\tau$. These terms dominate the matrix.

The diagonal elements of A^* are the eigenvalues of the original system. All of the eigenvalues are negative, indicating that the system is stable. The system has one coupled oscillatory mode, -1.56, 1.34 in the upper right corner of A^* . This mode corresponds to the model and will be referred to as the model mode throughout the remainder of this study. The eigenvalue -47.48, row 3 column 3 of A^* , is the mode which represents the output of the controller. We refer to this as the controller mode. It physically represents the real pole whose location corresponds to the value of KRL as discussed in the root locus analysis of section III-C. Similarly the eigenvalue -10.00, row 4 column 4 of A^* , is the compensator mode. The other three eigenvalues correspond to the noise filter time constant, $-1/T_r$. From the transformed system, the controllability and observability of each of the previously mentioned modes with respect to the noise input can be determined.

In the B^* matrix the Q_v above the first column indicates that column 1 is the input vector corresponding to velocity error measurement input. The other columns are annotated similarly. The first two rows of the B^* matrix indicate that the model and controller modes are affected by all three

measurement errors and that acceleration measurement error is least significant. The zeroes in row 4 of the B^* matrix indicate that the compensator mode is unaffected by measurement noise. This indicates that the compensator does not contribute to the uncertainty of the system.

The C^* matrix has been annotated in a way similar to B^* so the X_v^* , X_a^* , and X_p^* correspond to the velocity, acceleration, and position error modes respectively. From the C^* matrix it is seen that the observation of position, corresponding to the first row of the matrix, is affected by all three measurement errors but that velocity and acceleration are only slightly affected. We conclude from the C^* matrix that measurement errors will affect the position, which is the quantity being controlled, but that the dynamic behavior, velocity and acceleration are only slightly affected. This result is perhaps due to the low frequency error model which results from the choice of T_r equal to 10 seconds.

From the modal analysis it is concluded that sensor errors can affect the model and controller mode of the closed loop system and that the errors can be observed in the measurement of the position. The exact relationship between the output quantities of position, velocity and acceleration will be determined in the next section where the variances of state variable X_1 , X_2 , and X_3 will be found by solving the Lyapunov equation for the system.

B. COVARIANCE ANALYSIS

The object of the covariance analysis is to determine the standard deviations of the error in the states X_1 , X_2 , and X_3 of the system developed in the previous section. The standard deviation of X_1 and X_2 are of interest because they represent position and velocity tracking accuracy. X_3 is of interest because it is the input to the plant. A large deviation in X_3 due to measurement error would mean unnecessarily high amounts of control energy lost because of measurement errors. The state variable representation of the system developed in section 4-1, where the inputs to the system are noise sources representing position, velocity and acceleration measurement error, will again be used.

The problem of determining the covariance of the states of a system in the presence of disturbances is typically encountered in the design of optimal estimators, the Kalman filter. In the estimator problem the system is expressed in the following way

$$\dot{X} = AX + BU + GW_t(t) \quad 4-11$$

where A is the matrix representation of the plant, B the control input matrix, $W_t(t)$ white noise disturbance to the plant states with

$$E[W_t(t)] = 0, \quad E[W_t(t), W_t^T(t)] = \mu$$

and G the input matrix of the disturbances. In estimation problems one assumes that measurements of the system are made

which can be expressed in terms of the states of the system by the relationship

$$\underline{z}_N = H\underline{x} + \underline{v}_N$$

Here N quantities are measured with an expected error of \underline{v}_N .

In the developement of the SRFIMF controller, sensor noise was defined as a state of the system and the A matrix was augmented to include these states. The covariance analysis assumes quiescent operation of the controller, therefore, the only input to the system is white noise of strength, μ , given by equation 4-3. The white noise acts only to disturb the sensor error states. The governing equation for the covariance of the states is given by the Lyapunov differential equation

$$\dot{P} = AP + PA^T + GQG^T \quad 4-12$$

where P is the matrix of the state variable covariances defined as

$$P_{ij} = \sigma_i \sigma_j$$

and Q is as before, the matrix of white noise input whose power is μ . We have chosen to rename the matrix G of equation 4-11 to B because the white noise sources are considered to be the inputs to the system.

Again a unit value of standard deviations was assumed and, because the system is linear with respect to the noise inputs, we can apply later the set of sensors. We will consider the

same plant as used in section 4-1. The transfer function for the plant is given by

$$\frac{G(s)}{U(s)} = \frac{CPG}{s^2 + .6s + 2.16} \quad 4-13$$

At time equal to zero no uncertainties exist in the system, therefore the initial condition on P is zero.

A computer program, Vary, listed in Appendix A, was developed to solve the Lyapunov equation. The program uses an International Mathematical and Statistical Library (IMSL) subroutine called DVERK. This subroutine solves a system of first order differential equations using a Runge-Kutta Algorithm. The resulting covariance matrix, P, is printed by the program as a function of time, at a number of discrete times. The diagonal elements of the P matrix are interpreted as the square of the standard deviation or RMS value (σ_{ii}^2) of each of the state variable uncertainties as a result of the noise input. The data obtained from the computation of the P matrix is plotted in figures 4-3 to 4-5 and tabulated in Appendix B, table B-1. The figures show the standard deviation (sigma) of the states X_1 , X_2 and X_3 as functions of time from zero to ten seconds. When necessary, the steady state value is shown by a "+" on the figure.

Figures 4-3 to 4-5 can be interpreted in the following way. Each individual curve represents the contribution to the total state variable error as a result of one measurement

source. For example, in figure 4-3 we see that a unit value of standard deviation error in position measurement results in a standard deviation error in X_1 of approximately 0.8° at six seconds, and a steady state error of 0.98° . The total expected value of the uncertainty in X_1 is the sum of the errors resulting from position, velocity and acceleration measurements as given by

$$\sigma_i = \sigma_{ip} + \sigma_{iv} + \sigma_{ia} \quad 4-14$$

Where the notation σ_{ij} refers to the i th state variable and j refers to a noise source. Thus, σ_{ip} refers to the standard deviation of X_1 as a result of position measurement error.

Table 4-2 summarizes the steady state values of the components of the state variable errors.

	X_1	X_2	X_3
Position measurement error	<u>.980</u>	<u>.360</u>	<u>2.13</u>
Velocity measurement error	.735	.270	1.60
Acceleration measurement error	.245	.089	0.53

Table 4-2 Steady state errors as a result of measurement errors

The actual measurements are made either by inertial navigation sensors or by strapdown sensors whose standard deviations are given by table 4-1. We can now apply the results obtained from the covariance analysis to obtain an estimate of the state variable errors for actual measurement

cases. For example, the steady state standard deviation of the error in X_1 when the measurements are made by an inertial system is given as

$$\sigma_1 = q_p \sigma_{1p} + q_v \sigma_{1v} + q_a \sigma_{1a} \quad 4-15$$

where q_p , q_v and q_a are the standard deviations of the inertial sensor measurements given by table 4-1 as

$$q_p = 0.1^\circ$$

$$q_v = 0.5^\circ/\text{sec}$$

$$q_a = 0.1^\circ/\text{sec}^2$$

and σ_{1p} , σ_{1v} and σ_{1a} are given in table 4-2. The resulting expected error in X_1 in steady state is found from equation 4-15 to be 0.49° . In a similar way, the steady state errors in X_1 , X_2 and X_3 for both inertial measurements and strapdown measurements can be evaluated. The results are shown in table 4-3.

	X_1	X_2	X_3
Inertial sensors	0.49°	$0.18^\circ/\text{sec}$	$1.07^\circ/\text{sec}^2$
Strapdown sensors	1.6°	$0.58^\circ/\text{sec}$	$3.46^\circ/\text{sec}^2$

Table 4-3 Steady state tracking errors produced by strapdown and inertial navigation sensors

The result of the covariance analysis indicates that the expected uncertainty in X_1 and X_2 as a result of measurement errors are not significant. For example, in the case of strapdown sensors, the expected error in position, X_1 , is 1.6°

while measurement errors had standard deviation values of 1° , $0.5^\circ/\text{sec}$ and $1^\circ/\text{sec}^2$.

To interpret the significance of the expected value of the error in X_3 , the value of X_3 will be determined when a 1° input is applied to the controller. Refer to figure 4-2 and, for this example, disregard the effect of the control actuator at the input to the plant. Assuming that initially the controller is in steady operation with feedbacks equal to zero, at the instant the 1° input is applied the value of X_3 is determined to be

$$X_3 = X_c \cdot K_x \cdot K = 20 \quad 4-16$$

Comparing the value of the standard deviation in X_3 to the value of X_3 when a 1° unit step input is applied to the controller, we conclude that the value of the standard deviation error in X_3 is only 17.3 percent of the value of X_3 when a 1° input is applied to the system.

From both the modal analysis and the variance analysis it can be concluded that high quality acceleration measurements are not necessary and that errors in the measurement of position and velocity are not amplified. The errors in the states are most affected by position measurement error. This result might have been expected because the controller is attempting to track to the commanded position and errors in the position measurement should dominate the uncertainty in the other states. Figures 4-3 thru 4-5 show that the uncertainty in the states reaches a

SIGMA XI VS. TIME

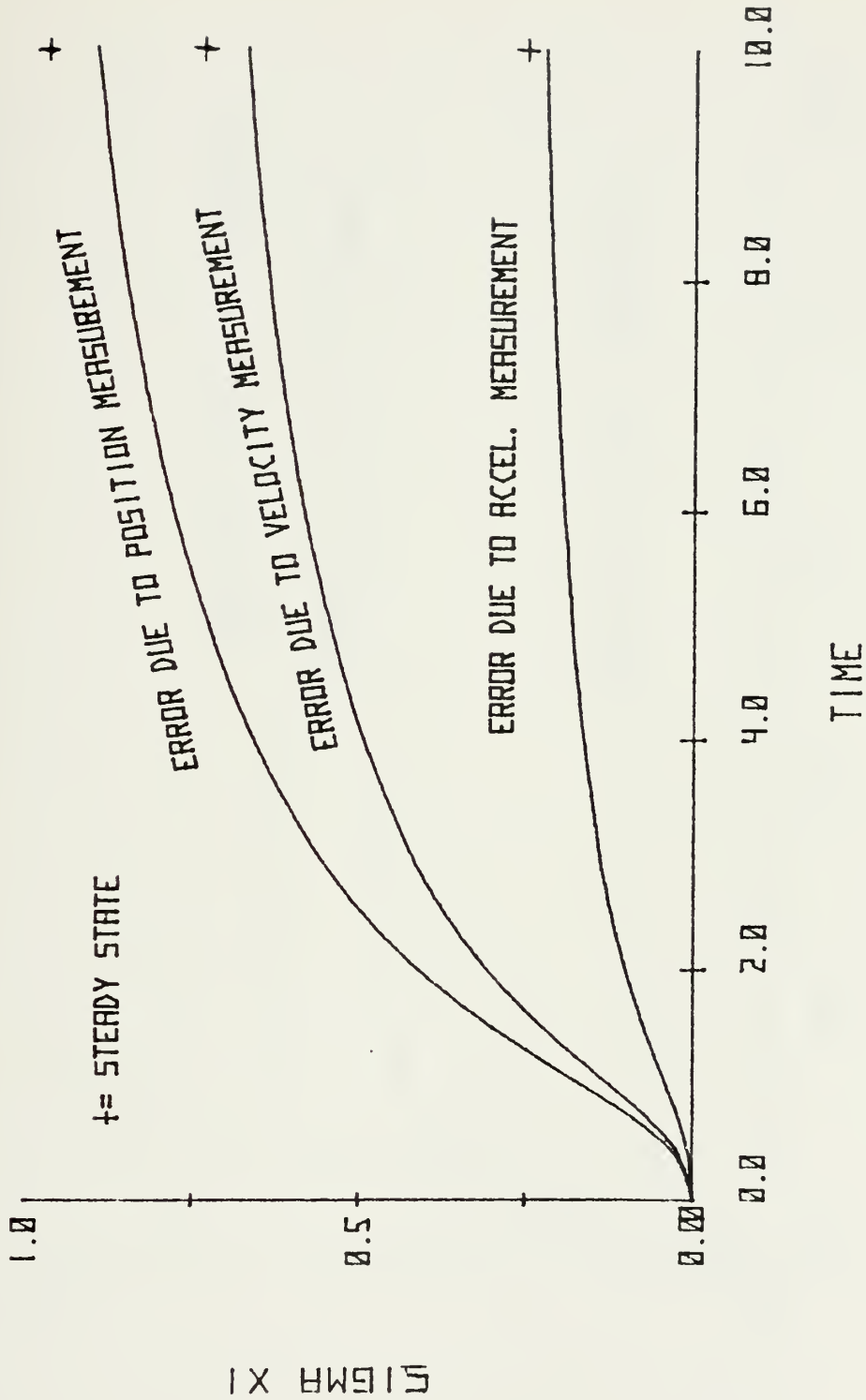


Figure 4-3 Tracking errors in X_1 as a result of measurement error in position, velocity and acceleration.

SIGMA X2 VS. TIME

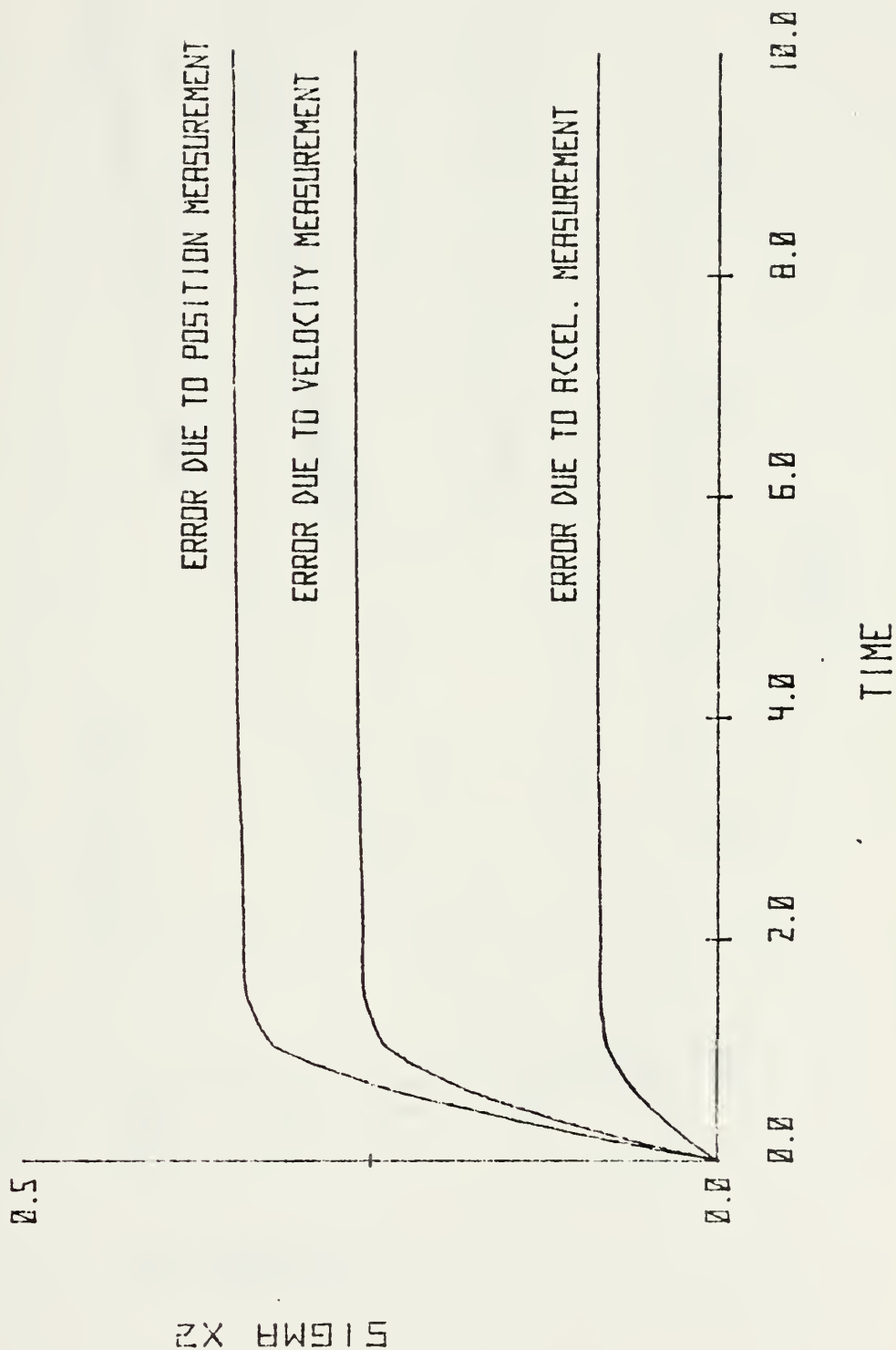


Figure 4-4 Tracking errors in X_2 as a result of measurement error position, velocity and acceleration.

SIGMA X3 VS. TIME

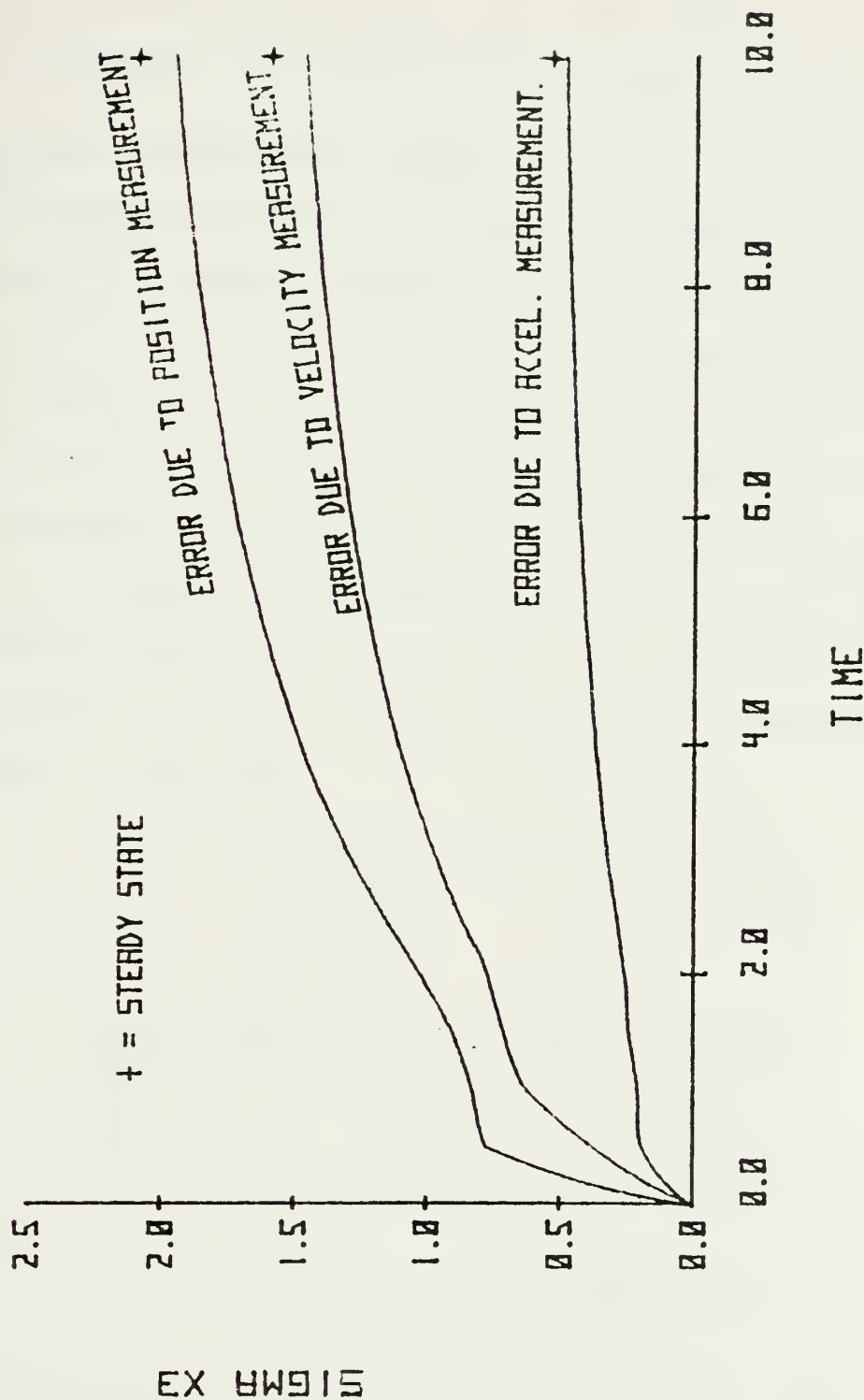


Figure 4-5 Tracking errors in X_3 as a result of measurement error in position, velocity and acceleration.

near steady state value in a short time, particularly in the case of X_2 . The rise time of the errors, seen in the figures, should not be interpreted as a lag in the response, since the figures represent the expected error in each of the states.

C. ALTERNATE MEASUREMENT SCHEMES

Two possible methods of reducing the number of measurements required by the SRFIMF controller will be considered. The first case is to measure acceleration and integrate to obtain velocity and position. In the second scheme, position and velocity will be measured and acceleration will be estimated from knowledge of the plant. The second case will be used to obtain an estimate of the added uncertainty caused by the acceleration measurement. Figure 4-6 is a schematic representation of the first case. As before the state representation of the system is obtained.

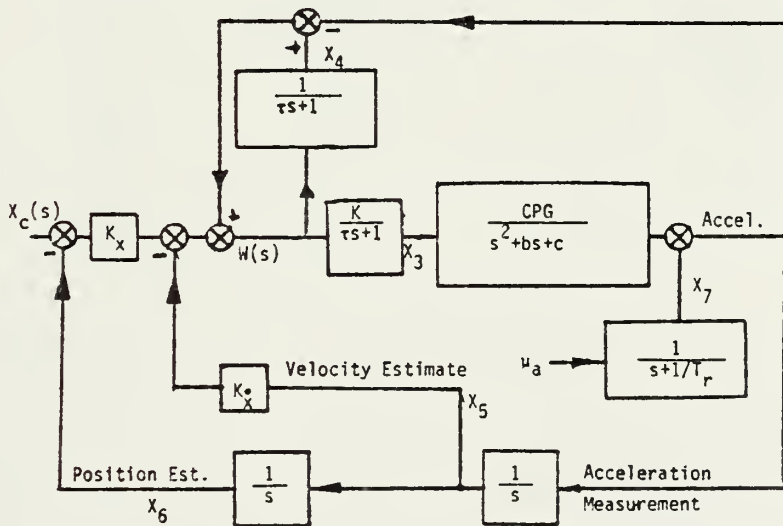


Figure 4-6 First alternate measurement scheme. Measured acceleration and implied position and velocity.

The state variables are defined as

x_1 = position

x_2 = velocity

x_3 = output of the control actuator

x_4 = output of the compensator

x_5 = velocity estimate

x_6 = position estimate

x_7 = acceleration error

The control input, from figure 4-5 is written as

$$W(s) = cx_1 + bx_2 - CPGx_3 + x_4 - K_x x_5 - x_7 \quad 4-16$$

Following a development analogous to that used in section 2-3

we obtain the state representation of the system to be

$$\dot{\mathbf{X}} = \mathbf{AX} + \mathbf{BQ}$$

$$\mathbf{A} = \begin{bmatrix} 0 & 0 & 0 & 0 & 0 & 0 & 0 \\ -c & -b & CPG & 0 & 0 & 0 & 0 \\ K \cdot c / \tau & b \cdot K / \tau & -(CPG \cdot K + 1) / \tau & K / \tau & -K \cdot K_x / \tau & -KK_x / \tau & -K / \tau \\ c / \tau & b / \tau & -CPG / \tau & 0 & -KX / \tau & -KX / \tau & -1 / \tau \\ -c & -b & CPG & 0 & 0 & 0 & 1 \\ 0 & 0 & 0 & 0 & 1 & 0 & 1 \\ 0 & 0 & 0 & 0 & 0 & 0 & -1 / T_r \end{bmatrix}$$

$$\mathbf{B} = \begin{Bmatrix} 0 \\ 0 \\ 0 \\ 0 \\ 0 \\ 0 \\ 1 \end{Bmatrix}$$

$$\mathbf{Q} = \begin{bmatrix} \frac{2\sigma_a}{T_r} \end{bmatrix}$$

We apply the modal computer program to this system using the plant defined by equation 4-10 in order to determine the observability and controllability. The resulting system in modal coordinates is

$$\dot{X}^* = A^* X^* + B^* Q$$

$$A^* = \begin{bmatrix} -47.48 & 0.0 & 0.0 & 0.0 & 0.0 & 0.0 & 0.0 \\ 0.0 & -1.56 & 1.34 & 0.0 & 0.0 & 0.0 & 0.0 \\ 0.0 & -1.34 & -1.56 & 0.0 & 0.0 & 0.0 & 0.0 \\ 0.0 & 0.0 & 0.0 & 0.0 & 0.0 & 0.0 & 0.0 \\ 0.0 & 0.0 & 0.0 & 0.0 & 0.0 & 0.0 & 0.0 \\ 0.0 & 0.0 & 0.0 & 0.0 & 0.0 & -10.0 & 0.0 \\ 0.0 & 0.0 & 0.0 & 0.0 & 0.0 & 0.0 & -0.1 \end{bmatrix}$$

$$B^* = \begin{bmatrix} -1.07 \\ .17 \\ -.20 \\ -211.0 \\ 9989.68 \\ 0.0 \\ 237.0 \end{bmatrix}$$

$$C^* = \begin{bmatrix} 0.0 & -0.03 & -0.05 & 0.46 & 0.0 & -0.01 & -0.42 \\ 0.02 & 0.12 & 0.04 & 0.0 & 0.0 & 0.08 & 0.04 \\ -0.99 & -0.24 & 0.09 & 0.0 & 0.0 & -0.82 & 0.0 \end{bmatrix} \begin{matrix} X_a^* \\ \\ \end{matrix}$$

From the A^* matrix we can see that this system has two zero eigenvalues meaning that the modes of the system which correspond to the open loop integrators are neutrally stable. The modal control vector B^* indicates that the velocity and position estimate modes of this system are strongly affected by the noise input. In particular, mode five (row 5 of B^*) which represents the position estimate mode has a control coefficient from the noise source four orders of magnitude greater than the model mode (rows 2 and 3 of B^*). We expect that in this case acceleration sensor noise significantly affects the performance of the controller.

Applying the algorithm used in the previous section to this case we obtain the covariance estimate. Figure 4-7 is a plot of the standard deviation (σ) of X_1 , X_2 and X_3 assuming

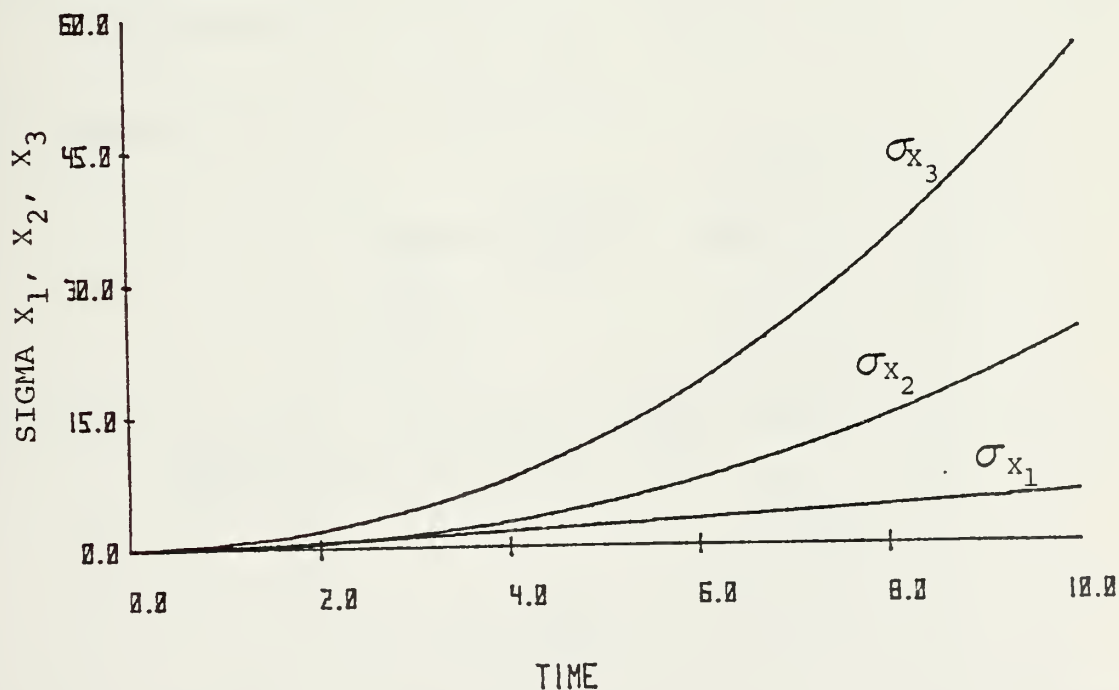


Figure 4-7 Error in X_1 , X_2 , and X_3 as a result of measurement errors in acceleration.

a unit standard deviation noise source as the acceleration measurement error. Data used to plot figure 4-7 is also tabulated in Appendix B, table B-2. It is seen from the figure that acceleration measurement error causes unbounded errors in X_1 and X_3 . Unbounded errors in any of the states are unacceptable in the controller and unless we can improve the method of estimating the position and velocity, we will be required to measure these quantities. A Luenberger observer could be used to estimate position and velocity, however the design of the observer would require use of knowledge of the plant. We wish to avoid using detailed knowledge of the plant.

The second alternate measurement scheme is the case of measured position and velocity with acceleration estimated from the plant parameters b and c . The estimation is given by

$$\text{Acceleration} = -cX_1 - bX_2 + \text{CPG } X_3 \quad 4-17$$

This scheme is shown in figure 4-8.

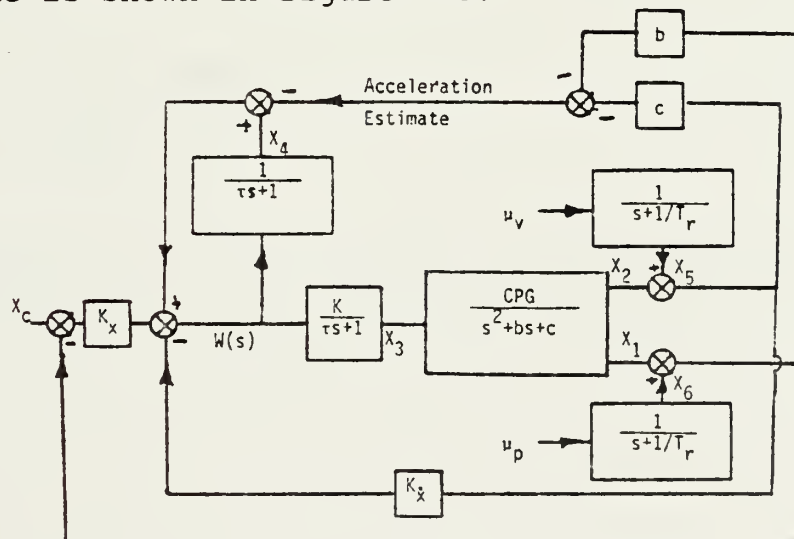


Figure 4-8 Second alternate measurement scheme, measured position and velocity. Estimated acceleration.

Following the same procedures as before we define the state variable as

X_1 = position

X_2 = velocity

X_3 = output of the control actuator

X_4 = output of the compensator

X_5 = position measurement error

X_6 = velocity measurement error

From figure 4-8 we obtain the control law $W(t)$ as

$$\begin{aligned} W(t) = & (-K_x + c) X_1 + (-K_{\dot{x}} + b) X_2 - CPG X_3 + X_4 \\ & + (-K_x + c) X_5 + (-K_{\dot{x}} + b) X_6 \end{aligned} \quad 4-18$$

Assuming the same second order plant given by equation 4-10 we obtain the modal transformation of the system.¹

$$\dot{X} = AX + BQ$$

$$Y = CX$$

$$\dot{X}^* = A^*X^* + B^*Q$$

$$Y = C^*X^*$$

¹Matricies A, B, C, A*, B* and C* are shown on the following pages.

$$A = \begin{bmatrix} 0.0 & 1.0 & 0.0 & 0.0 & 0.0 \\ -2.16 & -.6 & 0.0 & 0.0 & 0.0 \\ -92.0 & -120.0 & -60.0 & -50.0 & -92.0 \\ -18.0 & 24.0 & -10.0 & 0.0 & -18.0 \\ 0.0 & 0.0 & 0.0 & 0.0 & -.1 \\ 0.0 & 0.0 & 0.0 & 0.0 & -.1 \end{bmatrix}$$

$$B = \begin{bmatrix} 0.0 & 0.0 \\ 0.0 & 0.0 \\ 0.0 & 0.0 \\ 0.0 & 0.0 \\ 1.0 & 0.0 \\ 0.0 & 1.0 \end{bmatrix}$$

$$C = \begin{bmatrix} 1.0 & 0.0 & 0.0 & 0.0 & 0.0 \\ 0.0 & 1.0 & 0.0 & 0.0 & 0.0 \\ -2.16 & -.6 & 1.0 & 0.0 & 0.0 \end{bmatrix}$$

$$A^* = \begin{bmatrix} -1.56 & 1.34 & 0.0 & 0.0 & 0.0 & 0.0 \\ -1.34 & -1.56 & 0.0 & 0.0 & 0.0 & 0.0 \\ 0.0 & 0.0 & -47.48 & 0.0 & 0.0 & 0.0 \\ 0.0 & 0.0 & 0.0 & -10.0 & 0.0 & 0.0 \\ 0.0 & 0.0 & 0.0 & 0.0 & -1 & 0.0 \\ 0.0 & 0.0 & 0.0 & 0.0 & 0.0 & -1 \end{bmatrix}$$

$$B^* = \begin{bmatrix} Q_v & Q_p \\ 9.49 & 12.38 \\ 10.99 & 14.33 \\ -2.09 & -2.73 \\ 0.0 & 0.0 \\ 1.55 & 0.0 \\ 0.0 & 1.83 \end{bmatrix}$$

$$C^* = \begin{bmatrix} 0.05 & 0.0 & 0.0 & 0.01 & -0.32 & x_v^* \\ -0.08 & 0.07 & 0.02 & -0.08 & 0.03 & x_p^* \\ 0.03 & -0.22 & -0.99 & 0.82 & 0.0 & -0.35 \\ & & & & & 0.04 \\ & & & & & 0.0 \end{bmatrix}$$

The results of the modal analysis are similar to those obtained when acceleration was a measured quantity rather than calculated as in this case. The model and controller modes are controllable from the noise sources. The position and velocity outputs (rows 1 and 2 of the C* matrix) contain sensor noise terms.

The covariance analysis results are shown in figures 4-9 to 4-11 and listed in Appendix B, table B-3. Here it is seen that the standard deviation of X_1 , X_2 and X_3 is slightly less than in the case when acceleration was measured. This is because the quantity taken to be acceleration does not contain the additional error of actual acceleration measurement. In this case the system requires only measurements of position and velocity.

The second alternate measurement scheme can be used to compare a state rate feedback control scheme to a state variable feedback controller, from the viewpoint of increased uncertainty in the state variable resulting from the additional measurement of acceleration. To make the comparison, assume that the measurements are made by strapdown type sensors whose measurement errors are given in table 4-1. Table 4-4 lists the total uncertainty of X_1 , X_2 and X_3 for both measurement schemes. It can be seen from table 4-4 that the overall uncertainty of X_1 , X_2 and X_3 is increased when acceleration is measured, as compared to the second alternate measurement scheme when acceleration is obtained without measurement. In a practical

SIGMA XI VS. TIME

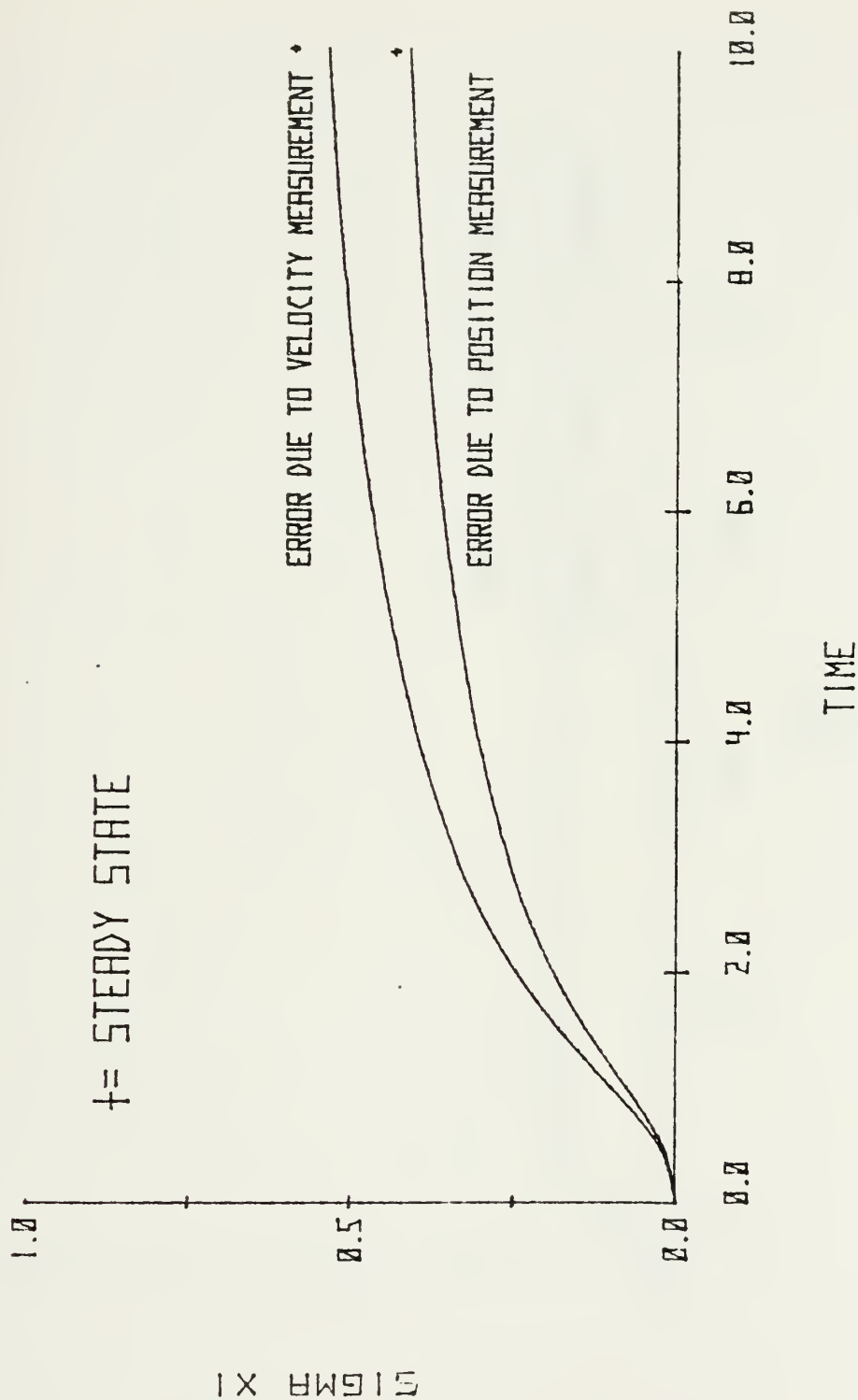


Figure 4-9 Tracking errors of X_1 as a result of measurement errors in position and velocity.

SIGMA X2 VS. TIME

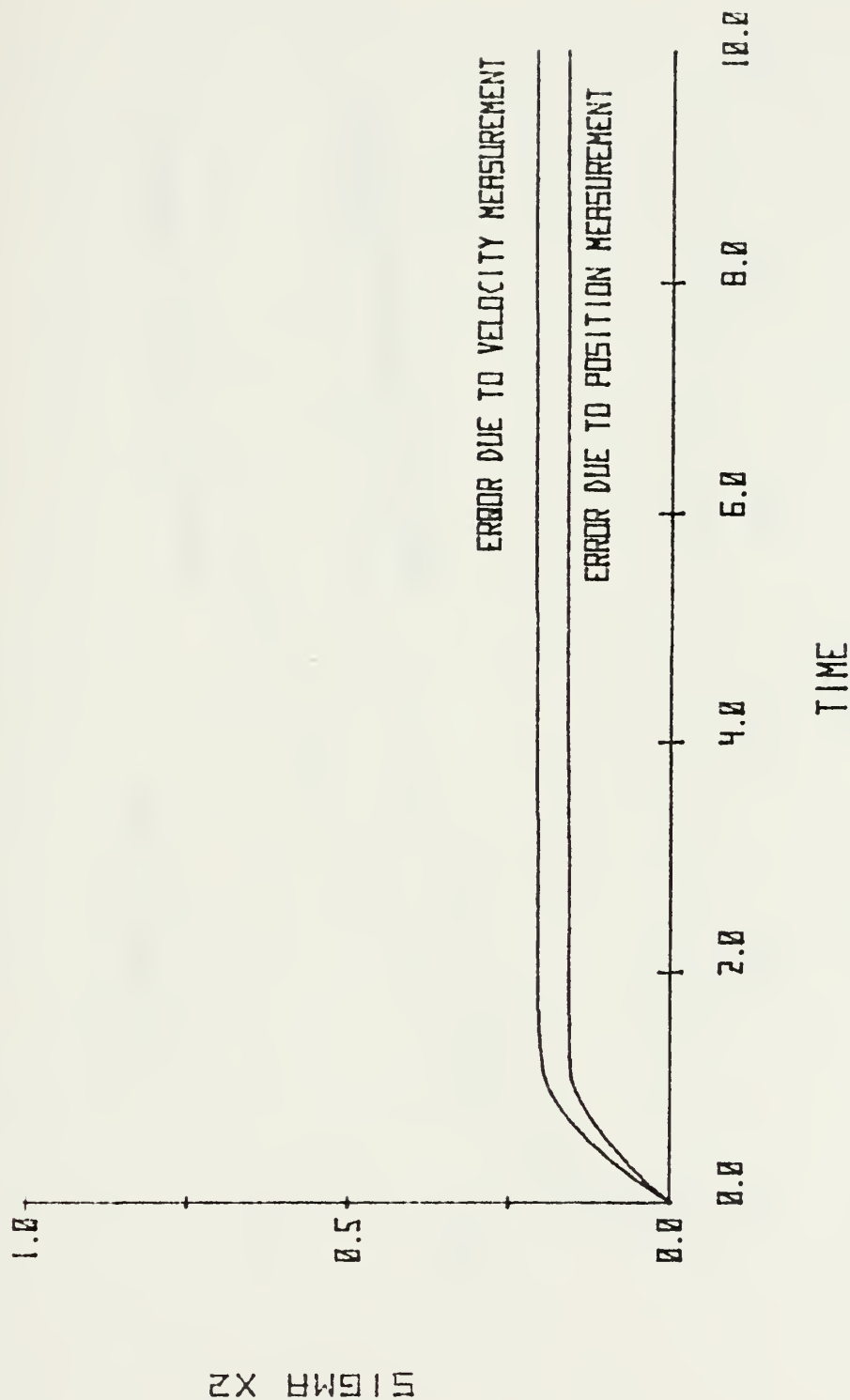


Figure 4-10 Tracking errors in X_2 as a result of measurement errors in position and velocity.

SIGMA X3 VS. TIME

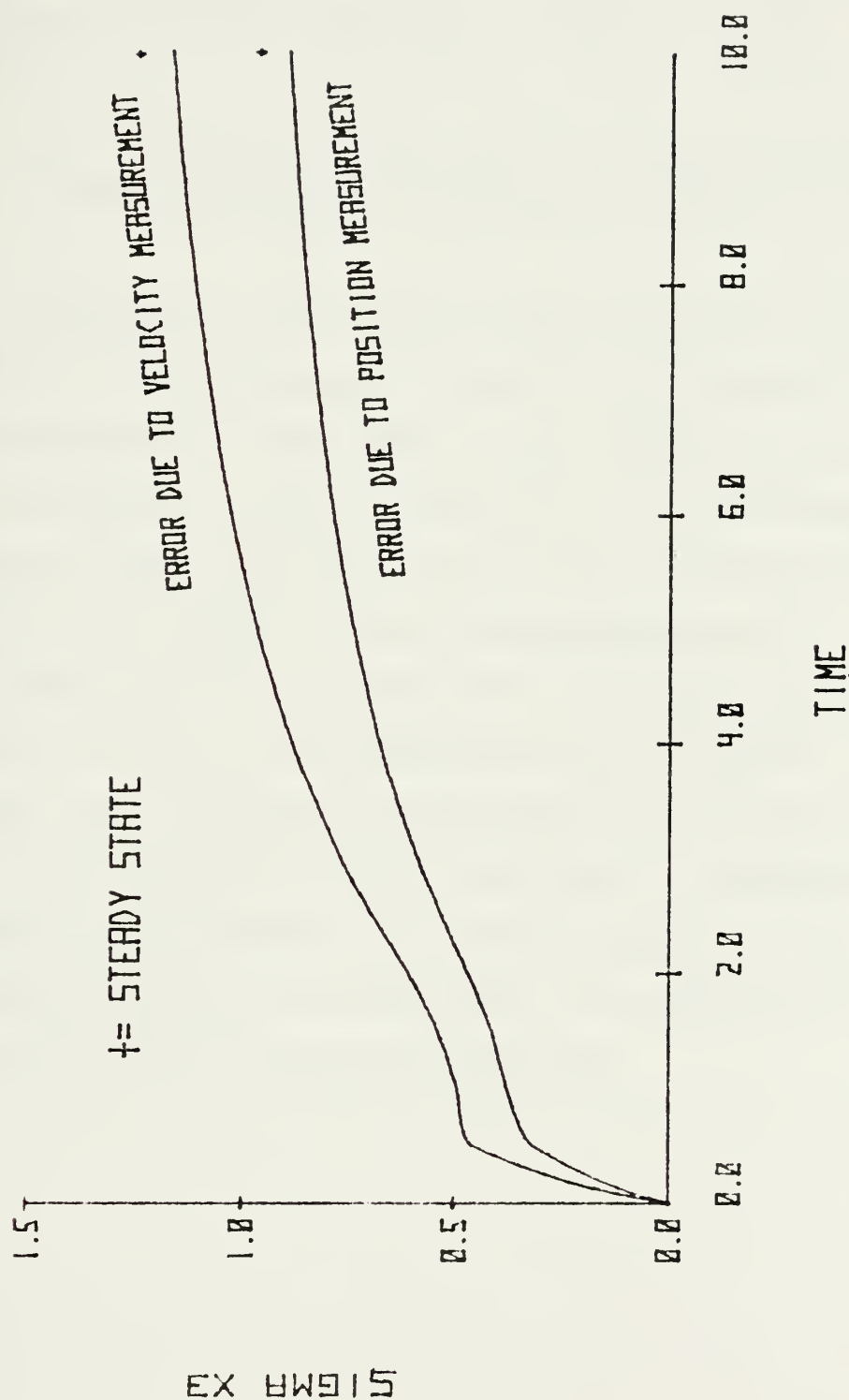


Figure 4-11 Tracking errors in X_3 as a result of measurement errors in position and velocity.

	$\overline{x_1}$	$\overline{x_2}$	$\overline{x_3}$
Second Alternate Measurement Scheme, Calculated Acceleration	0.75'	0.267'/s	1.6'/s ²
Measured Acceleration	1.6'	0.58'/s	3.46'/s ²
Percent increase of expected error	113%	117%	116%

Table 4-4 Steady state error in x_1 , x_2 and x_3 for measurements made by strapdown sensors.

system, uncertainty would exist in the knowledge of constants b and c and it could be expected that this would result in additional uncertainty in the value of the state variables. It might be possible that the uncertainty in the knowledge of the plant could negate the advantage gained by estimating acceleration as in the second alternate measurement scheme.

In conclusion, it has been shown that sensor noise does not adversely affect the SRFIMF position controller. It was also shown that acceleration measurement alone is not sufficient for acceptable operation of the controller. The analysis technique used in this section will next be applied to the analysis of a SRFIMF controller when the plant is assumed to be the longitudinal axis of the Harrier aircraft.

V. APPLICATION OF THE SRFIMF CONCEPT TO THE HARRIER AIRCRAFT

A. PITCH ATTITUDE CONTROL

The preceeding discussion dealt with the SRFIMF controller with the plant assumed to be a general second order system. In this section, the closed loop system will be modeled using the transfer function of a VSTOL aircraft. For this purpose the AV-8A Harrier, a jet-lift type VTOL aircraft, was chosen. The stability derivatives and transfer functions were obtained from reference [12]. The SRFIMF controller concept will be applied to the pitch attitude control of the aircraft and the analysis will be similar to that done earlier when the plant was assumed to be that of a second order system. As before, we will examine the root locus, time response and the effect of measurement errors. The effect of gust inputs to the plant will also be considered.

The transfer function between the pilot's stick and the pitch attitude of the Harrier, at 60 kts, 100 ft/sec, as given by reference [12] is

$$\frac{\theta(s)}{\delta_e(s)} = \frac{0.25 (s^2 + .246s + .00756)}{s^4 + .4896s^3 - .4495s^2 + .06736s + .00747} \quad 5-1a$$

$$= \frac{0.25 (s + .21) (s + .036)}{(s + 1) (s + .073) (s^2 - .1864s + .1024)} \quad 5-1b$$

$\theta(s)$ is given in radians and $\delta_e(s)$ in inches of stick displacement. The above transfer function does not include the effect of the control actuator which we include, as before, in the model of the controller.

The denominator factors of equation 5-1b indicate that at 60 kts the Harrier has an unstable oscillatory mode with a natural frequency, of 0.32 and damping ratio of -0.91, and that the constant plant gain, CPG, is 0.25. The plant, given by equation 5-1, is used to compute the root locus for the system by applying equation 3-21, developed for the controller in section III and rewritten here for convenience

$$1 + \frac{KRL(s^2 + K_{\dot{x}}s + K_x)}{s} G'(s) = 0 \quad 3-21$$

where $G'(s)$ is the open loop plant given by

$$G'(s) = \frac{G(s)}{CPG}$$

For the root locus evaluation, KRL was varied from 1 to 100. The value of the actuator time constant, τ , was chosen to be 0.1 sec and $K_{\dot{x}}$ and K_x were 3 and 4 respectively.

The root locus of the oscillatory pole is given in figure 5-1. The trajectory of this pole is similar to those given in section III where the plant was assumed to be a second order system. As before, the closed loop system oscillatory poles are near those of the model (-1.5, 1.32) at KRL values of about 25 and greater. Because of the scale of the figure,

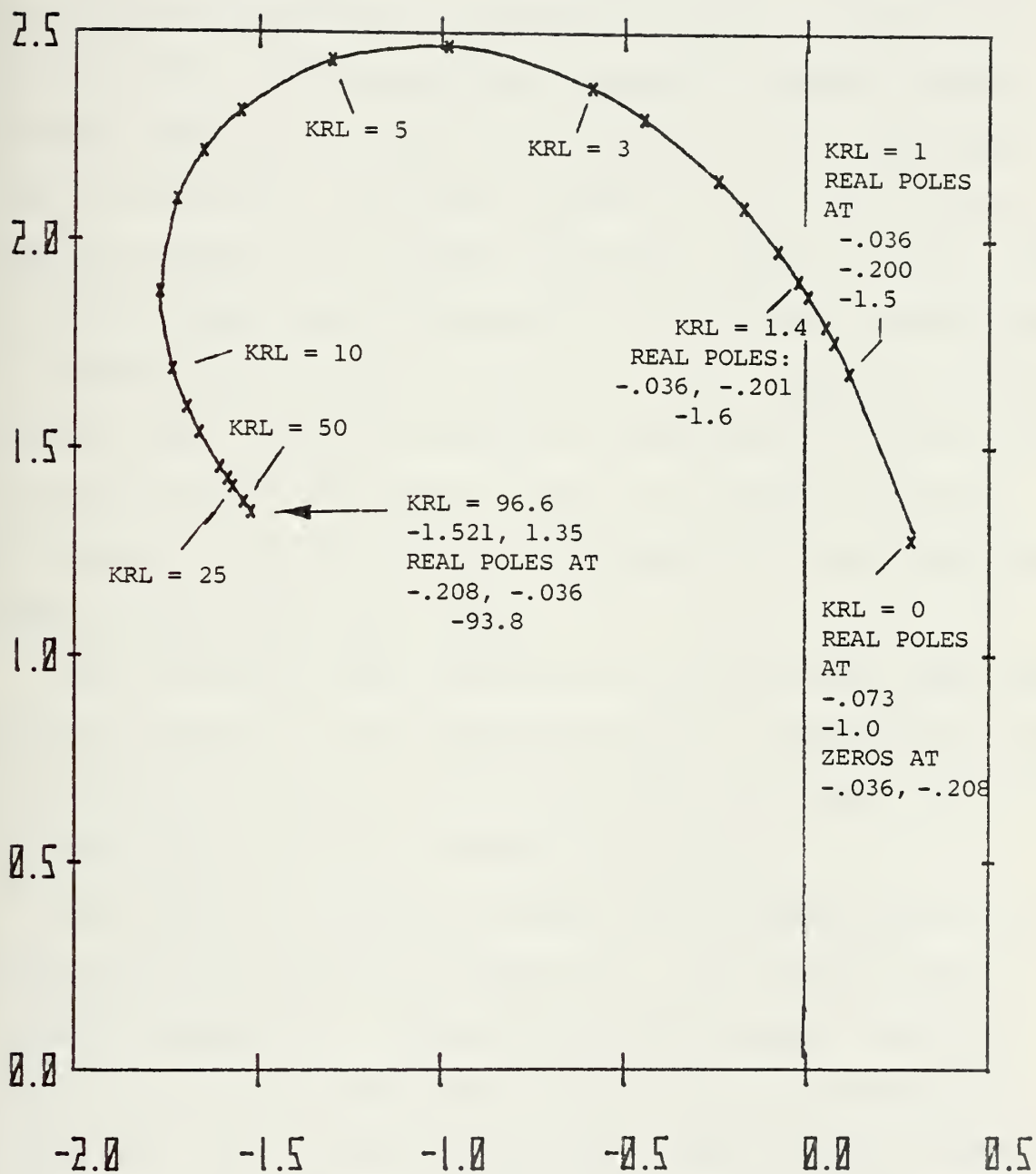


Figure 5-1 Root locus of the oscillatory poles of the longitudinal axis of the Harrier using SRFIMF position control. Note that the open loop zeros are nearly canceled at KRL = 1.0.

the real poles are not plotted, however their values are listed on the figure for various values of KRL. At the final value of KRL (96.6), the system's real poles were located at -93.82, -.2079 and -.036. The pole at -93.28 corresponds to the controller mode and its location is nearly equal to the value of KRL. This result was discussed in section three. The two other poles located at -.036 and -.2079 cancel the open loop zeroes of the plant located at -.036 and -.21 as seen in the open loop transfer function, equation 5-1b. Zero cancellation by a pole could be very detrimental to the response if the open loop zeroes are located in the right half of the complex plane, because it would be unreasonable to expect perfect pole-zero cancellation. This is a problem typically encountered in model following techniques when the plant has zeroes in the right half plane.

From the root locus, figure 5-1, it can be seen that the dynamic behavior of the SRFIMF controller is unchanged by the introduction of a more complicated plant. We shall now consider the time response of the closed loop system.

The controller and plant system was simulated using the CSMP program discussed in section III. The source code is listed in Appendix A. Simulation of the Harrier transfer function is illustrated using a signal flow graph shown in figure 5-2. The outputs of position, velocity and acceleration are shown in the figure as part of the overall transfer function simulation. For the simulation, KRL was chosen to be 50, τ was

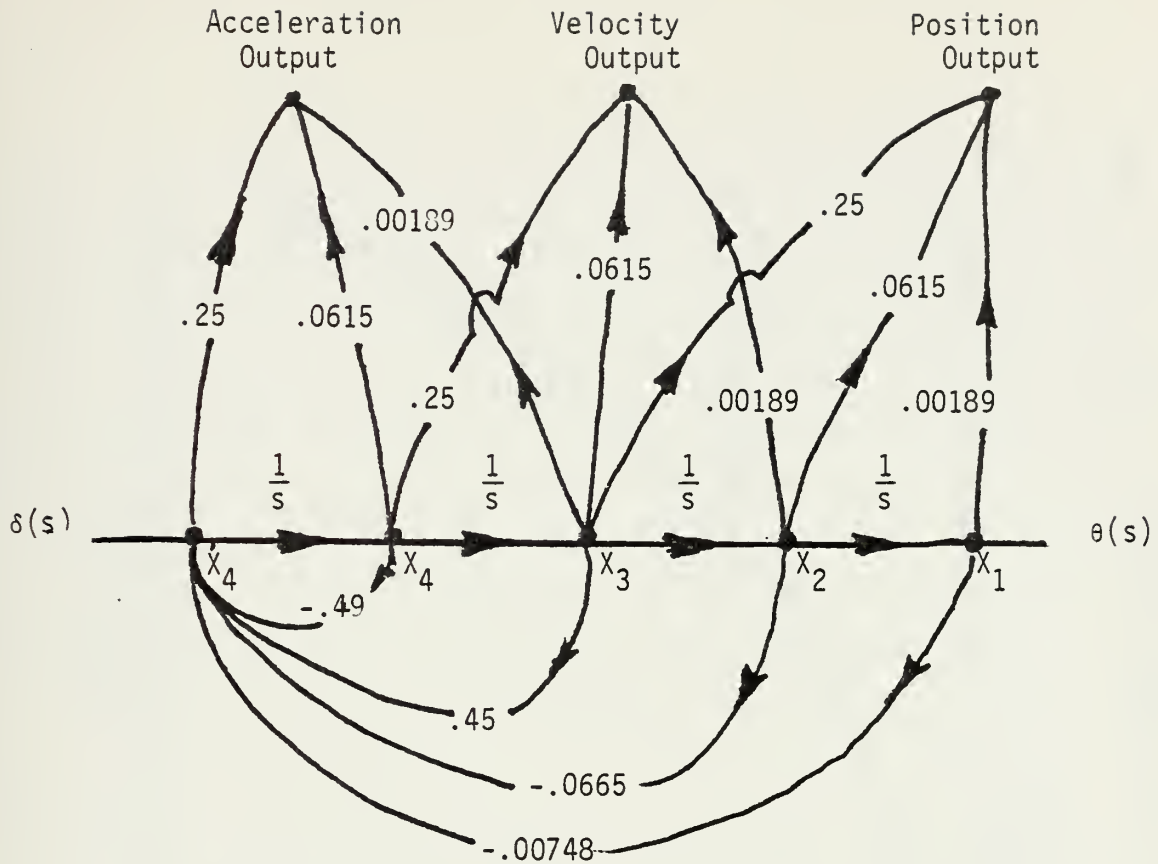


Figure 5-2 Harrier longitudinal signal flow graph transfer function simulation.

0.1 sec, K_x and K_x were 3 and 4. Plots of the time histories of the closed and open loop position, $\theta(t)$, as a result of the simulation, are given in figure 5-3. The figure indicates that the closed loop dynamic response is nearly identical to that of the model as shown in figure 3-5.

To evaluate the effect of the sensor noise, the state space representation of the system is required. Four states represent the plant. Defining X_1 and position and X_2 as velocity we write the transfer function for the Harrier, given

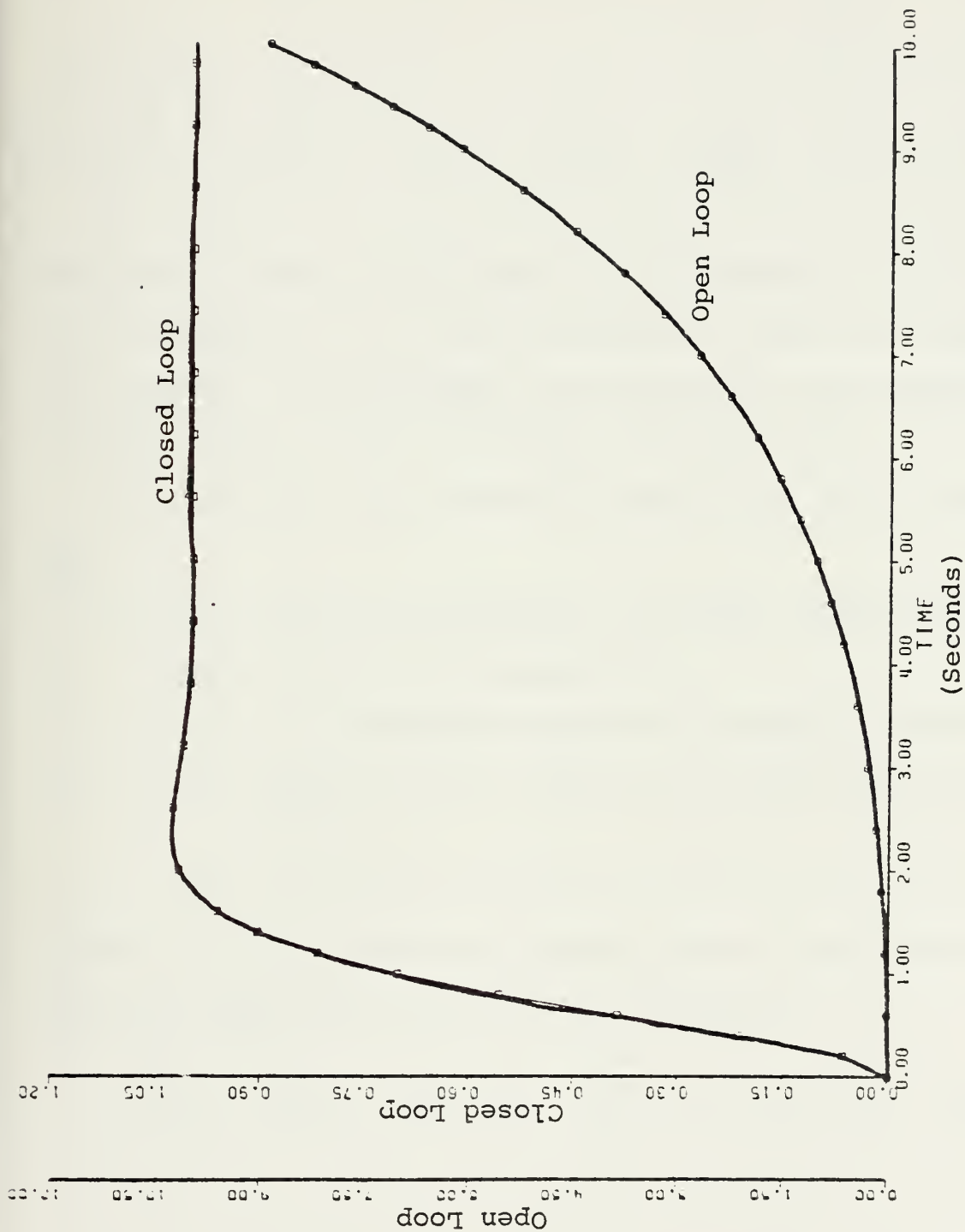


Figure 5-3 Simulation of the unit step response of the pitch attitude of the AV-8A Harrier with SRFIMF control.

in equation 5-1 in matrix notation as

$$\begin{Bmatrix} \dot{x}_1 \\ \dot{x}_2 \\ \dot{x}_3 \\ \dot{x}_4 \end{Bmatrix} = \begin{bmatrix} 0 & 1 & 0 & 0 \\ 0 & 0 & 1 & 0 \\ 0 & 0 & 0 & 1 \\ -.00747 & -.06736 & +.4495 & -.4896 \end{bmatrix} \begin{Bmatrix} x_1 \\ x_2 \\ x_3 \\ x_4 \end{Bmatrix} + \begin{Bmatrix} 0 \\ .25 \\ -.061 \\ .1443 \end{Bmatrix} \delta e \quad 5-2$$

The control vector of equation 5-2 is determined by the numerator of equation 5-1 so that the states x_1 and x_2 are position and velocity. The algorithm for determining the required control vector is given by Ogata, reference [13].

The remaining state variables are defined in the following way

x_5 = output of the control actuator, input to the plant

x_6 = output of the compensator

x_7 = state variable representing velocity sensor error

x_8 = state variable representing acceleration sensor error

x_9 = state variable representing position sensor error

Figure 5-4 is the schematic representation of the system and from the figure the control law is obtained as

$$W(t) = -K_x x_1 - K_v x_2 - x_3 - CPG x_5 + x_6 - K_a x_7 - x_8 - K_p x_9$$

5-3

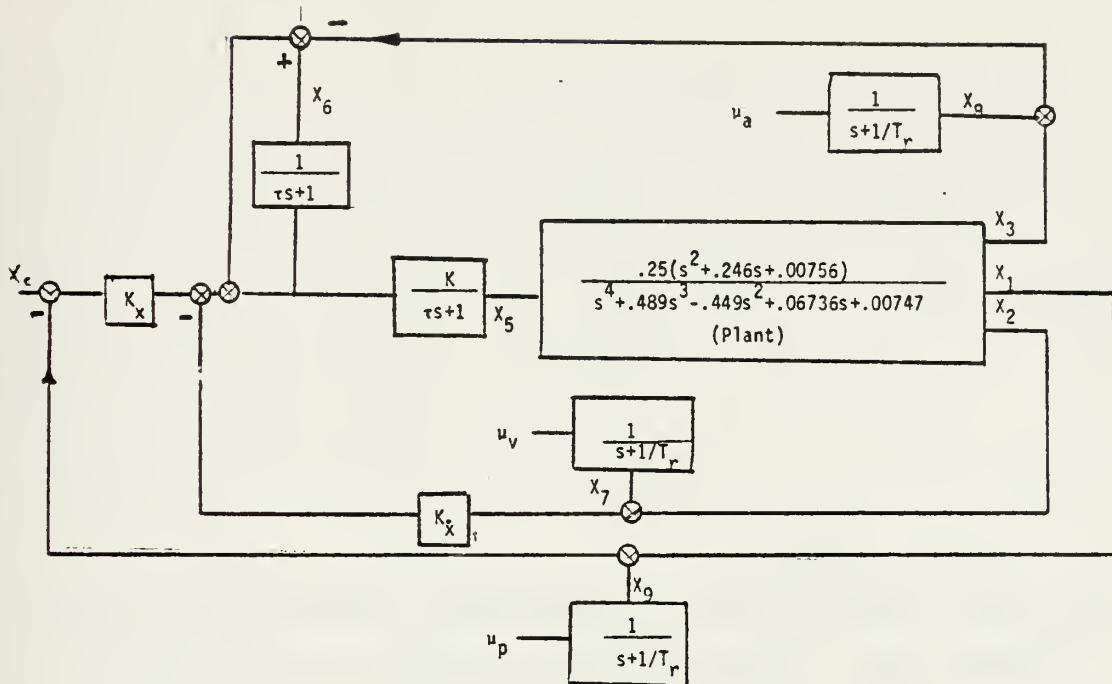


Figure 5-4 Schematic representation of the AV-8A Harrier pitch axis with the SRFIMF controller. Including sensor noise.

Combining and expressing the system in matrix form, the closed loop system is given by

$$\dot{\hat{X}} = A\hat{X} + BQ \quad 5-4$$

$$A = \begin{bmatrix} 0 & 1 & 0 & 0 & 0 & 0 & 0 & 0 & 0 \\ 0 & 0 & 1 & 0 & .25 & 0 & 0 & 0 & 0 \\ 0 & 0 & 0 & 1 & -.06115 & 0 & 0 & 0 & 0 \\ .00748 & -.0675 & .45 & -.4906 & .1443 & 0 & 0 & 0 & 0 \\ -KK_x/\tau & -KK_x/\tau & -K/\tau & 0 & -(.25K+1)/\tau & K/\tau & -KK_x/\tau & -K/\tau & -KK_x/\tau \\ -K_x/\tau & -K_x/\tau & -1/\tau & 0 & -.25/\tau & 0 & -K_x/\tau & -1/\tau & -K_x/\tau \\ 0 & 0 & 0 & 0 & 0 & 0 & -1/T_r & 0 & 0 \\ 0 & 0 & 0 & 0 & 0 & 0 & 0 & -1/T_r & 0 \\ 0 & 0 & 0 & 0 & 0 & 0 & 0 & 0 & -1/T_r \end{bmatrix}$$

$$B = \begin{bmatrix} 0 & 0 & 0 \\ 0 & 0 & 0 \\ 0 & 0 & 0 \\ 0 & 0 & 0 \\ 0 & 0 & 0 \\ 0 & 0 & 0 \\ 1 & 0 & 0 \\ 0 & 1 & 0 \\ 0 & 0 & 1 \end{bmatrix} \quad Q = \begin{bmatrix} 2\sigma_v^2/T_r & 0 & 0 \\ 0 & 2\sigma_a^2/T_r & 0 \\ 0 & 0 & 2\sigma_p^2/T_r \end{bmatrix}$$

Having the system, represented in state space, the technique used in the previous section can be applied. The general solution will be obtained for a unit value of sensor error standard deviation and later applied to the specific sensor suits assumed earlier. The constants required to obtain the numerical solution are: $K = 20$; $\tau = 0.1$; $K_x = 4$; $K_{\dot{x}} = 3$; $KRL = K \cdot CPG/\tau = 50$. The resulting system is

$$\dot{X} = AX + BQ \quad 5-5$$

$$Y = CX$$

$$\dot{X}^* = A^*X^* + B^*Q \quad 5-6$$

$$Y = C^*X^*$$

(Matricies A, B, C, A*, B* and C* are shown on the following pages.)

The result of the modal transformation is that the noise sources have about the same controllability and observability as in the

$$A = \begin{bmatrix} 0.0 & 1.0 & 0.0 & 0.0 & 0.0 & 0.0 & 0.0 & 0.0 \\ 0.0 & 0.0 & 1.0 & 0.0 & 0.25 & 0.0 & 0.0 & 0.0 \\ 0.0 & 0.0 & 0.0 & 1.0 & -0.06 & 0.0 & 0.0 & 0.0 \\ -0.01 & -0.07 & 0.45 & -0.49 & 0.14 & 0.0 & 0.0 & 0.0 \\ -800.0 & -800.0 & -200.0 & 0.0 & -60.0 & 200.0 & -600.0 & -800.0 \\ -40.0 & -30.0 & -10.0 & 0.0 & -2.5 & 0.0 & -30.0 & -40.0 \\ 0.0 & 0.0 & 0.0 & 0.0 & 0.0 & 0.0 & -0.1 & 0.0 \\ 0.0 & 0.0 & 0.0 & 0.0 & 0.0 & 0.0 & 0.0 & 0.0 \\ 0.0 & 0.0 & 0.0 & 0.0 & 0.0 & 0.0 & -0.1 & 0.0 \\ 0.0 & 0.0 & 0.0 & 0.0 & 0.0 & 0.0 & 0.0 & -0.1 \end{bmatrix}$$

$$B = \begin{bmatrix} 0.0 & 0.0 & 0.0 & 0.0 & 0.0 & 0.0 & 0.0 & 0.0 \\ 0.0 & 0.0 & 0.0 & 0.0 & 0.0 & 0.0 & 0.0 & 0.0 \\ 0.0 & 0.0 & 0.0 & 0.0 & 0.0 & 0.0 & 0.0 & 0.0 \\ 0.0 & 0.0 & 0.0 & 0.0 & 0.0 & 0.0 & 0.0 & 0.0 \\ 0.0 & 0.0 & 0.0 & 0.0 & 0.0 & 0.0 & 0.0 & 0.0 \\ 1.0 & 0.0 & 0.0 & 0.0 & 0.0 & 0.0 & 0.0 & 0.0 \\ 0.0 & 1.0 & 0.0 & 0.0 & 0.0 & 0.0 & 0.0 & 0.0 \\ 0.0 & 0.0 & 0.0 & 0.0 & 0.0 & 1.0 & 0.0 & 0.0 \end{bmatrix}$$

B =

$$C = \begin{bmatrix} 1.0 & 0.0 & 0.0 & 0.0 & 0.0 & 0.0 & 0.0 & 1.0 \\ 0.0 & 1.0 & 0.0 & 0.0 & 0.0 & 0.0 & 1.0 & 0.0 \\ 0.0 & 0.0 & 1.0 & 0.0 & 0.0 & 0.0 & 0.0 & 0.0 \end{bmatrix}$$

C =

$$A^* = \begin{bmatrix} -47.17 & 0.0 & 0.01 & 0.0 & 0.0 & 0.0 & 0.0 & 0.0 \\ 0.0 & -1.54 & 1.37 & 0.0 & 0.0 & 0.0 & 0.0 & 0.0 \\ 0.0 & -1.37 & -1.54 & 0.0 & 0.0 & 0.0 & 0.0 & 0.0 \\ 0.0 & 0.0 & 0.0 & -0.21 & 0.0 & 0.0 & 0.0 & 0.0 \\ 0.0 & 0.0 & 0.0 & 0.0 & -0.03 & 0.0 & 0.0 & 0.0 \\ 0.0 & 0.0 & 0.0 & 0.0 & 0.0 & -10.0 & 0.0 & 0.0 \\ 0.0 & 0.0 & 0.0 & 0.0 & 0.0 & 0.0 & -0.1 & 0.0 \\ 0.0 & 0.0 & 0.0 & 0.0 & 0.0 & 0.0 & -0.1 & -0.1 \end{bmatrix}$$

$$\begin{matrix} Q_v & Q_a & Q_p \end{matrix} \begin{bmatrix} -13.55 & -4.52 & -18.07 \\ 10.18 & 3.39 & 13.57 \\ -7.15 & -2.38 & -9.53 \\ 5.41 & 1.80 & 7.21 \\ 1.25 & 0.42 & 1.67 \\ 0.0 & 0.0 & 0.0 \\ 2.26 & 0.0 & 0.0 \\ 0.0 & 1.21 & 0.0 \\ 0.0 & 0.0 & 2.88 \end{bmatrix}$$

$$B^* =$$

$$C^* = \begin{bmatrix} 0.0 & 0.01 & -0.1 & 0.0 & 0.0 & 0.0 & -0.36 & -0.03 \\ 0.01 & 0.11 & 0.16 & 0.0 & 0.0 & -0.03 & 0.48 & 0.04 \\ 0.0 & -0.01 & -0.1 & -0.24 & 0.24 & 0.01 & 0.19 & 0.20 \end{bmatrix} \begin{matrix} x_v^* \\ x_a^* \\ x_p^* \end{matrix}$$

earlier cases. It can be seen from the A^* matrix that the closed loop system has two additional eigenvalues. These correspond to the shifted poles of the system. Variance analysis was done in the same way as in the earlier examples and the results are shown plotted in figures 5-5 through 5-8 and tabulated in Appendix B, table B-4. Table 5-1 lists the steady state values of the expected error in states X_1 , X_2 and X_5 .

	X_1	X_2	X_5
Position measurement error	0.98	0.36	3.85
Velocity measurement error	0.73	0.27	2.90
Acceleration measurement error	0.25	0.089	0.96

Table 5-1 Steady state values of σ_1 , σ_2 and σ_5 as a result of position, velocity and acceleration measurement error.

Comparison of table 5-1 with table 4-2 indicates that the values of the standard deviation of the X_1 and X_2 errors are identical in both cases even though the two plants are very different. The standard deviation of the plan input error (X_5 here, X_3 in section IV) is slightly different in the two cases. This should be expected because of the difference in the value of control gain K , required to yield a value of KRL equal to 50 and the large difference between the two plants. From the variance analysis, we obtain an estimate of the expected errors in X_1 , X_2 and X_5 which result from the sensor suit assumed in section IV. These values are listed in table 5-2.

SIGMA XI VS. TIME

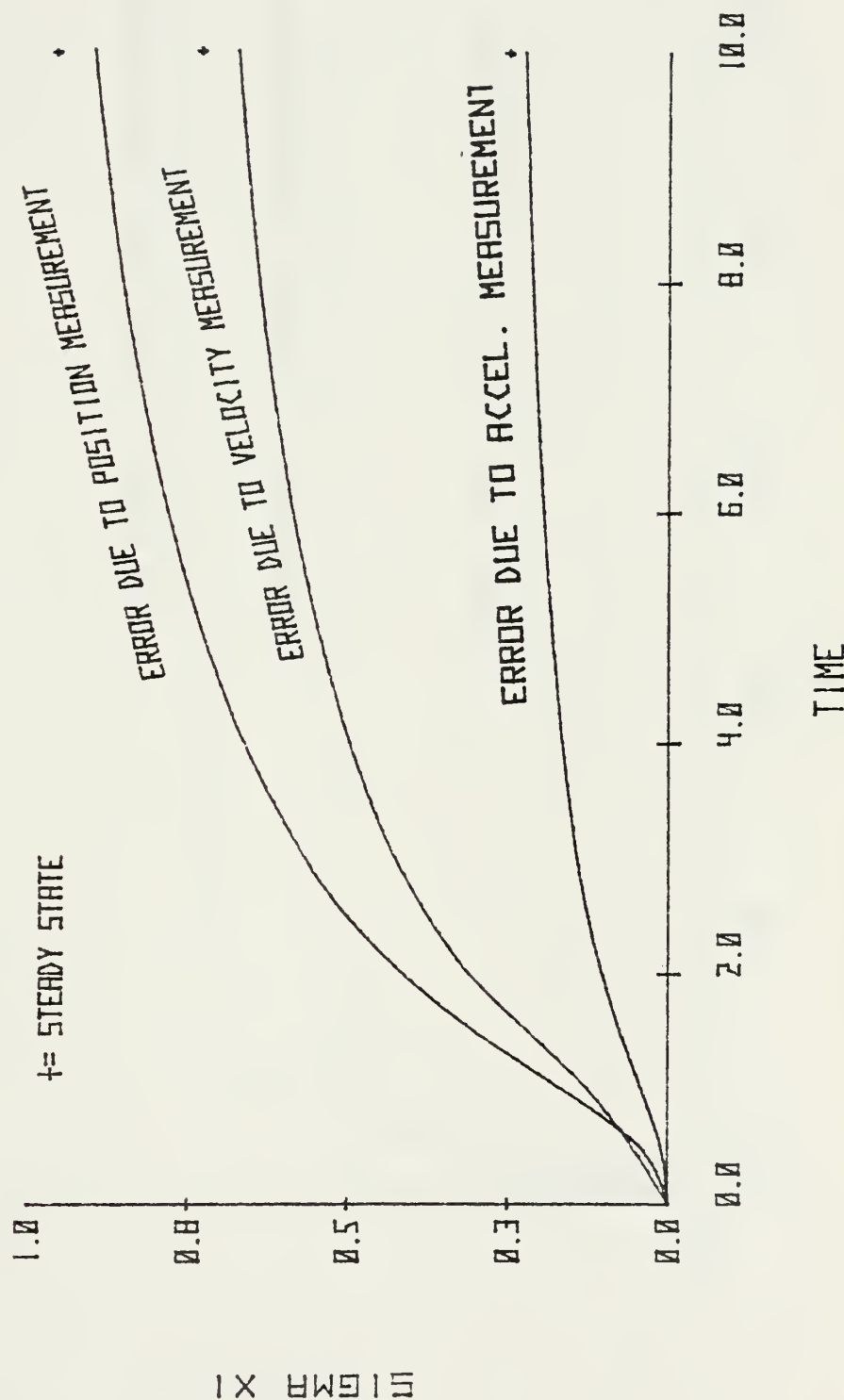


Figure 5-5 Tracking error in X_1 as a result of measurement error in position, velocity and acceleration for the Harrier longitudinal axis position control.

SIGMA X2 VS. TIME

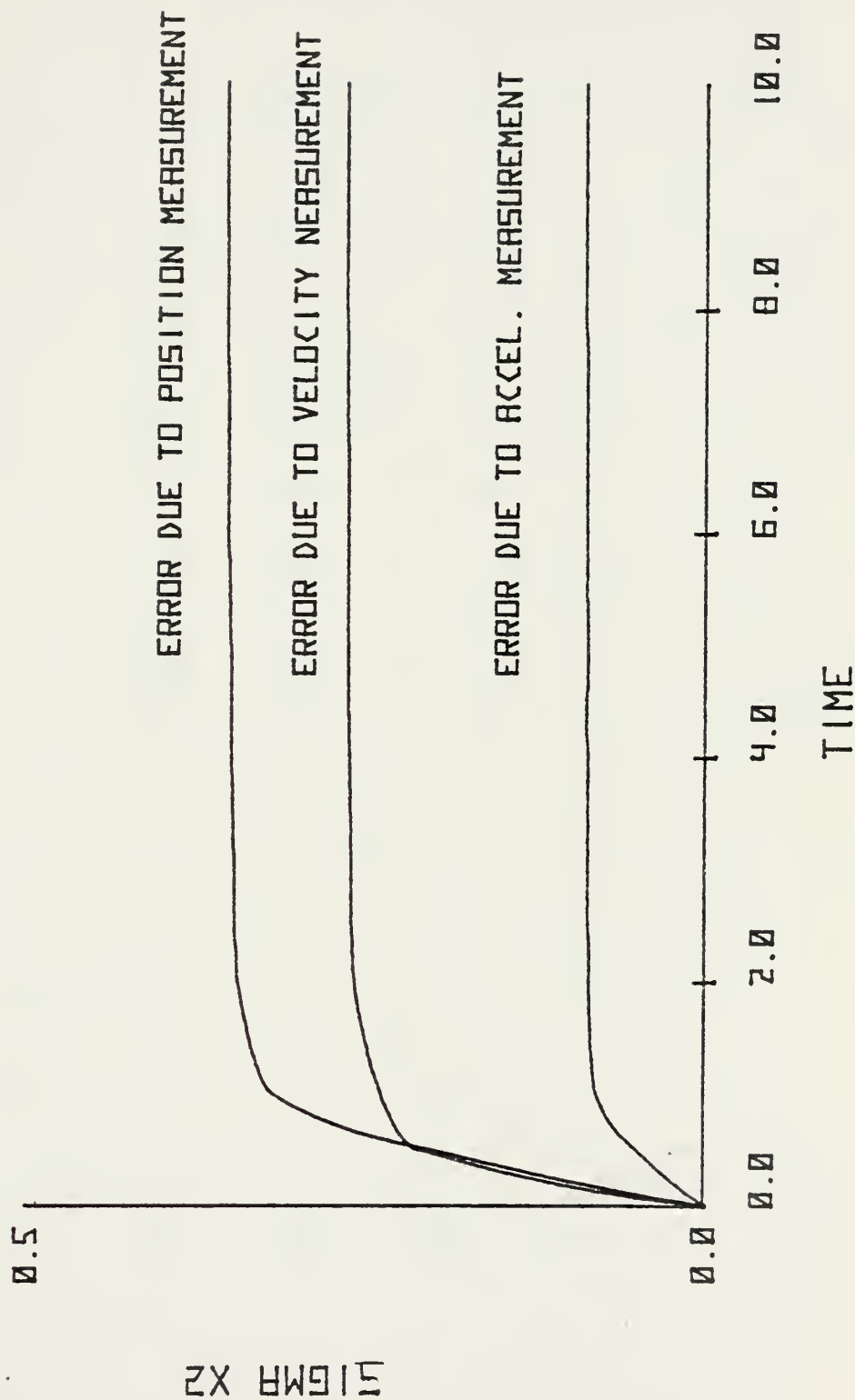


Figure 5-6 Tracking error in X_2 as a result of measurement error in position, velocity and acceleration for the Harrier longitudinal axis position control.

SIGMA X5 VS. TIME

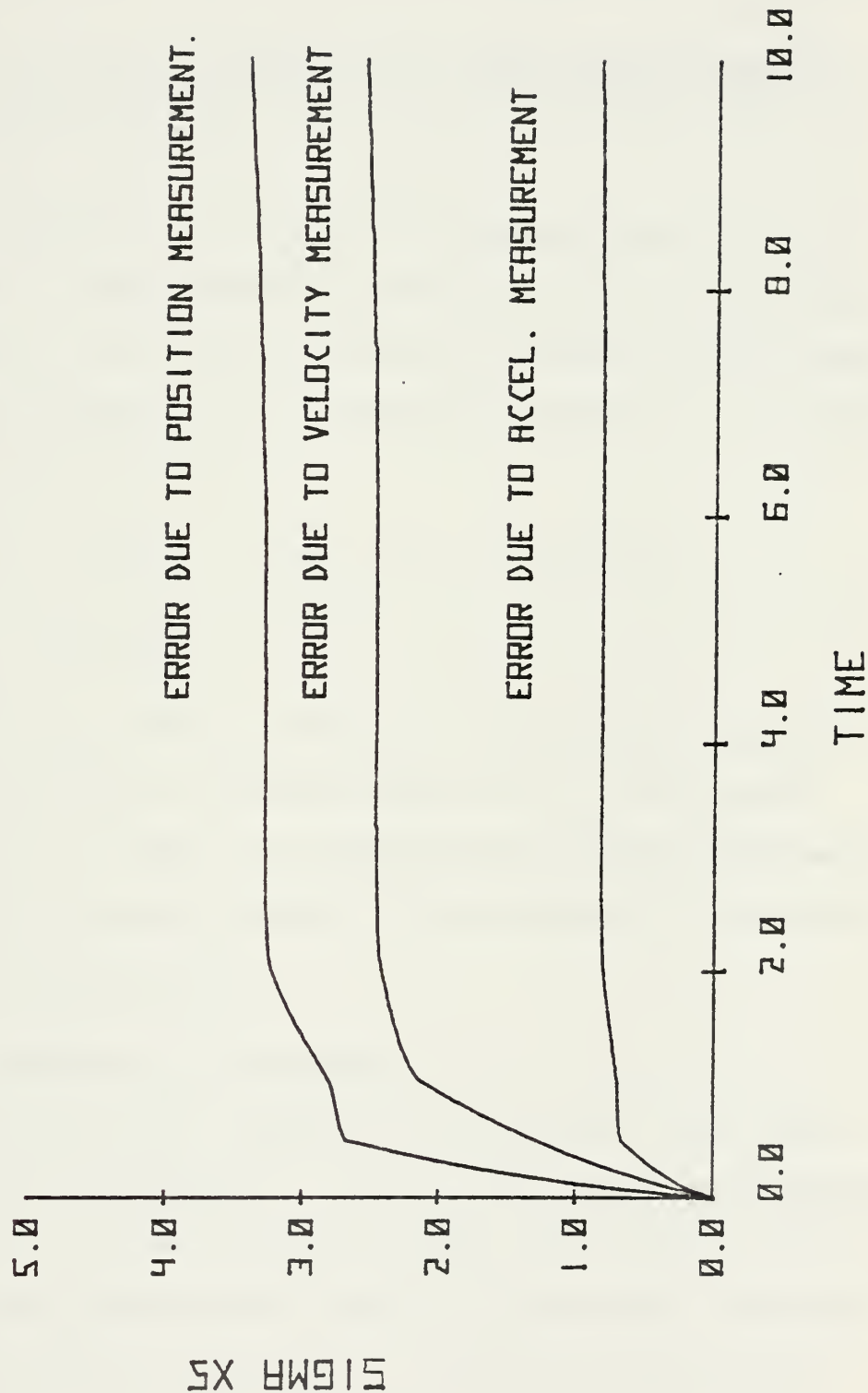


Figure 5-7 Tracking error in X_5 as a result of measurement error in position, velocity and acceleration for the Harrier longitudinal axis position control.

	<u>X₁</u>	<u>X₂</u>	<u>X₅</u>
Inertial sensors	0.49	0.18/sec	1.93/sec ²
Strapdown sensors	1.575	0.584/sec	6.26/sec ²

Table 5-2 Standard deviation of steady state tracking errors in X₁, X₂ and X₅ as a result of sensor noise in the Harrier aircraft.

The Significance of the total tracking error in X₅ is determined by comparing the standard deviation of the error to the value of X₅ when a 1° input is applied to the system. In quiescent operation, a 1° step input results in an instantaneous value of X₅ of

$$\begin{aligned}
 X_5 &= .0175\text{rad} \cdot 1^\circ K_x \quad K = 1.4 \text{ rad/sec}^2 \\
 &= 80^\circ/\text{sec}^2
 \end{aligned}$$

The value of X₅ given in table 5-2 for strapdown sensors whose expected error is in the order of 1° is not large compared to a 1° input. We conclude that sensor measurement errors do not adversely affect the performance of the SRFIMF Harrier pitch controller.

B. PITCH ATTITUDE GUST RESPONSE

The pitch attitude response of the Harrier from a gust input will be considered by applying the same type of analysis used earlier. For this purpose assume that the gust acts as an additional, uncontrolled input to the system. The symbol δ_g is used to denote this input. The gust input will be

modeled as an exponentially correlated noise source in the same way that the sensor noise was modeled. The schematic representation of an external exponentially correlated noise source was shown in figure 4-1. In this case the output of the noise source, $\xi(s)$, is the gust input to the system and $W_t(s)$ is the white noise input of strength μ_g as given by equation 4-12. The standard deviation and correlation time for the gust can be determined by examining the Dryden wind model used in simulation by NASA. At altitudes of 500 ft. and above the Dryden model assumes that the RMS value of atmospheric turbulence, σ_g , is given as

$$\sigma_g = 0.2 V_{\text{wind}}$$

The correlation time, T_g , is determined by a characteristic length, L_w , divided by the vehicle speed, V , or

$$T_g = L_w/V$$

The Dryden model gives the characteristic length of the turbulence as

$$150 \text{ ft.} + h = L_w$$

where h is the altitude. Choosing 500 ft. as the flight altitude, a flight speed of 60 kts and 15 kts as the value of the wind, the standard deviation and correlation time is

$$\sigma_g = 5 \text{ ft/sec}, T_g = 6.5 \text{ sec}$$

The gust input is represented schematically by figure 5-8.

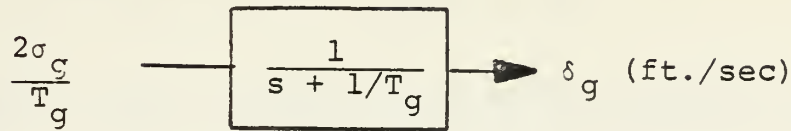


Figure 5-8 Gust shaping filter.

The transfer function between the gust and position, velocity and acceleration of the vehicle can be determined from the stability derivatives given by reference [14]. For This example we chose pitch attitude position control as was done in the previous example therefore the denominator of the gust transfer function is the same as the denominator of equation 5-1. The numerator is given by McRuer [14] for a vertical gust as

$$\frac{U_o N_g^w}{s} = (M_q - M_\alpha) s^2 + (M_\alpha - Z_w (M_q - M_\alpha)) s + X_u (M_\alpha + Z_w M_q) - X_w (V \cdot M_u + Z_u M_q) \quad 5-5$$

The stability derivatives for the Harrier at 60 kts are (6)

$$\begin{aligned} M_q &= -2.6 \\ M_\alpha &= V \cdot M_w = .54 \\ Z_w &= -.190 \\ Z_u &= -.036 \\ X_u &= -0.43 \\ X_w &= -0.27 \\ M_u &= .022 \end{aligned}$$

From equation 5-5 and 5-1, we obtain the transfer function for the pitch attitude from a gust input

$$\frac{\theta(s)}{\delta_g(s)} = \frac{-.0026s [s^2 + 2.31s + .073]}{s^4 + .4896s^3 - .4495s^2 + .0636s + .00747} \quad 5-6$$

The transfer function from the pilot's stick to the pitch angle is given by equation 5-1 where the input to the plant is δ_e . Expressing the plant, with multiple inputs of stick and gust load, in matrix notation with states X_1 and X_2 defined as position and velocity we have

$$\begin{Bmatrix} \dot{X}_1 \\ \dot{X}_2 \\ \dot{X}_3 \\ \dot{X}_4 \end{Bmatrix} = \begin{bmatrix} 0 & 1 & 0 & 0 \\ 0 & 0 & 1 & 0 \\ 0 & 0 & 0 & 1 \\ -.00747 & -.06736 & +.4495 & -.4896 \end{bmatrix} \begin{Bmatrix} X_1 \\ X_2 \\ X_2 \\ X_4 \end{Bmatrix} + \begin{bmatrix} 0 & -.0026 \\ .25 & -.00473 \\ -.061 & .00306 \\ .1443 & .00345 \end{bmatrix} [\delta_e \quad \delta_g]$$

The B matrix has been determined as before so that states X_1 and X_2 represent position and velocity.

Having the plant transfer function defined by 5-7 we can develop the equation to represent the closed loop controller. The additional state variables required are defined

X_5 = output of the control actuator, input to plant

X_6 = output of the compensator

X_7 = gust input to the plant, $\delta_g(s)$, figure 5-5.

The schematic of the closed loop system is shown in figure 5-9.

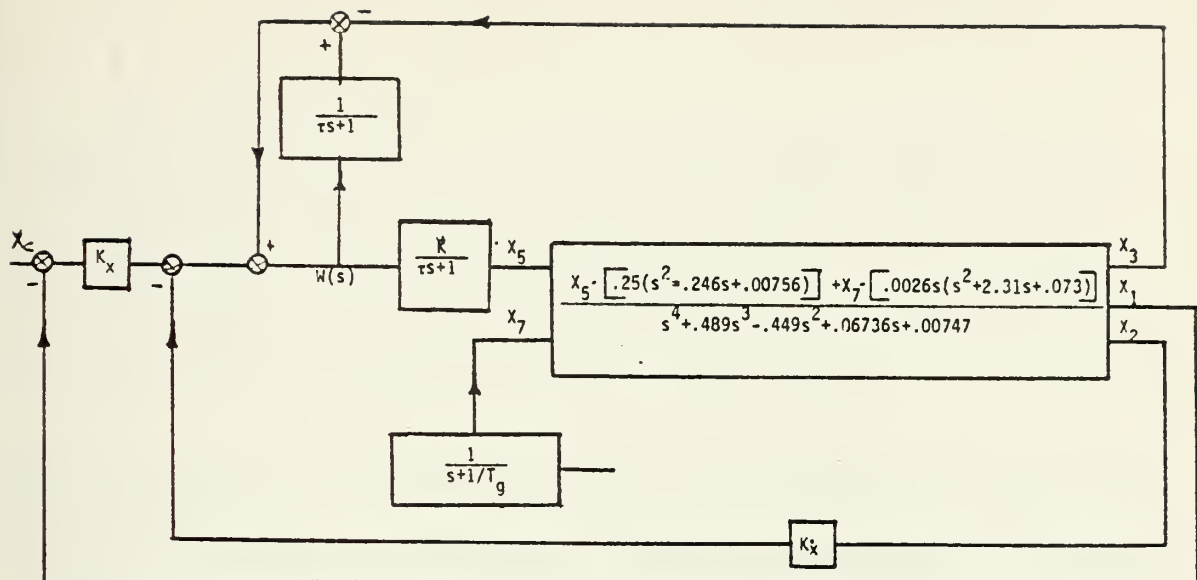


Figure 5-9 Schematic representation of the AV-8A Pitch control using a SRFIMF controller with wind gust input.

With $X_c = 0$, the control law $W(t)$ is

$$W(t) = -K_x X_1 - K_x X_2 - X_3 - .25X_5 + X_6 + (K_x \cdot .0026 + .00473)X_7$$

Rearranging in a manner similar to earlier work, we write the closed loop equation in matrix notation as

$$\dot{X} = AX + BQ \quad 5-8$$

$$A = \begin{bmatrix} 0 & 1 & 0 & 0 & 0 & 0 & -.0026 \\ 0 & 0 & 1 & 0 & .25 & 0 & -.00473 \\ 0 & 0 & 0 & 1 & -.061 & 0 & .00306 \\ -.00748 & -.0675 & .45 & -.49 & .1443 & 0 & .00346 \\ -K \cdot K_x / \tau & -K K_x / \tau & -K / \tau & 0 & -(.25 \cdot K + 1) / \tau & K / \tau & (K_x \cdot .0026 + .00473) K / \tau \\ -K_x / \tau & -K_x / \tau & -1 / \tau & 0 & -.25 / \tau & -K_x / \tau & (K_x \cdot .0026 + .00473) / \tau \\ 0 & 0 & 0 & 0 & 0 & 0 & -1 / T_g \end{bmatrix}$$

$$B = \begin{pmatrix} 0 \\ 0 \\ 0 \\ 0 \\ 0 \\ 0 \\ 1 \end{pmatrix}$$

$$Q = \begin{bmatrix} 2\sigma_g/T_g \end{bmatrix}$$

The covariance of the states were calculated for the system described above as was done in previous examples. The results of the covariance analysis was that the RMS values of X_1 and X_2 are very small and quickly reach the steady state values of

$$\sigma_p = \sigma_{X_1} = .0017$$

$$\sigma_v = \sigma_{X_2} = .0134$$

In the case of the gust we are interested in the pitch acceleration of the vehicle as a result of the gust input. Acceleration is given as \dot{X}_2 and from equation 5-8 is

$$\text{Acceleration} = X_3 + .25X_5 - .00473X_7 \quad 5-9$$

Recalling that the elements of the covariance matrix, P , are the squares of the standard deviations of the state variables, we write from equation 5-9 that

$$\sigma_{\text{accel}}^2 = P_{33}^{\frac{1}{2}} + .25P_{55}^{\frac{1}{2}} - .00473P_{77}^{\frac{1}{2}}$$

The standard deviation in pitch acceleration as a result of a gust input was plotted along with the gust input and the RMS value of X_5 as a function of time in figure 5-7. The results are also listed in Appendix B table B-5. The gust is shown for comparison of response time.

It is seen from the figure that the rise time in the RMS value of the vehicle acceleration is much slower than the gust itself. This result can be interpreted as a smoothing of the gust by the aircraft. This is primarily due to the slow response of the aircraft to the gust. The controller has a relatively fast reaction time and can maintain the output X_1 with only very small errors as a result of a gust input.

The analysis of the SRFIMF controller applied to the Harrier has indicated that the qualities of the controller found by analysis when the plant is assumed to be a second order system apply equally well when the plant is an actual VSTOL aircraft. We have also seen that the controller does not produce undesirable dynamic response when the vehicle is subjected to gust inputs and that the dynamic response of the aircraft and controller is due to the response of the aircraft alone to the gust.

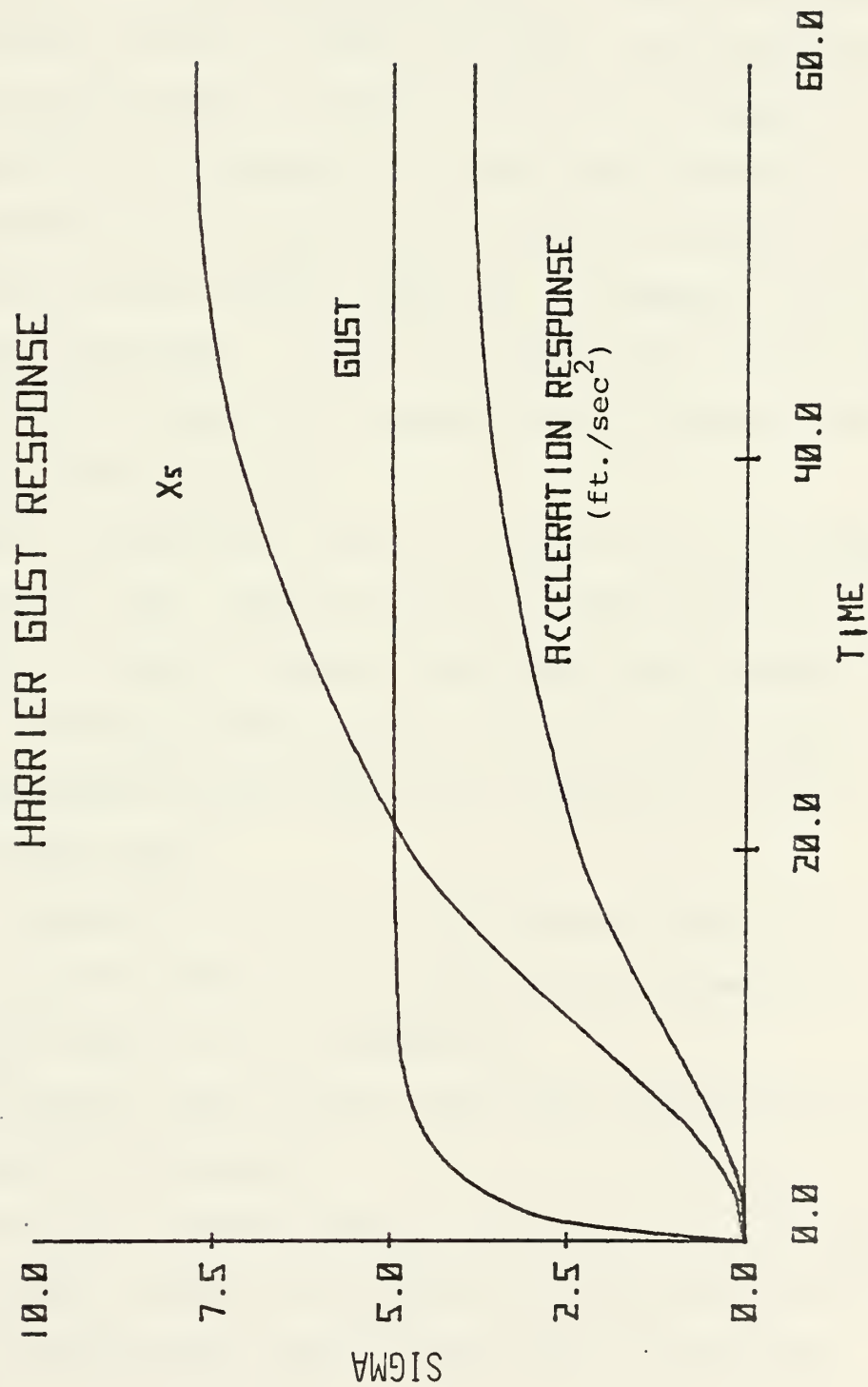


Figure 5-10 Standard deviation of vehicle pitch acceleration and plant input, X_5 , as a result of a gust.

VI. CONCLUSIONS

The use of State Rate Feedback Implicit Model Following, for the attitude control of VSTOL aircraft, has been studied. The SRFIMF control scheme is simple, easy to implement and can be expected to be reliable. It was shown that the dynamic response of the closed loop system is a second order response and that the natural frequency and damping are free choices of the designer. It was also shown that sensor noise does not adversely affect the operation of the system. Detailed conclusions of this study are:

1. Model following was shown in section III-D by simulations to be very good. Despite changing plant dynamics, representing a variety of flight conditions, the closed loop system had a response characteristic of that of the model and that the output of the closed loop system was driven to the value of the input.

2. The frequency response of the system is that of a low pass filter and that there was no phase shift between the output and the input at low frequencies.

3. Non-minimum phase system, pole-zero cancellation can lead to unstable performance.

4. High quality sensors are not required. It was shown by the covariance analysis in section IV-B that the error in position is approximately equal to the error in position

measurement plus 75 percent of the error in velocity measurement plus 25 percent of the error in acceleration measurement. The general result is that sensor errors do not adversely affect the performance of the system.

5. Estimation of position and velocity by integration of acceleration was shown to lead to unstable performance because of neutrally stable modes resulting from the integration. It was shown in section IV-C that acceleration sensor noise disturbs the neutrally stable modes with the result that the system diverges. It is then concluded that the quantities of position and velocity must be measured in order to have a stable system which does not require knowledge of the plant.

6. The system is capable of compensating for gust inputs. The analysis of section V-C showed that the error in position output was small as a result of the gust. Secondly, the response of the system to the gust is smoothed by the action of the uncontrolled plant.

APPENDIX A

COMPUTER LISTINGS

```

*****
*
*       ***   SRFIMF SIMULATION SOURCE CODE   ***
*
*       CSMP SOURCE CODE USED TO SIMULATE THE RESPONSE OF
*       THE SRFIMF AND AN ARBITRARY SECOND ORDER PLANT.
*       THE FUNCTIONS INTGRL AND REALPL ARE CSMP FUNCTIONS
*       WHICH PERFORM INTEGRATION OR SIMULATE A FIRST ORDER
*       RESPONSE. THE ORDER OF THE STATEMENTS IS UNIMPORTANT IN
*       CSMP.
*
*****
// EXEC CSMPXV
//X.COMPRINT DD DUMMY
//X.SYSPRINT DD DUMMY
//X.SYSIN DD *
    AS=REALPL(0,TOU,WS)
    X=INTGRL(0,VX)
    VX=INTGRL(0,AX)
    AX1=REALPL(0,TOU,IS)
    AX=AX1*CPG-C*X-B*VX
    IS=WS*K
    WS=-KXD*VX+(XC-X)*KX+VS
    VS=AS-AX
*
*       SIMULATION OF THE OPEN LOOP PLANT
*
    XDD=CPG*AX2-C*XP-VXP*B
    AX2=REALPL(0.,TOU,XC)
    VXP=INTGRL(0,XDD)
    XP=INTGRL(0,VXP)
    XC=G*STEP(0)
    G=1.
    CPG=4.
    TOU=.1
    K=5.
    KXD=3.
    KX=4.
    B=.6
    C=2.16
TIMER  FINTIM=10,OUTDEL=.2
OUTPUT X,XP
OUTPUT TIME,XP
PAGE  XYPLOT
      END
      STOP

```


A(2,2)=-BP
 A(2,3)=CPG
 A(3,1)=(CP-KX)*K/TOU
 A(3,2)=(BP-KXD)*K/TOU
 A(3,3)=- (CPG*K+1.)/TOU
 A(3,4)=K/TOU
 A(3,5)=-KXD*K/TOU
 A(3,6)=-K/TOU
 A(3,7)=-K*KX/TOU
 A(3,8)=-A(3,7)
 A(4,1)=A(3,1)/K
 A(4,2)=A(3,2)/K
 A(4,3)=-CPG/TOU
 A(4,4)=-KXD/TOU
 A(4,5)=-1./TOU
 A(4,6)=-KX/TOU
 A(4,7)=KX/TOU
 A(4,8)=KX/TOU
 A(5,5)=-1./TR(1)
 A(6,6)=-1./TR(2)
 A(7,7)=-1./TR(3)
 A(8,8)=-1./TR(4)

C

C

1

DO 1 I=1,M
 DO 1 J=1,N
 H(I,J)=0.
 H(1,1)=1.
 H(1,7)=1.
 H(2,2)=1.
 H(2,5)=1.
 H(3,1)=-CP
 H(3,2)=-BP
 H(3,3)=CPG
 H(3,6)=1.

C

4
20

DO 4 I=1,L
 DO 4 J=1,L
 Q(I,J)=0.
 Q(1,1)=(2./TR(1))*SIGMA1**2
 Q(2,2)=(2./TR(2))*SIGMA2**2
 Q(3,3)=(2./TR(3))*SIGMA3**2
 Q(4,4)=(2./TR(4))*SIGMA4**2

C

NPT=3
 T1=0.0

MOD00520
 MOD00530
 MOD00540
 MOD00550
 MOD00560
 MOD00570
 MOD00580
 MOD00590
 MOD00600
 MOD00610
 MOD00620
 MOD00630
 MOD00640
 MOD00650
 MOD00660
 MOD00670
 MOD00680
 MOD00690
 MOD00700
 MOD00710
 MOD00720
 MOD00730
 MOD00740
 MOD00750
 MOD00760
 MOD00770
 MOD00780
 MOD00790
 MOD00800
 MOD00810
 MOD00820
 MOD00830
 MOD00840
 MOD00850
 MOD00860
 MOD00870
 MOD00880
 MOD00890
 MOD00900
 MOD00910
 MOD00920
 MOD00930
 MOD00940
 MOD00950
 MOD00960
 MOD00970
 MOD00980
 MOD00990


```

A(3,1)=CP*K/TOU
A(3,2)=BP*K/TJJ
A(3,3)=-(CPG*K+1.)/TOU
A(3,4)=K/TOU
A(3,5)=-K*KXD/TOU
A(3,6)=-K*KX/TOU
A(3,7)=-K/TOU
A(3,8)=K*KX/TJU
A(4,1)=CP/TOU
A(4,2)=BP/TOU
A(4,3)=-CPG/TOU
A(4,5)=-KXD/TOU
A(4,6)=-KX/TOU
A(4,7)=-1./TOU
A(4,8)=KX/TOU
A(5,1)=-CP
A(5,2)=-BP
A(5,3)=CPG
A(5,7)=1.
A(6,5)=1.
A(7,7)=-1./TR(1)
A(8,8)=-1./TR(2)

```

C

136

```

B(7,1)=1.
B(8,2)=0.
H(1,1)=1.
H(2,2)=1.
H(3,1)=-CP
H(3,2)=-BP
SIGMA1=1.
SIGMA2=1.
H(3,7)=1.

```

C

```

Q(1,1)=(2./TR(1))*SIGMA1**2
Q(2,2)=(2./TR(2))*SIGMA2**2

```

```

NPT=1
T1=0.0
T2=.5

```

```

CALL ECHO(A,B,Q,H,TR,N,M,L)
CALL VARY(B,L,NPT,T1,T2)
CALL MODAL(A,B,H,N,M,L)

```

1151

```

STOP
END

```

MAIN 3

MAIN 3 IS THE CODE USED TO GENERATE THE A,B AND C MATRICES

C
C
C

MOD01480
MOD01490
MOD01500
MOD01510
MOD01520
MOD01530
MOD01540
MOD01550
MOD01560
MOD01570
MOD01580
MOD01590
MOD01600
MOD01610
MOD01620
MOD01630
MOD01640
MOD01650
MOD01660
MOD01670
MOD01680
MOD01690
MOD01700
MOD01710
MOD01720
MOD01730
MOD01740
MOD01750
MOD01760
MOD01770
MOD01780
MOD01790
MOD01800
MOD01810
MOD01820
MOD01830
MOD01840
MOD01850
MOD01860
MOD01870
MOD01880
MOD01890
MOD01900
MOD01910
MOD01920
MOD01930
MOD01940
MOD01950


```

C      FOR THE SECOND ALTERNATE MEASUREMENT SCHEME. IN THIS
C      CASE POSITION AND VELOCITY ARE MEASURED AND ACCELERATION IS
C      ESTIMATED.
C      *****
100  DIMENSION B(7,3), TR(3), H(3,7)
      REAL K, KX, KXD
      COMMON BP, CP, K, KX, KXD, TOU, CPG, N, PD(49), Q(7,7), A(7,7)
      WRITE(6,100)
      FORMAT(20X,90(' '),40X,'MODEL 3 MEASURED POSITION AND VELOC',
1      'ITY IMPLIED ACCELERATION',//,20X,90(' '),)
      N=7
      M=3
      L=3
      NCOUNT=0
      WRITE(6,502)
      FORMAT(//,10X,' ERROR DUE TO POSITION MEASUREMENT',//)
      SIGMA1=1.
      SIGMA2=1.
      SIGMA3=1.
      COMPUTE A,B,C,Q
      INITIALIZE ALL MATRICES
      DO 1 I=1,N
      DO 1 J=1,N
      A(I,J)=0.0
      DO 2 I=1,N
      DO 2 J=1,L
      B(I,J)=0.0
      DO 3 I=1,L
      DO 3 J=1,L
      Q(I,J)=0.0
      DO 4 I=1,M
      DO 4 J=1,N
      H(I,J)=0.0
      A(1,2)=1.
      A(2,1)=-CP
      A(2,2)=-BP
      A(2,3)=CPG
      A(3,1)=K*(CP-KX)/TOU
      A(3,2)=K*(BP-KXD)/TOU
      A(3,3)=-(K*CPG+1.)/TOU
      A(3,4)=K/TOU
      A(3,5)=A(3,1)
      A(3,6)=A(3,2)
MOD01960
MOD01970
MOD01980
MOD01990
MOD02000
MOD02010
MOD02020
MOD02030
MOD02040
MOD02050
MOD02060
MOD02070
MOD02080
MOD02090
MOD02100
MOD02110
MOD02120
MOD02130
MOD02140
MOD02150
MOD02160
MOD02170
MOD02180
MOD02190
MOD02200
MOD02210
MOD02220
MOD02230
MOD02240
MOD02250
MOD02260
MOD02270
MOD02280
MOD02290
MOD02300
MOD02310
MOD02320
MOD02330
MOD02340
MOD02350
MOD02360
MOD02370
MOD02380
MOD02390
MOD02400
MOD02410
MOD02420
MOD02430

```


MOD02920
MOD02930
MOD02940
MOD02950
MOD02960
MOD02970
MOD02980
MOD02990
MOD03000
MOD03010
MOD03020
MOD03030
MOD03040
MOD03050
MOD03060
MOD03070
MOD03080
MOD03090
MOD03100
MOD03110
MOD03120
MOD03130
MOD03140
MOD03150
MOD03160
MOD03170
MOD03180
MOD03190
MOD03200
MOD03210
MOD03220
MOD03230
MOD03240
MOD03250
MOD03260
MOD03270
MOD03280
MOD03290
MOD03300
MOD03310
MOD03320
MOD03330
MOD03340
MOD03350
MOD03360
MOD03370
MOD03380
MOD03390

```

KX=4.
KXD=3.
TOU=.1
SIGMA1=1.
SIGMA2=1.
SIGMA3=1.
TR(1)=10.
TR(2)=10.
TR(3)=10.

      CALCULATE THE A MATRIX

      DO 1 I=1,N
      DO 1 J=1,N
      A(I,J)=0.0
      A(1,2)=1.
      A(2,3)=1.
      A(2,5)=.25
      A(3,4)=1.
      A(3,5)=-.06115
      A(4,1)=-.00748
      A(4,2)=-.0675
      A(4,3)=.45
      A(4,4)=-.4906
      A(4,5)=.14428
      A(5,1)=-K*KX/TOU
      A(5,2)=-K*KXD/TOU
      A(5,3)=-K/TOU
      A(5,5)=-(.25*K+1.)/TOU
      A(5,6)=K/TOU
      A(5,7)=-K*KXD/TOU
      A(5,8)=-K/TOU
      A(5,9)=-K*KX/TOU
      A(6,1)=-KX/TOU
      A(6,2)=-KXD/TOU
      A(6,3)=-1./TOU
      A(6,5)=-.25/TOU
      A(6,7)=-KXD/TOU
      A(6,8)=-1./TOU
      A(6,9)=-KX/TOU
      A(7,7)=-1./TR(1)
      A(8,8)=-1./TR(2)
      A(9,9)=-1./TR(3)

      B MATRIX

      DO 2 I=1,N
      DO 2 J=1,L

```

C C C

1

C C C


```

2      B(I,J)=0.0
      B(7,1)=1.
      B(8,2)=1.
      B(9,3)=1.
      CONTINUE
20     C
      C
      C      Q MATRIX
      DO 3 I=1,M
      DO 3 J=1,M
      Q(I,J)=0.0
      Q(I,1)=(2./TR(1))*SIGMA1**2
      Q(2,2)=(2./TR(2))*SIGMA2**2
      Q(3,3)=(2./TR(3))*SIGMA3**2
      C
      C      C MATRIX
      DO 4 I=1,M
      DO 4 J=1,N
      H(I,J)=0.0
      H(1,1)=1.0
      H(1,9)=1.
      H(2,2)=1.0
      H(2,7)=1.0
      H(3,3)=1.0
      H(3,8)=1.
      NPT=40
      T1=0.
      T2=20.
      CALL ECHO(A,B,Q,H,TR,N,M,L)
      CALL MODAL(A,B,H,N,M,L)
      CALL VARY (B,L,NPT,T1,T2)
      STOP
      END
C*****
C      HARRIER G
C
C      HARRIER G IS THE CODE USED TO GENERATE THE A,B AND C
C      MATRICES FOR THE COVARIANCE CALCULATION OF THE HARRIER
C      LONGITUDINAL AXIS SRFIMF CONTROL WITH A GUST INPUT.
C*****
C      DIMENSION B(10,4),H(3,10),TR(4)
C      REAL K,KX,KXD
C      COMMON BP,CP,K,KX,KXD,TDU,CPG,N,PD(100),Q(10,10),A(10,10)
C      WRITE(6,100)
C      FORMAT(/,20X,90(' '),//,40X,'HARRIER MODEL ',
100

```



```

1. ALL QUANTITIES MEASURED',//,20X,90('*'),//)
N=10
L=4
M=3
K=20.
KX=4.
KXD=3.
TOU=.1
SIGMA1=1.
SIGMA2=1.
SIGMA3=1.
SIGMA4=1.
TR(1)=10.
TR(2)=10.
TR(3)=10.
TR(4)=6.5
CALCULATE THE A MATRIX
DO 1 I=1,N
DO 1 J=1,N
A(I,J)=0.0
A(1,2)=1.
A(1,10)=-.0026
A(2,3)=1.
A(2,5)=.25
A(2,10)=-.00473
A(3,4)=1.
A(3,5)=-.06115
A(3,10)=-.00306
A(4,1)=-.00748
A(4,2)=-.0675
A(4,3)=.45
A(4,4)=-.4906
A(4,5)=.14428
A(4,10)=-.00346
A(5,1)=-K*KX/TOU
A(5,2)=-K*KXD/TOU
A(5,3)=-K/TOU
A(5,5)=-(.25*K+1.)/TOU
A(5,6)=K/TOU
A(5,7)=-K*KXD/TOU
A(5,8)=-K/TOU
A(5,9)=-K*KX/TOU
A(5,10)=(KXD*.0026+.00473)*K/TOU
A(6,1)=-KX/TOU
A(6,2)=-KXD/TOU
A(6,3)=-1./TOU

```

C C C 1

MOD03880
MOD03890
MOD03900
MOD03910
MOD03920
MOD03930
MOD03940
MOD03950
MOD03960
MOD03970
MOD03980
MOD03990
MOD04000
MOD04010
MOD04020
MOD04030
MOD04040
MOD04050
MOD04060
MOD04070
MOD04080
MOD04090
MOD04100
MOD04110
MOD04120
MOD04130
MOD04140
MOD04150
MOD04160
MOD04170
MOD04180
MOD04190
MOD04200
MOD04210
MOD04220
MOD04230
MOD04240
MOD04250
MOD04260
MOD04270
MOD04280
MOD04290
MOD04300
MOD04310
MOD04320
MOD04330
MOD04340
MOD04350


```

A(6,5)=-.25/TOU
A(6,7)=-KXD/TOU
A(6,8)=-1./TOU
A(6,9)=-KX/TOU
A(6,10)=A(5,10)/K
A(7,7)=-1./TR(1)
A(8,8)=-1./TR(2)
A(9,9)=-1./TR(3)
A(10,10)=-1./TR(4)

```

C C C

```

B MATRIX

```

```

DO 2 I=1,N
DO 2 J=1,L
B(I,J)=0.0
B(7,1)=1.
B(8,2)=1.
B(9,3)=1.
B(10,4)=1.

```

2

```

Q MATRIX

```

```

DO 3 I=1,L
DO 3 J=1,L
Q(I,J)=0.0
Q(1,1)=(2./TR(1))*SIGMA1**2
Q(2,2)=(2./TR(2))*SIGMA2**2
Q(3,3)=(2./TR(3))*SIGMA3**2
Q(4,4)=(2./TR(4))*SIGMA4**2

```

3

```

C MATRIX

```

```

DO 4 I=1,M
DO 4 J=1,N
H(I,J)=0.0
H(1,1)=1.0
H(2,2)=1.0
H(3,3)=1.0
NPT=60
T1=0.
T2=60.
ECHO(A,B,Q,H,TR,N,M,L)
CALL MODAL(A,B,H,N,M,L)
CALL VARY(B,L,NPT,T1,T2)
STOP
END

```

C C C

4

```

MOD04360
MOD04370
MOD04380
MOD04390
MOD04400
MOD04410
MOD04420
MOD04430
MOD04440
MOD04450
MOD04460
MOD04470
MOD04480
MOD04490
MOD04500
MOD04510
MOD04520
MOD04530
MOD04540
MOD04550
MOD04560
MOD04570
MOD04580
MOD04590
MOD04600
MOD04610
MOD04620
MOD04630
MOD04640
MOD04650
MOD04660
MOD04670
MOD04680
MOD04690
MOD04700
MOD04710
MOD04720
MOD04730
MOD04740
MOD04750
MOD04760
MOD04770
MOD04780
MOD04790
MOD04800
MOD04810

```



```

MOD000520
MOD000530
MOD000540
MOD000550
MOD000560
MOD000570
MOD000580
MOD000590
MOD000600
MOD000610
MOD000620
MOD000630
MOD000640
MOD000650
MOD000660
MOD000670
MOD000680
MOD000690
MOD000700
MOD000710
MOD000720
MOD000730
MOD000740
MOD000750
MOD000760
MOD000770
MOD000780
MOD000790
MOD000800
MOD000810
MOD000820
MOD000830
MOD000840
MOD000850
MOD000860
MOD000870
MOD000880
MOD000890
MOD000900
MOD000910
MOD000920
MOD000930
MOD000940
MOD000950
MOD000960
MOD000970
MOD000980
MOD000990

FNORM=0.0
IF(AIMAG(W(J)).NE.0) GO TO 4
EIGENVECTOR IS REAL
DO 2 I=1,N
  FNORM=FNORM+REAL(Z(I,J)**2)
DO 3 I=1,N
  T(I,J)=REAL(Z(I,J))/SQRT(FNORM)
GO TO 7
COMPLEX NORMALIZATION
DO 5 I=1,N
  TAT=REAL(Z(I,J)**2)
  IF(TAT.LE.FNORM) GO TO 5
  IMAX=I
  FNORM=TAT
CONTINUE
THE I*TH ROW WILL BE NORMALIZED TO 1+0I
XN1=REAL(Z(IMAX,J))
XN2=AIMAG(Z(IMAX,J))
ENORM=CMPLX(XN1/(XN1+XN2**2),-XN2/(XN1+XN2**2))
DO 6 I=1,N
  VNORM=Z(I,J)*ENORM
  T(I,J)=REAL(VNORM)
  T(I,J+1)=AIMAG(VNORM)
  J=J+1
  J=J+1
  IF(J.LE.N) GO TO 10
WRITE THE NORMALIZED MATRIX
WRITE(5,203)
FORMAT(/,10X,'THE NORMALIZED TRANSFER MATRIX IS',/)
WRITE(6,100) ((T(I,J),J=1,N),I=1,N)
INVERT T
IDGT=0
CALL LINV2F(T,N,IA,A,IDGT,WK,IER)
WRITE(6,204)
FORMAT(/,10X,'THE INVERSE OF THE TRANSFORM IS',/)
WRITE(6,100) ((A(I,J),J=1,N),I=1,N)
TAKE T INV*A*T

```



```

C          CALL VMULFF(A,AC,N,N,N,N,IA,C,N,IER)
          CALL VMULFF(C,T,N,N,N,IA,IA,AC,N,IER)
          WRITE(6,205)
          FORMAT(//,10X,'THE DIAGONAL MATRIX IS',//)
          WRITE(6,100) ((AC(I,J),J=1,N),I=1,N)
C
C          CALCULATE THE CONTROL MATRIX
C
          WRITE(6,206)
          FORMAT(//,10X,'THE CONTROL MATRIX IS',//)
          CALL VMULFF(A,B,N,N,L,N,N,D,N,IER)
          DO 30 I=1,N
          WRITE(6,104) (D(I,J),J=1,L)
          FORMAT(//,8(2X,F7.2,2X))
C
C          CALCULATE Y=CI
C
          WRITE(6,207)
          FORMAT(//,10X,'THE MEASUREMENT VECTOR IS',//)
          CALL VMULFF(H,T,M,N,N,M,IA,G,M,IER)
          WRITE(6,100) ((G(I,J),J=1,N),I=1,M)
          FORMAT(//,10(2X,F7.2))
          RETURN
          END
C
C          SUBROUTINE VARY (B,L,NPT,I1,I2)
C
C          VARY IS USED TO CALCULATE THE COVARIANCE OF THE STATES OF
C          A SYSTEM. THE COVARIANCE IS FOUND BY SOLVING THE LYAPUNOV
C          DIFFERENTIAL EQUATION USING THE ISML SUBROUTINE DVERK.
C
C          SUBROUTINE VARY (B,L,NPT,I1,I2)
C          DIMENSION B(10,4),P(100),PDOT(100),D(10,10),W(100,10),
C          1G(10,10),C(24)
C          EXTERNAL FCN
C          COMMON BP,CP,K,KX,KXD,TOU,CPG,N,PD(100),Q(10,10),A(10,10)
C          WRITE(6,200)
C          FORMAT(//,20X,90(' '),//,40X,'VARIANCE ANALYSIS',
C          1//,20X,90(' '),//)
C
C          START CLACULATIONS

```



```

C
1  C C C
  TST=.00005
  NSQ=N*N
  NW=NSQ
  TIME=T1
  TOL=.001
  XNPT=NPT
  STEP=(T2-T1)/XNPT
  DO 1 I=1,N
  DO 1 J=1,N
  G(I,J)=0.0
  DO 1 K=1,L
  G(I,J)=G(I,J)+B(I,K)*Q(K,J)
  G=B*QA
  DO 2 I=1,N
  DO 2 J=1,N
  Q(I,J)=0.0
  DO 2 K=1,L
  Q(I,J)=Q(I,J)+G(I,K)*B(J,K)
  Q=B*Q*BT
  NOW SET INITIAL VALUES OF P
  DO 3 I=1,N
  DO 3 J=1,N
  G(I,J)=0.0
  G IS THE MATRIX OF THE P VECTOR SET TO 0.0
  SET UP TO CALL DVERK
  DO 4 I=1,24
  C(I)=0.0
  WRITE(6,700) TIME
  FORMAT(/,10X,'AT TIME= ',F5.2,/)
  CALL MTM(N,NSQ,G,P)
  TIMEE=TIME+STEP
  IND=1
  CALL DVERK(NSQ,FCN,TIME,P,TIMEE,TOL,IND,C,NW,W,IER)
  WRITE(6,750) IND
  FORMAT(10X,'IND=',I3,' AFTER CALL TO DVERK')
  CALL VTM(N,NSQ,G,P)
  WRITE(6,700) TIME
  WRITE(6,800)
  FORMAT(/,20X,'THE P MATRIX IS',/)
2  C C C C C
3  C C C C C
4
700
20
750
800

```

```

MOD01480
MOD01490
MOD01500
MOD01510
MOD01520
MOD01530
MOD01540
MOD01550
MOD01560
MOD01570
MOD01580
MOD01590
MOD01600
MOD01610
MOD01620
MOD01630
MOD01640
MOD01650
MOD01660
MOD01670
MOD01680
MOD01690
MOD01700
MOD01710
MOD01720
MOD01730
MOD01740
MOD01750
MOD01760
MOD01770
MOD01780
MOD01790
MOD01800
MOD01810
MOD01820
MOD01830
MOD01840
MOD01850
MOD01860
MOD01870
MOD01880
MOD01890
MOD01900
MOD01910
MOD01920
MOD01930
MOD01940
MOD01950

```



```

C      801      WRITE(6,100) ((G(I,J),J=1,N),I=1,N)
C      CALL VTM(N,NSQ,D,PD)
C      WRITE(6,801)
C      FORMAT(//,20X,'P DOT IS',//)
C      WRITE(6,100) ((D(I,J),J=1,N),I=1,N)
C      SUM=0.0
C      DO 5 I=1,NSQ
C        SUM=SUM+ABS(PD(I))
C      WRITE(6,802) SUM
C      802      FORMAT(10X,'THE SUM OF THE P DOT TERMS IS ',E15.5)
C      IF(SUM.LE.1ST) GO TO 50
C      IF(TIMEE-GE.12) GO TO 51
C      GO TO 20
C      50      WRITE(6,710)
C      710      FORMAT(//,20X,'THE LAST P IS A STEADY STATE',//)
C      RETURN
C      51      CALL VTM(N,NSQ,G,PD)
C      WRITE(6,720)
C      720      FORMAT(//,20X,'END OF RUN THE FINAL PDOT IS',//)
C      100      WRITE(6,100) ((G(I,J),J=1,N),I=1,N)
C      FORMAT(10(2X,E10.4),//)
C      RETURN
C      END
C
C      SUBROUTINE FCN(NSQ,TIME,P,PDOT)
C
C      FCN IS USED BY DVERK.IT PROVIDES THE FORM OF THE
C      DIFFERENTIAL EQUATION.
C
C      SUBROUTINE FCN(NSQ,TIME,P,PDOT)
C      DIMENSION D(10,10),G(10,10),P(NSQ),PDOT(NSQ)
C      COMMON BP,CP,KX,KX,TOU,CPG,N,PD(100),Q(10,10),A(10,10)
C      CALL VTM(N,NSQ,G,P)
C      DO 1 I=1,N
C      DO 1 J=1,N
C        D(I,J)=Q(I,J)
C        DO 1 K=1,N
C          D(I,J)=D(I,J)+A(I,K)*G(K,J)+G(I,K)*A(J,K)
C        CALL MTV(N,NSQ,D,PDOT)
C      DO 2 I=1,NSQ
C        PD(I)=PDOT(I)
C      RETURN
C      END
C
C      SUBROUTINES MTV AND VTM
C
C      SUBROUTINE MTV(N,NSQ,A,B)

```

```

MOD01960
MOD01970
MOD01980
MOD01990
MOD02000
MOD02010
MOD02020
MOD02030
MOD02040
MOD02050
MOD02060
MOD02070
MOD02080
MOD02090
MOD02100
MOD02110
MOD02120
MOD02130
MOD02140
MOD02150
MOD02160
MOD02170
MOD02180
MOD02190
MOD02200
MOD02210
MOD02220
MOD02230
MOD02240
MOD02250
MOD02260
MOD02270
MOD02280
MOD02290
MOD02300
MOD02310
MOD02320
MOD02330
MOD02340
MOD02350
MOD02360
MOD02370
MOD02380
MOD02390
MOD02400
MOD02410
MOD02420
MOD02430

```



```

DIMENSION A(N,N),B(NSQ)
K=1
DO 1 I=1,N
DO 1 J=1,N
B(K)=A(I,J)
K=K+1
DEBUG SUBCHK
RETURN
END
1

SUBROUTINE VTM(N,NSQ,A,B)
DIMENSION A(N,N),B(NSQ)
K=1
DO 1 I=1,N
DO 1 J=1,N
A(I,J)=B(K)
K=K+1
DEBUG SUBCHK
RETURN
END
1

```

```

MOD02440
MOD02450
MOD02460
MOD02470
MOD02480
MOD02490
MOD02500
MOD02510
MOD02520
MOD02530
MOD02540
MOD02550
MOD02560
MOD02570
MOD02580
MOD02590
MOD02600
MOD02610
MOD02620
MOD02630

```



```

*****
*
*      **      HARRIER LONUDITUDNAL SRFIMF CONTROL SIMULATION      **
*
*****
// EXEC CSMPXV
//X.COMPRINT DD DUMMY
//X.SYSPRINT DD DUMMY
//X.SYSIN DD *
*
*      SIMULATION OF OPEN LOOP PLANT
*
X1P=INTGRL(0.0,X2P)
X2P=INTGRL(0.0,X3P)
X3P=INTGRL(0.0,X4P)
X4P=INTGRL(0.0,X4PDOT)
X4PDOT=.25*XC-.49*X4P+.45*X3P-.0665*X2P-.00748*X1P
ACCELP=-.00189*X1P-.016625*X2P+.1144*X3P-.061*X4P+.25*XC
POSITP=.00189*X1P+.0615*X2P+.25*X3P
VELP=.00189*X2P+.0615*X3P+.25*X4P
*
*
*      CLOSED LOOP SYSTEM SIMULATION
*
X1=INTGRL(0.0,X2)
X2=INTGRL(0.0,X3)
X3=INTGRL(0.0,X4)
X4=INTGRL(0.0,X4DOT)
X4DOT=X5-.49*X4+.45*X3-.0665*X2-.00748*X1
ACCEL=-.00189*X1-.016625*X2+.1144*X3-.061*X4+.25*X5
POSIT=.00189*X1+.0615*X2+.25*X3
VEL=.00139*X2+.0615*X3+.25*X4
X5=REALPL(0.0,TOU,IS)
XC=STEP(0.0)
WS=-KXD*VX+KX*(XC-X)+VS
IS=K*WS
VS=AS-AX
AS=REALPL(0.0,TOU,WS)
AX=ACCEL
VX=VEL
X=POSIT
K=100.
KX=4.
KXD=3.
TOU=.1
TIMER FINTIM=10,OUTDEL=.2
OUTPUT POSIT,POSITP
OUTPUT TIME,POSIT,POSITP
PAGE XYPLOT
END
STOP

```


APPENDIX B
TABULATED DATA

Time (sec)	σ_{1p}	σ_{1v}	σ_{1a}	σ_{2p}	σ_{2v}	σ_{2a}	σ_{3p}	σ_{3v}	σ_{3a}
0	0	0	0	0	0	0	0	0	0
.5	.045	.033	.011	.191	.149	.050	.764	.573	.191
1.0	.164	.123	.074	.315	.236	.079	.825	.619	.206
2.0	.410	.307	.102	.342	.256	.085	1.022	.767	.256
3.0	.564	.423	.141	.344	.258	.086	1.283	.962	.321
4.0	.660	.495	.165	.347	.260	.087	1.475	1.106	.369
5.0	.728	.546	.182	.348	.261	.087	1.613	1.210	.403
6.0	.780	.585	.195	.349	.262	.087	1.717	1.288	.429
7.0	.819	.615	.205	.350	.262	.087	1.797	1.348	.449
8.0	.851	.638	.213	.351	.263	.088	1.861	1.395	.465
9.0	.875	.657	.219	.351	.263	.088	1.911	1.433	.478
10.0	.895	.671	.224	.352	.264	.088	1.950	1.464	.488
20.0	.968	.726	.242	.354	.265	.088	2.100	1.576	.525
40.0	.979	.734	.245	.354	.265	.089	2.123	1.592	.531
60.0	.979	.734	.245	.354	.266	.089	2.123	1.592	.531
S.S.	.979	.734	.245	.354	.266	.089	2.123	1.592	.531

Table B-1 Tabulated Data
for figures 4-4 through 4-6.

Time (sec)	σ_{1a}	σ_{2a}	σ_{3a}
0	0	0	0
2.0	.530	.675	2.005
4.0	2.858	1.781	7.745
6.0	8.070	3.060	18.515
8.0	14.649	4.412	34.742
10.0	24.399	5.791	56.569

The rate of change in P , \dot{P} after 10 seconds was

	$\sigma_{\dot{P}1}$	$\sigma_{\dot{P}2}$	$\sigma_{\dot{P}3}$
10.0	16.422	2.826	37.350

Table B-2
Tabulated data for figure 4-7.

Time (sec)	σ_{1p}	σ_{1v}	σ_{2p}	σ_{2v}	σ_{3p}	σ_{3v}
0	0	0	0	0	0	0
.5	.020	.026	.091	.119	.351	.458
1.0	.076	.099	.149	.189	.379	.495
2.0	.189	.246	.157	.205	.470	.613
3.0	.259	.338	.158	.206	.590	.770
4.0	.304	.396	.160	.208	.679	.885
5.0	.335	.437	.160	.209	.740	.968
6.0	.359	.468	.160	.209	.790	1.030
7.0	.377	.492	.161	.210	.827	1.078
8.0	.391	.510	.161	.210	.856	1.116
9.0	.403	.525	.162	.211	.879	1.147
10.0	.412	.537	.162	.211	.898	1.171
20.0	.445	.581	.163	.212	.966	1.261
S.S	.450	.590	.163	.212	.970	1.300

Table B-3 Tabulated data for figures 4-9 through 4-11.

Time (sec)	σ_{lp}	σ_{lv}	σ_{la}	σ_{2p}	σ_{2v}	σ_{2a}	σ_{5p}	σ_{5v}	σ_{5a}
0	0	0	0	0	0	0	0	0	0
.5	.440	.081	.011	.201	.210	.050	2.672	2.010	.668
1.0	.166	.125	.042	.319	.239	.080	2.807	2.106	.702
2.0	.413	.310	.103	.345	.259	.086	3.237	2.428	.809
3.0	.566	.425	.142	.348	.261	.087	3.286	2.465	.822
4.0	.662	.496	.165	.350	.263	.088	3.288	2.466	.822
5.0	.730	.547	.182	.351	.264	.088	3.291	2.468	.822
6.0	.781	.586	.195	.353	.264	.088	3.300	2.475	.825
7.0	.820	.615	.205	.353	.265	.088	3.320	2.490	.830
8.0	.852	.639	.213	.354	.266	.089	3.345	2.511	.837
9.0	.876	.657	.219	.355	.266	.089	3.384	2.538	.846
10.0	.896	.672	.224	.355	.266	.089	3.425	2.570	.856
20.0	.969	.727	.242	.357	.268	.089	3.821	2.866	.955
S.S.	.980	.734	.245	.360	.270	.089	3.900	2.900	.970

Table B-4 Tabulated data for figures 5-4 through 5-6.

Time (sec)	σ_{1g}	σ_{2g}	σ_{5g}	σ_{accg}	σ_g
0	0	0	0	0	0
1.0	.0013	.006	.076	.013	2.573
2.0	.0014	.009	.110	.040	3.390
3.0	.0014	.011	.227	.102	3.882
4.0	.0015	.011	.402	.191	4.207
5.0	.0015	.012	.622	.301	4.431
6.0	.0015	.012	.874	.427	4.588
7.0	.0016	.013	1.150	.564	4.701
8.0	.0016	.013	1.442	.701	4.782
9.0	.0016	.013	1.743	.860	4.840
10.0	.0016	.013	2.050	1.013	4.884
20.0	.0016	.013	4.750	2.360	4.959
40.0	.0016	.013	7.169	3.567	5.00
60.0	.0017	.013	7.783	3.874	5.00
S.S.	.0017	.013	7.800	4.00	4.00

Table B-5 Tabulated data for figure 5-7.

LIST OF REFERENCES

1. Merrick, V.K. and Gerdes, R.M., "Design and Piloted Simulation of a VTOL Flight Control System," Journal of Guidance and Control, v. 1 no. 3, May - June 1978.
2. NASA Technical Report 1040, Study of the Application of an Implicit Model Following Flight Controller to Lift Fan VTOL Aircraft, by V.K. Merrick, November 1977.
3. NASA Contractor Report 1519, Mathematical Model for Lift/Cruise for V/STOL Aircraft Simulator Programming Data, by M. P. Bland and B. Fajfar, 6 December 1976.
4. Tyler, J. S., Jr., "The Characteristics of Model Following Systems as Synthesized by Optimal Control," IEEE Trans. Automatic Control, v. 9 no. 4, p. 485-498, October 1964.
5. NASA Technical Note D-4663, On the Use of Algebraic Methods in the Analysis and Design of Model-Following Control Systems, by H. Erzberger, July 1968.
6. Nobel, B., Applied Linear Algebra, Prentice-Hall, 1969.
7. Melsa, J. L. and Jones, S. K., Computer Programs for Computational Assistance in the Study of Linear Control Theory, 2d ed., McGraw - Hill, 1973.
8. Speckhart, F. H. and Green, W. L., A Guide to Using CSMP - The Continuous System Modeling Program, Prentice - Hall, 1976.
9. Maybeck, P. S., Stochastic Models, Estimation, and Control, v. 1, Academic Press, 1979.
10. Analytical Mechanics Associates, Inc. Report No. 80-13, An Investigation of Automatic Guidance Concepts to Steer VTOL Aircraft to Small Aviation Facility Ships, Sorensen, J. A., Goka, T., Phatak, A., Schmidt, S. F., July 1980.
11. Bryson, A. E., "Kalman Filter Divergence and Aircraft Motion Estimators", Journal of Guidance and Control, v. 1 no. 1, January-February 1978.

12. Calspan Report AK-5876-F-1, A Study to Determine the Feasibility of Simulating the AV-8A Harrier With the X-22A Variable Stability Aircraft, J. V. Lebacqz and F. W. Aiken, July 1976.
13. Ogata, K., Modern Control Engineering, Prentice - Hall, 1970.
14. McRuer, D., Ashkenas, I., and Graham, D., Aircraft Dynamics and Automatic Control, Princeton University Press, 1973.

INITIAL DISTRIBUTION LIST

	No. Copies
1. Defense Technical Information Center Cameron Station Alexandria, Virginia 22314	2
2. Library, Code 0142 Naval Postgraduate School Monterey, California 93940	2
3. Department Chairman, Code 67 Department of Aeronautics Naval Postgraduate School Monterey, California 93940	1
4. Prof. D. J. Collins, Code 67fo Department of Aeronautics Naval Postgraduate School Monterey, California 93940	2
5. LT Lawrence E. Epley, USN HELANTISUBRON LIGHT THRITY-THREE NAS North Island San Diego, California 92135	1
6. Dr. Tsuyoshi Goka Analytical Mechanics Associates, Inc. Suite 210 2483 Old Middlefield Way Mountain View, California 94043	1
7. Prof. A. E. Fuhs, Code 67Fu Department of Aeronautics Naval Postgraduate School Monterey, California 93940	1
8. Mr. Vernon Merrick Mail Stop N211-2 NASA Ames Research Center NAS Moffett Field, California 94035	5

Thesis

E559

c.1

Epley

190865

A study of state rate
feedback implicit model rate
following control for model
VSTOL aircraft.

27 JUL 92

38237

7.

Thesis

E559

c.1

Epley

190865

A study of state rate
feedback implicit model
following control for
VSTOL aircraft.

thesE559

A study of state rate feedback implicit



3 2768 002 06193 9

DUDLEY KNOX LIBRARY